

Electronic Thesis and Dissertation Repository

1-31-2012 12:00 AM

A geobiological investigation of the Mazon Creek concretions of northeastern Illinois, mechanisms of formation and diagenesis

Andrea S. Fernandes
The University of Western Ontario

Supervisor

Dr. Gordon Southam
The University of Western Ontario Joint Supervisor

Dr. Cameron Tsujita
The University of Western Ontario

Graduate Program in Geology

A thesis submitted in partial fulfillment of the requirements for the degree in Master of Science
© Andrea S. Fernandes 2012

Follow this and additional works at: <https://ir.lib.uwo.ca/etd>



Part of the [Biogeochemistry Commons](#)

Recommended Citation

Fernandes, Andrea S., "A geobiological investigation of the Mazon Creek concretions of northeastern Illinois, mechanisms of formation and diagenesis" (2012). *Electronic Thesis and Dissertation Repository*. 398.

<https://ir.lib.uwo.ca/etd/398>

This Dissertation/Thesis is brought to you for free and open access by Scholarship@Western. It has been accepted for inclusion in Electronic Thesis and Dissertation Repository by an authorized administrator of Scholarship@Western. For more information, please contact wlsadmin@uwo.ca.

**A GEOBIOLOGICAL INVESTIGATION OF THE MAZON CREEK CONCRETIONS
OF NORTHEASTERN ILLINOIS, MECHANISMS OF FORMATION AND
DIAGENESIS**

(Spine title: A geobiological investigation of Mazon Creek concretions)

(Thesis format: Integrated-Article)

By

Andrea S. Fernandes

Graduate Program in Geology

A thesis submitted in partial fulfillment
of the requirements for the degree of
Master of Science

The School of Graduate and Postdoctoral Studies
The University of Western Ontario
London, Ontario, Canada

© Andrea S. Fernandes 2012

THE UNIVERSITY OF WESTERN ONTARIO
SCHOOL OF GRADUATE AND POSTDOCTORAL STUDIES

CERTIFICATE OF EXAMINATION

Supervisor	Examiners
_____ Dr. Gordon Southam	_____ Dr. Patricia Corcoran
_____ Co-Supervisor	_____ Dr. Susan Koval
_____ Dr. Cameron Tsujita	_____ Dr. Gordon Osinski

The thesis by

Andrea Sangeeta Fernandes

Entitled:

**A geobiological investigation of the Mazon Creek concretions of
northeastern Illinois, mechanisms of formation and diagenesis**

Is accepted in partial fulfilment of the
requirements for the degree of
Master of Science

Date: _____

Chair of the Thesis Examination Board

ABSTRACT

Siderite concretions from the mid-Pennsylvanian Francis Creek Shale of the Mazon Creek area, in northeastern Illinois, contain exceptionally preserved soft-tissue fossils. Scanning electron microscopy, energy dispersive spectroscopy, time of flight-secondary ion mass spectrometry and micro-x-ray diffraction on polychaete worm, jellyfish and holothurian samples highlighted detrital clay and quartz grains in siderite cement. The worm and jellyfish are pyritised and surrounded by pyrite halos, whereas the holothurian is preserved as a weathered impression. Specimens possessed either microbial textures or framboidal pyrite, in carbon-enriched zones. The carbon-enriched zones contained organic compounds, indicating that extensive degradation associated with high temperature diagenesis did not occur in this region. Laboratory diagenesis experiments using sulphate- and iron-reducing bacteria revealed the challenges of soft-tissue preservation; bacteria rapidly degrade buried labile organics. Concretion and model analysis suggest rapid burial and early diagenetic mineralisation is essential for the preservation of soft tissues, including microbial remains.

KEY WORDS: Mazon Creek, *Konservat-Lagerstätten*, Siderite Concretions, Pyritisation, SEM, EDS, ToF-SIMS, Biomarkers, Diagenesis, Taphonomy, SRB, Iron Reducers, *Shewanella oneidensis* MR-1, Microfossils

This thesis is dedicated to my family, for keeping me going,
and to my friends, for keeping me sane.

ACKNOWLEDGEMENTS

I would like to thank my supervisors, Cam Tsujita and Gord Southam. Cam, if it had not been for you, I would never have found this project. Thank you for introducing me to the world of paleontology. Gord, our meetings and conversations over the last few years, have been invaluable. Without your guidance and patience, this project would not have been possible.

A big thank you: to Todd Simpson and Tim Goldhawk at the Nanofabrication Laboratory for teaching me the intricacies of the SEM; to Brian Hart and Heng-Yong Nie at SSW for their help with ToF-SIMS; to Robbie Flemming, for teaching me everything I know about XRD and mineralogy, and for the use of the Bruker; to Gord and Stephen Wood at the Thin Section Laboratory, for sample preparation and for allowing me to hijack the fumehood; to Fred Longstaffe and the LSIS lab techs, for their assistance with powder XRD; to Charlie Wu, Monique Durr, Karen Nygard and everyone at the Biotron, for their advice and help with geochemical analyses and light microscopy; to Ian Glasspool and Paul Mayer from the Field Museum of Natural History, Illinois, for giving me access to the Paleobotany and Fossil Invertebrate Collections, and to Nick Wong for playing photographer; and last but definitely not least, to everyone at the Southam Lab for their scientific insights and friendship (I will miss our lab meetings!).

I would like to recognise the prior contributions of Alaina Hills and Leah Curtis to the Mazon Creek project, and take this opportunity to thank my examination committee: Patricia Corcoran, Susan Koval and Gordon Osinski. This research was supported through NSERC Discovery grants to Cameron Tsujita and Gordon Southam.

TABLE OF CONTENTS

Title Page.....	i
Certificate of Examination	ii
Abstract.....	iii
Dedication.....	iv
Acknowledgements.....	v
Table of Contents.....	vi
List of Tables.....	ix
List of Figures	x
List of Abbreviations	xii
1. Introduction	1
1.1 General introduction	2
1.2 Exceptional fossilisation	2
1.2.1 Konservat Lagerstätten.....	2
1.2.2 Taphonomy	6
1.2.3 Biostratinomic processes.....	6
1.2.4 Fossil diagenesis.....	7
1.2.5 Sedimentation and burial rates	8
1.2.6 Oxygen levels: clarification of terms	9
1.2.7 Obrution vs. stagnation deposits.....	10
1.3 The Mazon Creek area.....	12
1.3.1 Paleoenvironment	15
1.3.2 Stratigraphy and sedimentology	18
1.3.3 Flora and fauna	23
1.4 Diagenetic mineralisation.....	29
1.4.1 Mineralisation.....	29
1.4.2 Biomineralisation.....	31
1.5 Microbial metabolism.....	33
1.5.1 Iron oxidising bacteria	34
1.5.2 Iron reducing bacteria.....	37
1.5.3 Suphate reducing bacteria.....	38
1.5.4 Methanogens.....	40
1.6 Mazon Creek type fossil diagenesis.....	41
1.6.1 Concretions	41

TABLE OF CONTENTS (CONTINUED)

1.6.2 Pyrite	45
1.6.3 Siderite	48
1.6.4 Concretion lithification	51
1.7 Chapter outlines	53
1. References	55
2. Mineralogy and biogeochemistry of Mazon Creek concretions	75
2.1 Introduction	76
2.2 Methods	79
2.2.1 Sample preparation	79
2.2.2 Micro-X-ray diffraction	80
2.2.3 Scanning electron microscopy (SEM) and energy dispersive spectroscopy (EDS)	80
2.2.4 Time of flight-secondary ion mass spectrometry (ToF-SIMS)	81
2.3 Results	82
2.3.1 Polychaete worm (PW)	82
2.3.2 Jellyfish: <i>Essexella asherae</i>	88
2.3.3 Holothurian	91
2.4 Discussion	97
2.4.1 Sulphate reduction and pyritisation	97
2.4.2 Fossil impressions and weathering minerals	103
2.4.3 Extracellular polysaccharide substances in protoconcretions	104
2.4.4 Iron reduction and siderite precipitation	105
2.4.5 Detrital grains	106
2.4.6 Organic preservation	107
2. References	109
3. A laboratory model for the initial stages of soft body fossil diagenesis	114
3.1 Introduction	115
3.2 Methods	118
3.2.1 Bacteria and culture conditions	118
3.2.1.1 Iron reducing bacterium – <i>Shewanella oneidensis</i> MR-1	118
3.2.1.2 Sulfate reducing bacteria	119
3.2.1.3 Methanogenic archaea	119
3.2.2 Column set-up	122
3.2.2.1 Arkona Shale sampling	122
3.2.2.2 Diagenesis model	123
3.2.2.3 Half-marine synthetic seawater medium	125
3.2.2.4 Fe ³⁺ -stock solution	126
3.2.3 Column analysis	126
3.2.3.1 Inductively coupled plasma-atomic emission spectrometry (ICP-AES)	130

TABLE OF CONTENTS (CONTINUED)

3.2.3.2 Ion-exchange chromatography (IC)	131
3.2.3.3 Dry weight (DW), pH, total carbon (TC) and total organic carbon (TOC)	131
3.2.3.4 Microbial counts	132
3.2.3.5 Critical point drying (CPD) for scanning electron microscopy (SEM).....	133
3.2.3.6 LR-white embedding for scanning electron microscopy (SEM).....	134
3.3 Results.....	135
3.3.1 Ion-exchange chromatography (IC), inductively coupled plasma-atomic emission spectrometry (ICP-AES), pH and total carbon (TC) results	135
3.3.2 Most probable number (MPN) results	137
3.3.3 Scanning electron microscopy (SEM) and energy dispersive spectroscopy (EDS) results	139
3.4 Discussion	147
3.4.1 Column phenotypes, geochemistry and microbial populations.....	147
3.4.2 Carbonate formation and pH.....	153
3.4.3 Organism diagenesis and preservation of organics.....	154
3.4.4 Future recommendations	156
3. References	158
4. General Discussion	162
4.1 Synthesis and conclusions	163
4.2 Future experiments	168
4. References	171
Curriculum Vitae	174

LIST OF TABLES

3. A laboratory model for the initial stages of soft body fossil diagenesis

3.1 – *Shewanella* and SRB microbial counts..... 139

LIST OF FIGURES

1. Introduction

1.1 – Maps of the Mazon Creek area	13
1.2 – Stratigraphic sequence and cross sections of the Francis Creek Shale	14
1.3 – Paleogeographic reconstruction of the Mazonian delta complex	17
1.4 – Schematic of cyclic silt-clay lamina within the Francis Creek Shale	22
1.5 – Images of the Essex fauna	24
1.6 – Images of Mazon Creek flora	27
1.7 – Images of the Braidwood fauna.....	28
1.8 – Microbial redox succession in soil	35

2. Mineralogy and biogeochemistry of Mazon Creek concretions

2.1 – Polychaete worm polished and thin sections.....	83
2.2 – Polychaete worm XRD scans.....	85
2.3 – SEM micrographs of PW fossil and EDS spectrum of C-rich inclusion.....	86
2.4 – SEM micrograph and EDS spectra of PW matrix, fossil and inclusions	87
2.5 – ToF-SIMS spectra of PW C-rich inclusion.....	89
2.6 – Photographs of the jellyfish concretion and polished section, and SEM micrographs of the region of interest (ROI).....	90
2.7 – Magnified SEM micrograph and EDS spectra within the jellyfish ROI.....	92
2.8 – SEM micrograph and EDS spectrum of organic aggregates within the jellyfish ROI	93
2.9 – ToF-SIMS spectra of the jellyfish ROI.....	94
2.10 – Photographs of the holothurian concretion and polished section	95
2.11 – SEM micrograph and EDS spectra of reticulate cracks within the holothurian fossil region	96
2.12 – SEM micrographs of the holothurian ROI.....	98
2.13 – ToF-SIMS spectra of the holothurian ROI.....	99

3. A laboratory model for the initial stages of soft body fossil diagenesis

3.1 – Photograph of column set-up and outline of analyses	124
3.2 – Column photographs showing diagenetic phenotypes.....	128
3.3 – Graphs of nitrate, nitrite, sulphate, iron and phosphorus concentration with depth in columns	136
3.4 – Graphs of calcium and magnesium concentrations, pH, TOC and TIC with depth in columns	138
3.5 – SEM micrographs and EDS spectra of uninoculated and C column Arkona Shale.....	140
3.6 – SEM micrograph of a freshly killed brine shrimp	141
3.7 – SEM micrograph focal series showing brine shrimp microbiota.....	143

LIST OF FIGURES (CONTINUED)

3. A laboratory model for the initial stages of soft body fossil diagenesis (continued)

3.8 – SEM micrograph and EDS spectra of spheroidal aggregate forming in shale 144

3.9 – SEM micrographs of brine shrimp carcasses at 5, 8.5 and 9 months 145

3.10 – SEM micrograph and EDS spectrum of framboidal pyrite..... 146

3.11 – SEM micrographs of C-rich regions in 8.5 month sediments 148

3.12 – SEM micrographs and EDS spectra of framboidal pyrite and a mineralised cell within C-rich sediment 149

3.13 – SEM micrograph focal series and EDS spectrum of a C-rich rod 150

LIST OF ABBREVIATIONS

ANME	ANAerobic MEthane oxidisers
Anammox	ANAerobic AMMonium OXidation
ΔG_0	Standard Gibbs free energy change
μ XRD	Micro-X-Ray Diffraction
BSE-SEM	Backscattered Secondary Electron – Scanning Electron Microscopy
C	Control phenotype
cf.	Latin <i>confer</i> , meaning “bring together”
CPD	Critical Point Drying
CT	Computed Tomography
Da.	Daltons
DIC	Differential Interference Contrast
DL	Detection Limit
DO ₂	Dissolved Oxygen
DS	Diffuse-Sulphidic phenotype
DW	Dry Weight
EDS	Energy Dispersive Spectroscopy
EPS	Extracellular Polysaccharide Substances
EtOH	Ethanol
FIB	Focused Ion Beam
GC/MS	Gas Chromatography-Mass Spectrometry
IC	Ion-Exchange Chromatography
ICP	Inductively Coupled Plasma
ICP-AES	Inductively Coupled Plasma-Atomic Emission Spectroscopy
ka	Latin <i>kiloannum</i> , meaning “thousand years”
Ma	Latin <i>megaannum</i> , meaning “million years”
MPN	Most Probable Number
MS	Mid-Sulphidic phenotype
OC	Organic Carbon
PW	Polychaete Worm
RAS	Reducing Agent Supplement
ROI	Region Of Interest
ROM	Royal Ontario Museum
SE2	Secondary Electron
SEM	Scanning Electron Microscop(e/y)
SRB	Sulphate Reducing Bacteria
SSM	Synthetic Seawater Medium
TC	Total Carbon
TOC	Total Organic Carbon
ToF-SIMS	Time-of-Flight Secondary Ion Mass Spectrometry
TSB	Tryptic Soy Broth
US	Upper-Sulphidic phenotype
UWO	University of Western Ontario

LIST OF ABBREVIATIONS (CONTINUED)

vol.	volume
wt.	weight

CHAPTER 1

INTRODUCTION

1.1 GENERAL INTRODUCTION

The Mazon Creek area is one of the most famous sites for exceptionally preserved fossils in North America. This assemblage includes fossils of more than 350 plant and 250 animal species (Nitecki, 1979). The fauna contain mostly soft-bodied taxa, but include some vertebrates, such as fish. Rapid burial is indicated by the three-dimensional preservation of plant organs (Schopf, 1979), preservation of jellyfish, yolk sacs on young coelacanths, colour markings on bivalves and insects, setae on worms and radulas on chitons and cephalopods (Baird *et al.*, 1985a).

Mazon Creek organisms are preserved within concretions, which are hardened, oblate to spherical aggregates of mineral precipitates that form around a nucleus, such as organic matter (Ojanuga and Lee, 1973). Post-burial processes of decay, diagenesis and concretion formation have been studied, but are still poorly understood (Baird *et al.*, 1986). This study investigates these processes from a microbiological perspective using: 1) multiple analytical techniques to study concretions and 2) a laboratory diagenetic model to study the early stages of decay and fossilisation in soft-bodied organisms.

1.2 EXCEPTIONAL FOSSILISATION

1.2.1 *Konservat Lagerstätten*

Fossilisation may be more common in the rock record than is commonly believed (Bottjer, 2002), but some tissues are more easily preserved than others. Preservation capacity falls along a continuum based on mineral (high capacity) to organic (low capacity) content ratio as follows (Allison, 1988b; Briggs and Kear, 1993a,b): 1) mineralised tissues, such as shells, bones and teeth; 2) sclerotised structural polymers, such as exoskeletal chitin and hardened collagen; 3) non-sclerotised structural polymers, such as cuticular collagen; and 4) soft, primarily proteinaceous tissues, such as muscle (Briggs and Kear, 1993a,b; Bottjer, 2002). In recent years, several examples of exceptional soft tissue preservation have been discovered and studied (Briggs and Kear, 1993a,b; Bottjer, 2002).

Lagerstätten, a term coined by Seilacher in 1970 literally translates from German as “storage place”, and is used in paleontology to denote exceptional fossil deposits. There are two types of *lagerstätten*: *Konzentrat* (concentration) and *konservat* (conservation), depending on whether they are exceptional in terms of fossil abundance or quality of preservation (Allison, 1988a). Seilacher and Westphal (1971) further divided concentration and conservation deposits into three main types. The concentration deposits are: 1) condensation deposits (*e.g.*, subaerial or submarine cave deposits); 2) placer deposits, which contain beds where fossils have been biogenically and mechanically concentrated over time (Allison and Briggs, 1991) (*e.g.* river bone beds); and 3) concentration traps, such as fissures. The conservation deposits are: 1) stagnation deposits, where offshore sediments are deposited under conditions of restricted circulation (Jenkyns, 1980) (*e.g.*, lignitic shales, black shales, marine or non-marine

lithographic limestones); 2) obrution deposits, which are characterized by rapid burial (e.g., Burgess Shale, Hunsrück Slate, Gmünd echinoderm *Lagerstätte*); and 3) conservation traps, where organisms are caught or deposited in environments that prevent decay (e.g., permafrost crevices, amber, desiccation environments, peat bogs).

Some famous examples of *Konservat Lagerstätte* that preserve soft-bodied organisms are the Middle Cambrian Burgess Shale, Lower Devonian Hunsrück Slate, Jurassic Solnhofen Plattenkalk, Middle Triassic Voltzia Sandstone and Carboniferous Francis Creek Shale (Mazon Creek) (Shabica and Hay, 1997). These deposits vary widely in paleoenvironment and fossil diagenesis. The Burgess Shale was deposited in a deep outer shelf environment (Fritz, 1971; Piper, 1972; McIlreath, 1977). The Hunsrückschiefer preserves extraordinarily intact, multi-element skeletal remains of marine organisms that were rapidly buried, and possibly smothered, in a shallow to medium depth marine environment (Bartels and Brassel, 1990; Bartels *et al.*, 1998). Lithographic limestones of the Solnhofen were formed in a series of small hypersaline, oxygen-depleted basins enclosed by bioherms and reefs (Viohl, 1996). Both the Grès à Voltzia Sandstones and Francis Creek Shale were deposited in a deltaic to marginal marine environment (Shabica, 1979; Gall, 1985).

Fidelity of fossil preservation is determined by environmental conditions at the burial site and by sedimentation/burial rate (Clarkson, 1998). *Konservat Lagerstätten* often preserve lightly sclerotised and soft tissues. Taphonomic conditions that slow and/or prevent post-mortem decomposition and destruction are required for soft tissue preservation. These include rapid burial, anoxia and early diagenetic mineralisation.

Rapid burial kills organisms and immobilises carcasses before significant decomposition and disarticulation can occur. Rapid burial associated with high-volume influxes of fine-grained sediment can promote the development of anoxia by limiting the diffusion of oxygen from overlying water (Allison, 1988b). Fine-grained sediments without deep bioturbation are also more likely to become anoxic, because of smaller pore spaces and limited sediment water mixing. Sediments with more permeable, silt- to sand-sized particles are more likely to remain oxic (Brett *et al.*, 1986).

Aerobic and anaerobic microorganisms can promote the development of anoxia through decomposition of organic matter; after sediment porewaters are depleted in dissolved oxygen, the gases produced during anaerobic decay prevent reoxygenation as long as organic matter persists. Anaerobic decay progresses more slowly than aerobic decay (Allison, 1988b). This is especially important in soft tissue preservation.

Soft tissue preservation in sedimentary deposits can occur in several ways: 1) early diagenetic mineralisation by a variety of minerals (*e.g.*, hydrous aluminosilicates, pyrite, phosphate, iron oxides, and silicates); 2) as organic residues; 3) as sediment impressions or as casts (Bottjer, 2002). In some cases, such as in the Mazon Creek *lagerstätte*, it is evident that soft tissues were protected from compaction by virtue of encasement in concretions.

The higher concentration of fossil bodies in *lagerstätten* compared to more typical fossil occurrences allows a more comprehensive study of their genesis (Seilacher *et al.*, 1985). Their taphonomic study can give a more complete picture of ancient biodiversity, the extent of soft tissue and skeletal decay, environmental events and

conditions surrounding burial, and mineralisation of preserved tissues (Seilacher *et al.*, 1985).

1.2.2 Taphonomy

Taphonomy is the study of post-mortem processes, and encompasses two smaller subcomponents of investigation– biostratinomy and fossil diagenesis (Müller, 1979). Biostratinomy covers processes from organism death to its final burial within sediment, whereas diagenesis covers the processes following final burial. Variations in environmental conditions and in the susceptibility of the remains of organisms to destruction by these processes affect the quality of preservation.

1.2.3 Biostratinomic Processes

The biostratinomic processes are divided into four main categories: 1) Reorientation - the movement of an organism or carcass from its life position and/or its transport before burial; 2) disarticulation - the separation of skeletal elements caused by decay of connective tissues; 3) fragmentation - the breakage of skeletal elements, usually following reorientation and disarticulation; and 4) corrosion - a combination of mechanical abrasion, bioerosion and dissolution that mainly occurs when skeletal remains are left exposed at the sediment/water interface for a prolonged period of time (Brett *et al.*, 1986). For example, rapid burial in anoxic, quiet-water conditions can result in articulated preservation of organisms in life-position. Intact preservation of fragile structures suggests a low-energy environment of deposition with minimal reorientation.

1.2.4 Fossil diagenesis

Diagenetic processes that occur within the top few metres of uncompacted sediment include dissolution, and infilling of inter- and intra-skeletal voids by sediments and authigenic minerals (Boyd and Newell, 1972). Organisms' skeletal structures can have varying mineralogy across species. Knowledge of the stability fields of skeletal minerals combined with knowledge of the relative abundance of various skeletons in a deposit can give paleoenvironmental insights (Seilacher, 1982a; Brett and Baird, 1986). Anaerobic decay in organic-rich muds produces carbonic and sulphuric acids, accelerating calcium carbonate dissolution (Hecht, 1933). In these environments, refractory organic matter (*e.g.* periostracum) or post-dissolution diagenetic minerals may remain once carbonate shells have dissolved (Seilacher, 1971; Fisher and Hudson, 1985).

Sediment infillings and mineral diagenesis vary with depositional rate and sediment geochemistry. Rapid burial and soft-tissue decay can lead to sediment-free voids that can be filled by diagenetic minerals (*e.g.* pyrite, phosphate, carbonate, silica or chert) (Brett and Baird, 1986). Slow burial usually results in complete decay of soft parts, unless burial is in a euxinic basin. Slower burial and decay can lead to eventual infilling of skeletal voids with sediment. If geochemical conditions allow early cementation of infilled sediments by, for *e.g.*, carbonate or phosphate, the steinkerns could withstand subsequent compaction (Seilacher, 1971; Brett and Baird, 1986). Steinkerns are formed when sediment infilling a hollow organic structure is

consolidated, and maintains its form even after the structure has disintegrated. To preserve the forms of skeletal voids or soft tissues, mineralisation must occur before significant sediment compaction; therefore, steinkern mineralogy can be used to determine the geochemical conditions in the upper few metres of sediment (Brett and Baird, 1986). Rapid burial in anoxic environments slows organic decay and could lead to preservation of soft tissues (Zangerl, 1971).

1.2.5 Sedimentation and burial rates

Sedimentation rates vary between environments, and determine how rapidly carcasses are buried. Normal, background sedimentation rates can range from high (>100 cm/1000 yr) to intermediate (10-100 cm/1000 yr) to low (<10 cm/1000 yr) to none (Speyer and Brett, 1991). Determination of the background sedimentation rate can be complicated by overprinting, caused by episodic winnowing, resuspension and redeposition. Information from the fossil record (*e.g.*, level of corrosion, degree of articulation, types of structures preserved) can help in determining background sedimentation rates in these cases (Brett and Baird, 1986). For a discussion of normal background sedimentation as it pertains to epeiric seas, see Irwin (1965).

Episodic sedimentation events can deposit large amounts of sediment rapidly and abruptly (Speyer and Brett, 1991). They are caused by disturbances, such as large storms, floods, seismic shocks and slumps (*i.e.*, tempestites, turbidites, and inundates) (Brett and Baird, 1986), and can create a spectrum of deposits along a shore-to-basin transect (Speyer and Brett, 1991). Shelly deposits develop in nearshore environments

above normal wave base, grading downslope into shelly sand deposits between normal and storm wave bases, and into smothered bottom deposits below storm wave base (Speyer and Brett, 1991). There is no specific depth indicated in the literature for normal- or storm wave base, presumably because these can vary widely with underwater topography, current strength and wind speed; however, it may be possible to develop a complete spectrum for wave heights at a given location if data is collected for a few weeks (Denny *et al.*, 2004). Kumar and Sanders (1976) proposed a method for approximating the depth of normal- and storm-wave scour in modern and ancient nearshore sediments using a succession of basal lag, laminated sand and either wave-ripple or burrow-mottled sedimentary strata.

1.2.6 Oxygen levels: clarification of terms

Terms used to describe the level of oxygen are loosely defined, and can vary among authors. See Brett and Baird (1986) for a detailed explanation. For the purposes of this study: anoxic and anaerobic denote oxygen levels at or approaching zero (<0.1-0.3 mL/L); suboxic and dysaerobic denote low oxygen levels (0.3-0.7 mL/L); and oxic and aerobic denote higher oxygen levels (>0.7 mL/L) in sediment porewater and water (Thompson *et al.*, 1985; Brett *et al.*, 1986).

Brett and Baird (1986) compiled several naming schemes used to differentiate between low, medium and high oxygen, sulphide and/or organic carbon levels in sediments, water or shale. The compiled scheme describes the oxygen, sulphide and organic carbon conditions in the water column and bottom sediments of three “types”

of basins. “Normal” basins have fully aerobic bottom water (Dissolved Oxygen (DO₂) > 0.7 mL/L), and sediments that are oxic to several centimetres and organic poor. “Restricted” basins have low aerobic to dysaerobic bottom water (DO₂ 0.7-0.3 mL/L), and sediments that are organic poor, usually nonsulphidic and anoxic beneath a millimetres thick oxic layer. “Inhospitable bottoms” have dysaerobic to anaerobic bottom waters (DO₂ 0.3-0.1 mL/L), and sediments that are anoxic to the surface, organic-rich and sulphidic. In strata deposited in epeiric seas, all of these bottom water conditions should be present and overlapping to varying degrees, based on basin stratification conditions during deposition (Brett *et al.*, 1986).

1.2.7 Obrution vs. stagnation deposits

Seilacher *et al.* (1985) defined a ternary diagram into which various exceptional fossil biotas could be placed, based on environmental and diagenetic boundary conditions. The corners of the ternary diagram (obrution, stagnation and bacterial sealing) were considered the most dominant factors in the formation of conservation *lagerstätten*.

Obrution deposits are formed by sediment inundation in aqueous environments (Seilacher *et al.*, 1985). Finer-grained sediments are more likely to smother and trap entrained organisms (Bernier, 1981b). Obrution deposits usually form during the transgressive phases of stratigraphic cycles (Seilacher *et al.*, 1985). Reduced oxygen in pore waters is not necessary for their formation, but would aid preservation by inhibiting infaunal scavenging of carcasses (Seilacher, 1964). Some examples of obrution

deposits are the Burgess Shale, the Hunsrück Slate and the Gmünd echinoderm beds (Bottjer, 2002). The Burgess shale formed in a relatively deep outer shelf setting (Fritz, 1971; Piper, 1972; McIlreath, 1977). The environment of formation of the Hunsrück Slate is still under debate, but is believed to fall within the intertidal region to 200 m water depth (Mittmeyer, 1980; Briggs *et al.*, 1996). The Gmünd echinoderm beds were deposited on shallow, marine firm-grounds during the early Lower Jurassic transgression (Seilacher *et al.*, 1985).

Stagnation deposits are formed in marine basins when the water body becomes stratified during restricted circulation conditions (Seilacher *et al.*, 1985; Allison and Briggs, 1991). Stratification can be a result of thermoclines, haloclines, *etc.*, often accompanied by oxyclines (Keupp, 1977; Jenkyns, 1980; Allison and Briggs, 1991). Bottom anoxia can be limited to subseafloor pore waters or extend into the overlying water column (Seilacher *et al.*, 1985), analogous to the “inhospitable bottoms” of Brett and Baird (1986). Stagnation can be temporarily reduced by water mixing during storm events. Seilacher (1982b) classified Holzmaden, the locale of the Posidonia Shales, as a large stagnant basin.

In many cases, interplay between stagnation and obrution is apparent in the sedimentary record of *lagerstätten* formation. The lithographic limestones of the Solnhofen, for example, formed in permanently submerged restricted basins during the early Tithonian, before the regressive end of the Jurassic cycle in southern Germany (Viohl, 1985). The water was stratified, either due to a halocline (Keupp, 1977) or a combined halocline and oxycline (Seilacher *et al.*, 1985). The basins were smaller than at

Holzmaden, with steeper slopes. This confined storm wave action to the shallow margins, and allowed episodic inundation of anoxic deeper regions with fine-grained sediment and entrained benthic organisms from oxygenated nearshore environments (Seilacher *et al.*, 1985).

1.3 THE MAZON CREEK AREA

The Mazon Creek area, the source area of the fossiliferous concretions studied herein, encompasses several counties in northeastern Illinois (Fig. 1.1) (Smith, 1970). It derives its name from a local river (Fig. 1.1A) along which cutbank exposures first revealed the so-called Mazon Creek concretions to amateur collectors (Nitecki, 1979). The concretions occur in the mid to lower Francis Creek Shale Member of the mid-Pennsylvanian Carbondale Formation (Fig. 1.2A). The Francis Creek Shale is regionally underlain by the Colchester No. 2 Coal Member (Wanless and Weller, 1932; Wanless, 1939; Smith, 1970). Shaft and strip mining of the Colchester Coal greatly increased the number of exposures of the Francis Creek Shale (Fig. 1.1A), and led to the majority of fossil finds (Baird, 1979). 370 collecting localities are situated in a 200-square-kilometre region encompassing five counties: La Salle, Livingston, Grundy, Will and Kankakee (Baird *et al.*, 1985a). Pit 11, a Peabody Coal Company strip mine located just south of Braidwood in Will County, has been particularly important in yielding rare fossils of soft-bodied organisms (Fig. 1.1A) (Nitecki, 1979).

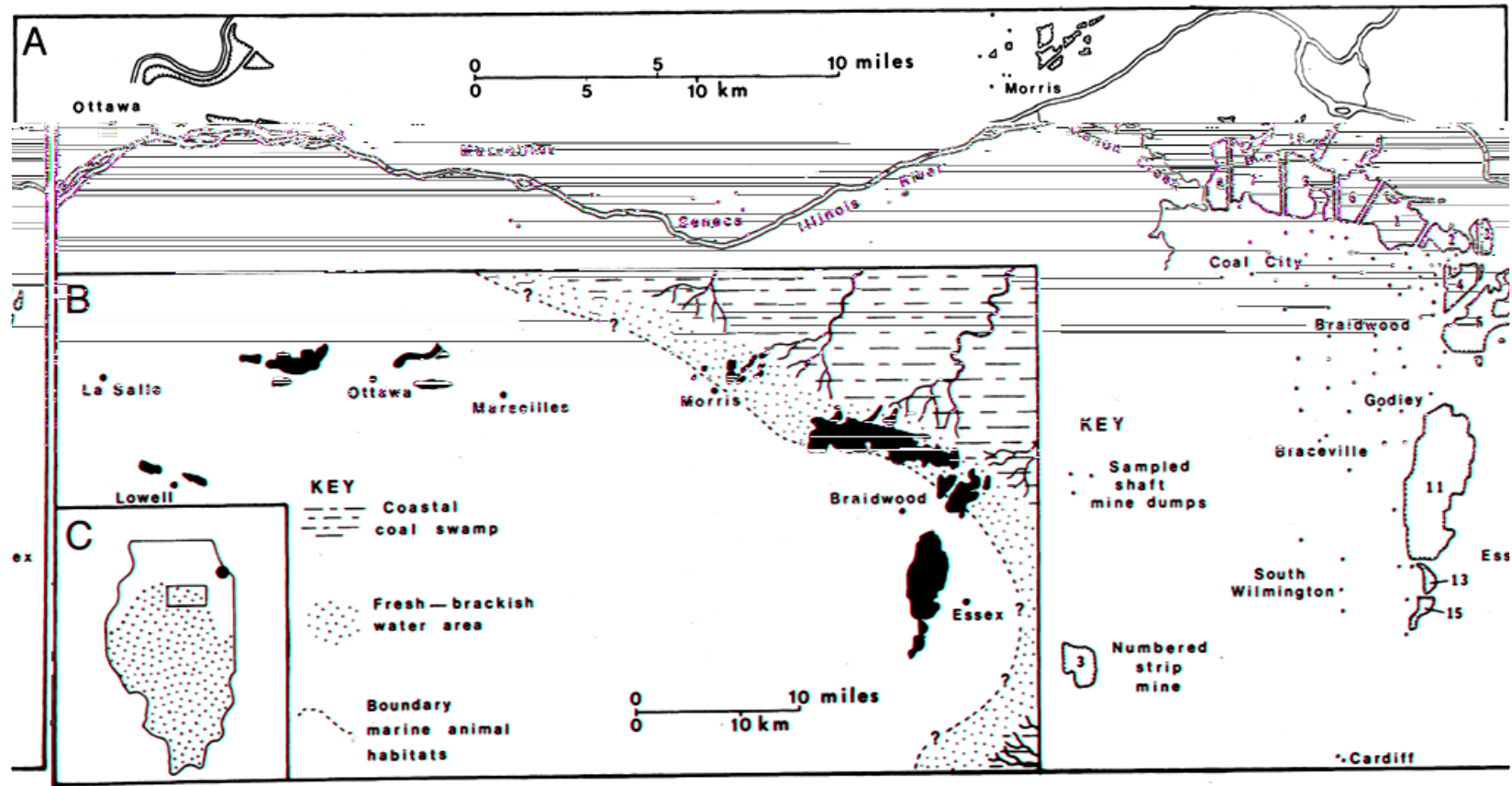


Figure 1.1: Map of Mazon Creek area, northeast Illinois. A) Distribution of fossil collecting localities (*i.e.*, shaft and strip mines indicated on map) around Mazon Creek. B) Inferred Pennsylvanian paleogeography of the Mazon Creek area. C) Location of Mazon Creek area (boxed region) southwest of Chicago, Illinois (black dot). The stippled region is the inferred location of an epeiric sea that covered most of Illinois during the Pennsylvanian (modified from Shabica and Hay, 1997).

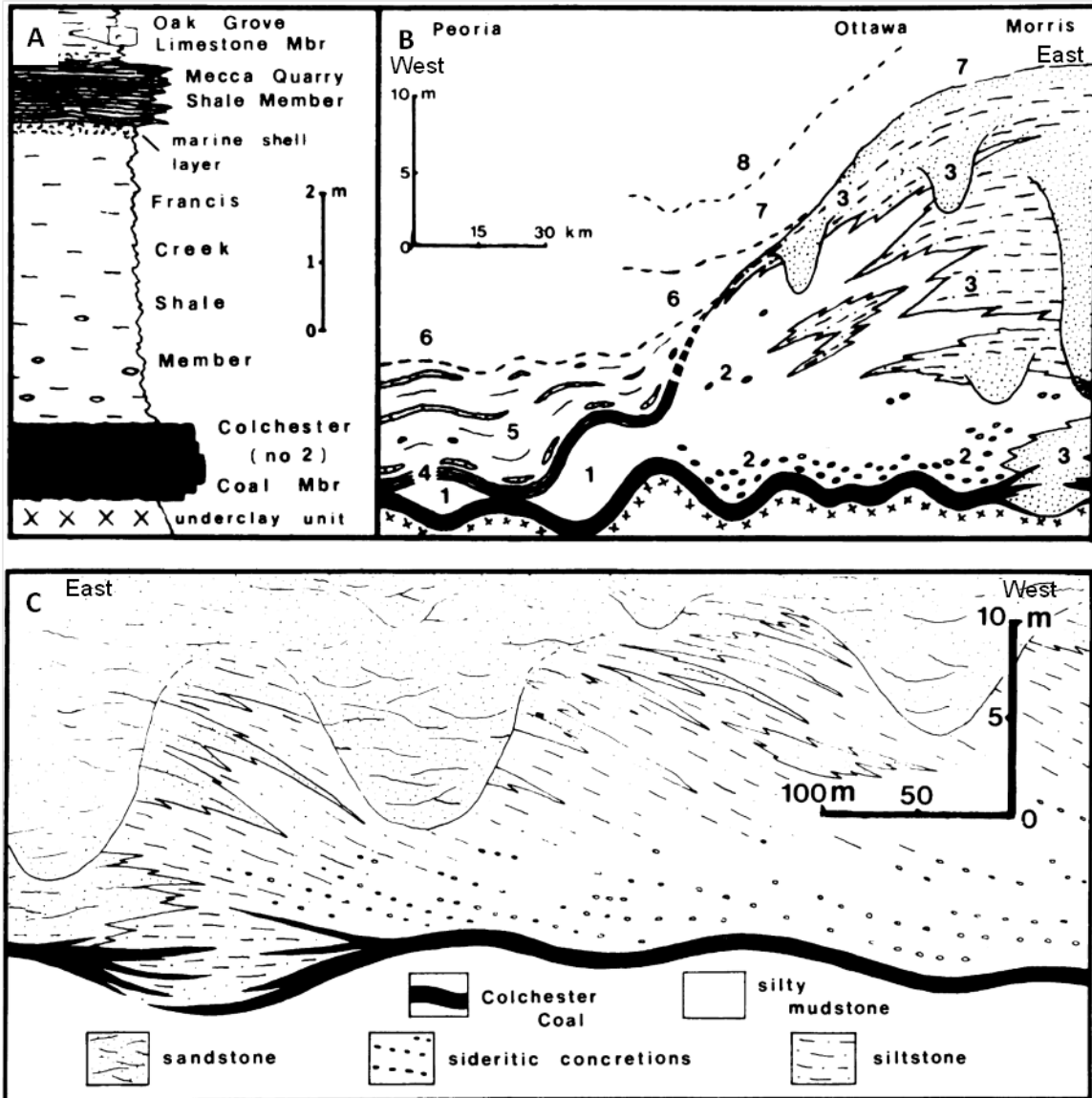


Figure 1.2: Lithofacies in the Francis Creek Shale. A) Schematic vertical stratigraphic sequence of Francis Creek thin facies from Lowell, Illinois. The Colchester Coal Member represents the base of the Carbondale Formation. B) Cross section of Francis Creek deposit showing thickening of facies from West to East. (xxx), Underclay unit beneath Colchester No. 2 Coal Member. 1. Burrowed mudstone. 2. Laminar silty mudstone containing siderite concretions. 3. Siltstone-sandstone layers. 4. Mecca Quarry Shale Member. 5. Marine strata. 6-8. Younger cyclic marine to non-marine strata. C) Cross-section of Mazon Creek silty-mudstone and thin siltstone lithofacies. Inclined strata indicate delta growth and progradation (modified from Baird *et al.*, 1985).

1.3.1 Paleoenvironment

The Francis Creek Shale formed during the mid-Pennsylvanian Westphalian D stage of the middle to upper Carboniferous period, approximately 296 million years (Ma) ago (Darrah, 1970; Baird, 1979; Pfefferkorn, 1979). This coincided with the “Coal Age.” During this time Illinois was located within 10° of the paleoequator, and was mostly covered by an epeiric sea from the southwest (Fig. 1.1C) (Wright, 1965; Scotese *et al.*, 1979; Shabica, 1979; Zeigler *et al.*, 1979). The climate was wet and tropical (Wegener, 1929; Chaloner and Creber, 1973; Phillips and Peppers, 1984). The Mazon Creek area was located in a coastal deltaic-estuarine environment (Fig. 1.1B) along the subsiding northeast structural margin of the Illinois Basin (Shabica, 1970; Baird *et al.*, 1985b). Terrigenous muds and detrital sediments produced by Appalachian tectonism were transported southwest into the Illinois Basin by major fluvial systems (Potter and Pryor, 1961; Shabica, 1971). Deposition of these sediments along the structural margin was controlled by sea-level fluctuations of the epeiric seaway. Factors affecting local sea-level fluctuations during the mid-Pennsylvanian were delta progradation, regional plate bending from the Laurasia-Gondwana collision and eustasy caused by the Gondwana glaciations (Heckel, 1986). This led to the formation of cyclothems deposited over periods of marine transgression and regression (Wanless and Weller, 1932; Wright, 1965). The Carbondale Formation is the lowest portion of the Liverpool Cyclothem (Shabica, 1979). The basal member of the Carbondale Formation is the Colchester (No. 2) Coal, which is irregularly overlain by the Francis Creek Shale, and in areas of marine

transgression, the Mecca Quarry Shale (Fig. 1.2A) (Shabica, 1971; Baird, 1979; Baird *et al.*, 1985).

Marine transgression occurred prior to delta progradation (Baird *et al.*, 1985a). Initial sea-level rise caused a coastal water table rise, creating conditions for deposition of the southwestward sloping Colchester Peat (which would eventually become the Colchester No. 2 Coal Member) (Baird, 1979; Baird *et al.*, 1985a, 1986). Continued transgression gradually inundated the coal swamp and Essex fauna (an assemblage of Mazon Creek fossils consisting of mostly marine organisms) inhabited an estuarine environment above the peat unit (Fig. 1.3) (Baird, 1979; Baird *et al.*, 1985). Subsequent delta-progradation deposited laminated muds over the depressions and swales of the peat layer, creating the irregular contact between the Francis Creek Shale and the Colchester Coal (Fig. 1.2B) (Baird and Shabica, 1980). This is seen in Francis Creek facies as upward coarsening clastic sediment filling distributary channels and subaqueous levee deposits (Baird *et al.*, 1985a). Sediment influx from rivers caused sudden burial episodes, and sediment anoxia promoted rapid fossilisation and preservation of organisms in interdistributary bay and proximal prodelta settings (Fig. 1.3) (Nitecki, 1979; Baird *et al.*, 1986). Mecca Quarry Shale sediments were deposited as the Colchester Peat and low lying delta sediments were inundated due to continued marine transgression (Shabica, 1970, 1971; Baird *et al.*, 1985a; Schellenberg, 2002).

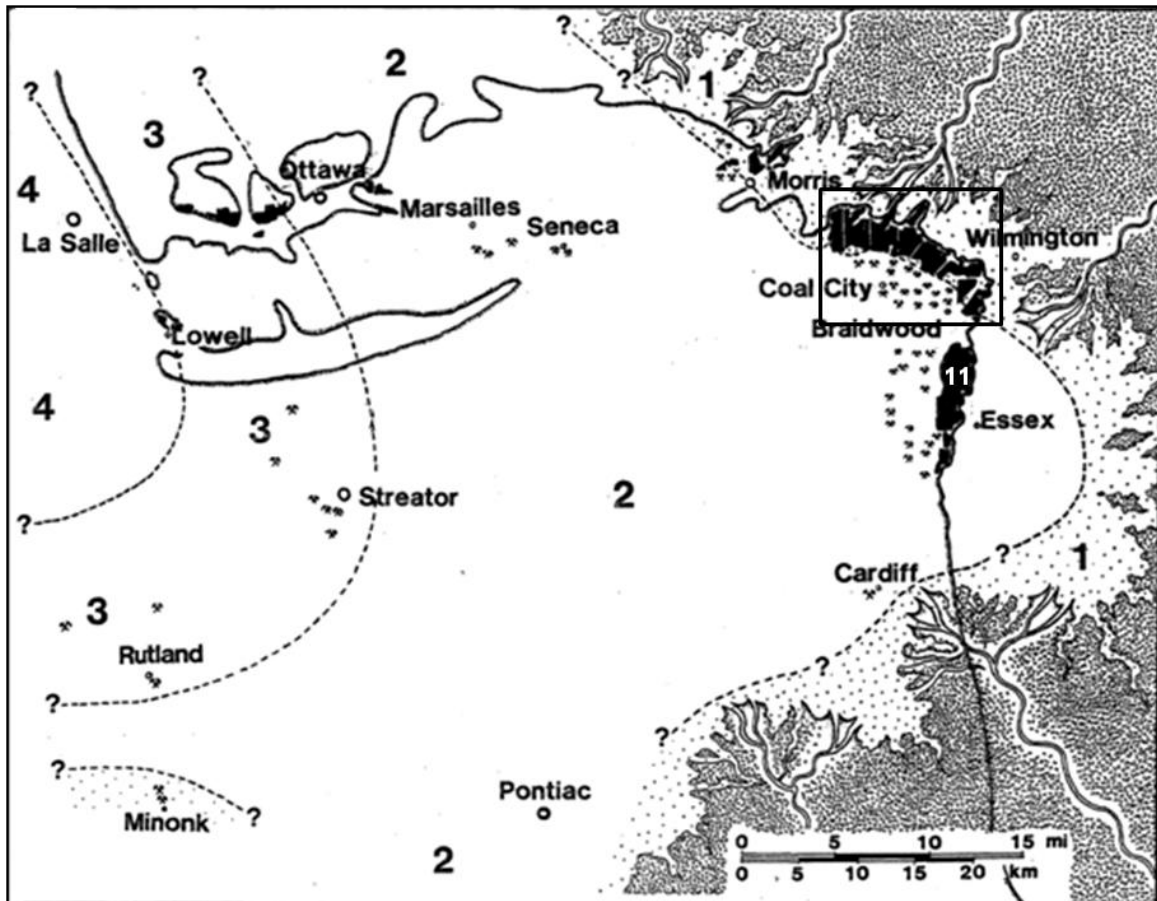


Figure 1.3: Paleogeographic reconstruction of the tidally-dominated Mazonian delta complex showing: Fresh-brackish water Braidwood areas (1); brackish-marginal marine Essex areas (2); marginally Essex areas (3); normal marine areas (4); Pits 1-10 (boxed); and Pit 11 (11) (modified from Shabica and Hay, 1997).

1.3.2 Stratigraphy and sedimentology

The Francis Creek Shale is regionally discontinuous and consists of lenticular wedges of clastic sediment overlying the Colchester (No. 2) Coal Member (Wright, 1965, 1979). These wedges are remnants of deltaic distributary systems. Lenticularity was caused by distributary channel, interdistributary bay and proximal prodelta deposits filling in irregularities caused by marine inundation of the coastal swamp, leading to an abrupt contact between the Colchester Coal and the Francis Creek Shale (Shabica, 1979; Baird and Shabica, 1980).

The coal unit is approximately 1 m thick and laterally widespread (Wright, 1979; Winston, 1986). The Francis Creek Shale ranges in thickness from 4-26 m (Smith, 1970). Kuecher *et al.* (1990) set the maximum thickness at 34 m. It is thickest and has the most stratigraphic variation in the east and thins irregularly towards the west (Fig. 1.2B) (Baird, 1979). Facies coarsen upwards from mudstone to siltstone to sandstone (Baird and Sroka, 1990). In some areas, basally argillaceous laminar mudstones grade upwards into alternating rhythmic silt and clay laminae that were deposited in a low energy environment (Baird *et al.*, 1985a). Several fossiliferous concretions are found within these laminae (Shabica, 1971; Baird, 1979). Above the graded silt-clay lamina, a silty to sandy mudstone interval is often found. Ripple cross-stratification within this interval indicates weak current influence (Baird *et al.*, 1986). In the Mazon Creek area, sparsely occurring fossiliferous siderite concretions are found within this facies. Rippled mudstone grades laterally and upwards into coarser siltstone and sandstone facies which contain climbing ripple sequences, indicative of episodic, torrential sedimentation

(Baird *et al.*, 1985a). Mudstone levels increase as the Francis Creek Shale thins towards the southwest (Baird, 1979). Where it is less than 10-12 m thick, it is overlain by the Mecca Quarry Shale Member (Fig. 1.2B) (Smith, 1970; Baird, 1979). Eventually it thins to disappearance and the Mecca Quarry Shale directly overlies the Colchester Coal (Baird, 1979). The black Mecca Quarry Shale is a half-metre thick unit with laminar bedding, phosphatic nodules and fish fragments (Zangerl and Richardson, 1975). Nodules, unlike concretions, do not require a nucleus to initiate formation.

Thick Francis Creek facies (> 10-12 m) are composed of gray, friable silty to sandy mudstone with irregularly distributed sandstone channels and lenses (Fig. 1.2B) (Baird *et al.*, 1985a). Trough cross-stratification is observed within sandstone channels, and strong currents are indicated by plane-bed stratification and concentrated bedloads of hiatus siderite concretions, underclay masses, palaeozoic pebbles and peat fragments (Baird *et al.*, 1985a). Fossiliferous concretions are usually found in the lower 3-5 m of mudstone within the thick facies (Baird and Sroka, 1990). Fossiliferous concretion bearing strata are often inclined at angles between 10-20° (Fig. 1.2C) (Baird *et al.*, 1985a, 1986). They are found adjacent to sandstone channels and lenses and along distributary margins, and individual beds coarsen up dip, suggesting they were deposited following fluvial transport. They record foreset deposition and crevasse splays during channel migration or progradation (Baird and Shabica, 1980). Deposited sediment intervals have vertical thicknesses of 10-12 m and show climbing ripple drift, local dewatering and slump structures, indicating torrential sedimentation. Several discrete horizons of concretions preserving soft bodied Essex fossils (See section 1.3.3) suggest episodic

flood-induced obrution events (Baird *et al.*, 1985a, 1986). Thinner facies (10-13 m thick) are found near Ottawa, Illinois, and yield poorly preserved fossiliferous concretions (Baird *et al.*, 1985a). This is attributed to slower deposition farther away from the deltaic mouth (Baird, 1979). Thin facies (<5 m thick) yield non-concretionized marine fossils in western Illinois (Smith *et al.*, 1970; Shabica, 1971). These fossils preserve stenotopic organisms in bioturbated sediment containing limestone concretions and pyrite nodules. Soft tissue preservation is rare, indicating a slower sedimentation rate (Shabica, 1971; Baird, 1979).

Where present, the cyclic graded silt-clay lamina appear within 3-7 m of the base of the Francis Creek Shale (Baird *et al.*, 1986). Silt bands show an alternation of thin (0.1-2 mm) and thick (0.5-10 mm) layers separated by clay bands (Kuecher, 1983; Baird *et al.*, 1985b). Clay bands can be grouped into couplets (Fig. 1.4). The variation in thickness of silty clay layers within and between clay band couplets can be used to determine cycles (Kuecher *et al.*, 1990). Alternation of thin and thick silt bands is caused by deposition during individual tidal cycles (Fig. 1.4A). Clay bands are deposited from sediment suspended during tidal slack water periods. Silt bands are deposited from bedload during periods of tidal flow (flood and ebb) (Kuecher, 1983). Thin silt layers are deposited during flood tides, and thick silt layers during ebb tides. This occurs because ebb currents are reinforced by river flow, making them stronger than flood currents. Sequences of silt layers between clay couplets can thicken over several cycles and then thin over several cycles (Fig. 1.4B). Alternation of thinning and thickening groupings of coupled clay band sequences occurs during neap and spring tidal cycles, respectively

(Kuecher, 1983). Silt bands are interpreted to thicken with spring tides, because they have larger tidal ranges and greater water velocities. Consequently, they would thin with neap tides. It is possible that no sediment may have been deposited during the flood phase of some neap tides, resulting in amalgamation of the clay bands in a couplet (Fig. 1.4B) (Kuecher *et al.*, 1990). Tidal rhythmites have been used to estimate sedimentation rates for the Mazonian delta complex. Baird *et al.* (1986) used the thickness of an individual cycle, which they averaged to be 1 mm. Assuming a diurnal tide (Baird *et al.*, 1985b) and sediment water content at or above 70%, they proposed a sedimentation rate of 3-4 mm/day. Kuecher *et al.* (1990) came up with a similar rate using entire thinning or thickening sequences. These represent spring-to-neap or neap-to-spring periods respectively, and would be seven days long if the tide was diurnal. Based on this, they proposed a (compacted) sedimentation rate of 1.0 m/yr during active tidal sedimentation; however, there is evidence that other layers took significantly longer to deposit (Kuecher *et al.*, 1990). In areas with irregular lamination, Kuecher *et al.* (1990) presumed overprinting by other sedimentation controls, such as seasonal fluctuation or channel switching. The tidal rhythmite interpretation for cyclic lamina is controversial. Rhythmites can repeat for intervals of several metres in some areas without scour surfaces, current-wave ripple bedforms or other evidence of reworking typically observed in tidal deposits (Reineck and Singh, 1973; Klein, 1977; Allen, 1981). Another explanation, suggested by Baird *et al.* (1986) is sudden major distributary diversion in the area. In this case lamina would have been produced by rapid deposition in response to increased sediment supply.

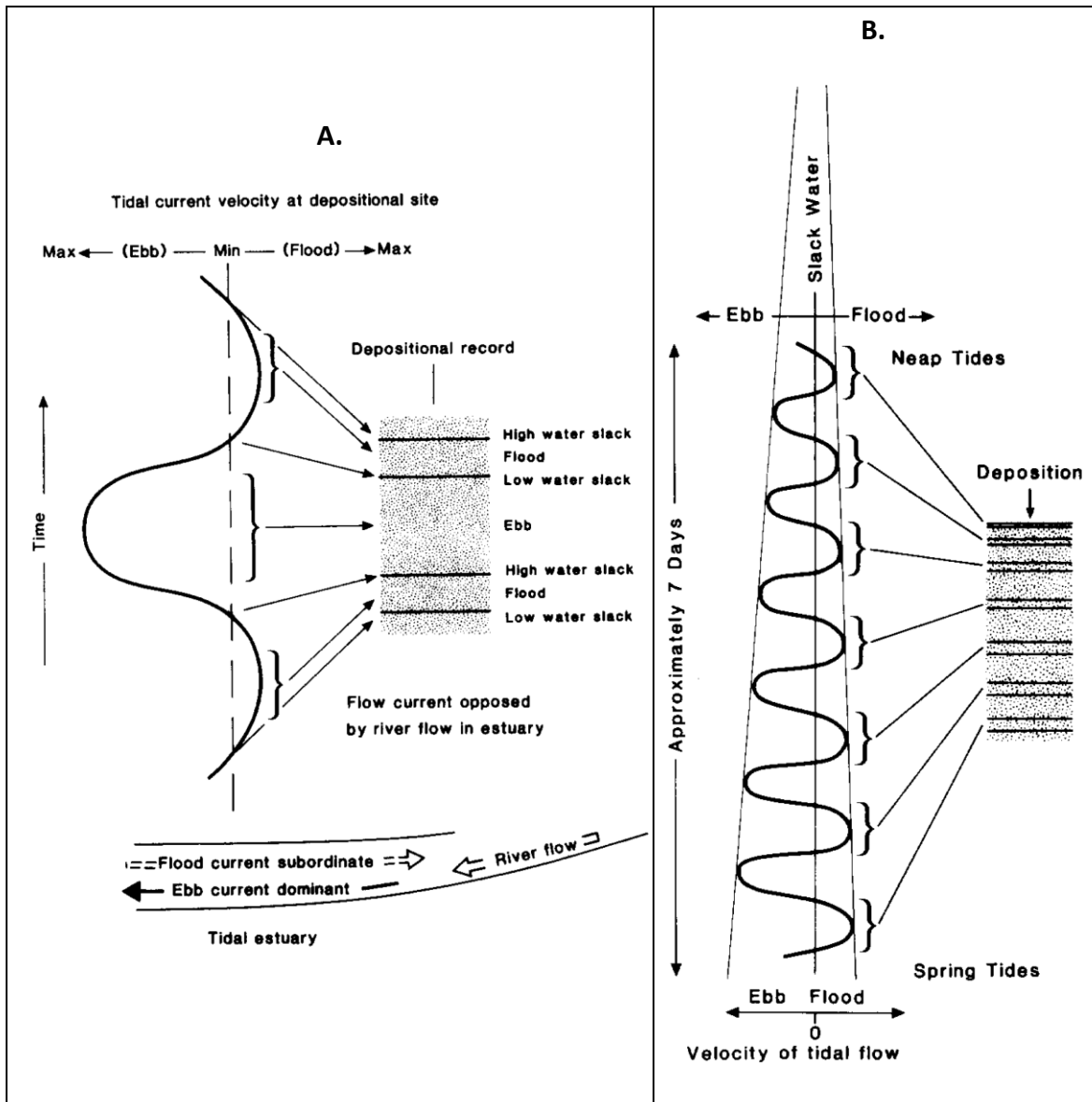


Figure 1.4: Schematic explanation of cyclic silt-clay lamina. A) Alternation in thickness of silty clay lamina within and between paired clay bands is caused by flood and ebb currents in individual tidal cycles. Clay bands are represented by dark lines in the sediment sequence on the right and the stippled regions are silty clay bands. One complete oscillation of the curve on the left represents one complete tidal cycle. B) Thinning or thickening of consecutive silty clay layers is caused by spring-to-neap or neap-to-spring tidal cycles, respectively (Kuecher *et al.*, 1990).

1.3.3 Flora and fauna

Various flora, terrestrial to freshwater fauna and invertebrate marine fauna are represented in Mazon Creek concretions. Some of these are the only known occurrences of ancestral forms, and others, such as *Tullimonstrum gregarium* (Fig. 1.5A), have not yet been classified (Richardson, 1966; Foster, 1979a; Beall, 1991). Uncrushed insects and coprolites have been found (Nitecki, 1979; Baird *et al.*, 1985a). Composite impressions of the jellyfish *Essexella asherae* (Fig. 1.5C) are preserved as “blobs” often located along the median plane of the concretion (Foster, 1979b). This exceptional preservation, accompanied by organism diversity, makes Mazon Creek fossils an important part of paleontological science.

The terrestrial flora and terrestrial and freshwater fauna are collectively referred to as the Braidwood Biota and represent over 200 animal and 250 plant species. The marine fauna are referred to as the Essex biota and are not as well preserved as the Braidwood organisms (Richardson and Johnson, 1971). There is a seaward decline in preservation quality of Braidwood organisms, due to excessive transport. While Braidwood organisms are transported seaward, Essex organisms are not transported landward. Essex fauna are found over a large part of the Mazon Creek area directly overlying the coal unit, suggesting initially marine-estuarine conditions that became less hospitable to stenotopic organisms as delta progradation pushed the biofacies boundary further to the southwest (Baird *et al.*, 1985a). Most well-preserved Braidwood specimens were found in the spoil piles of Pits 1 and 6, and most well-preserved Essex

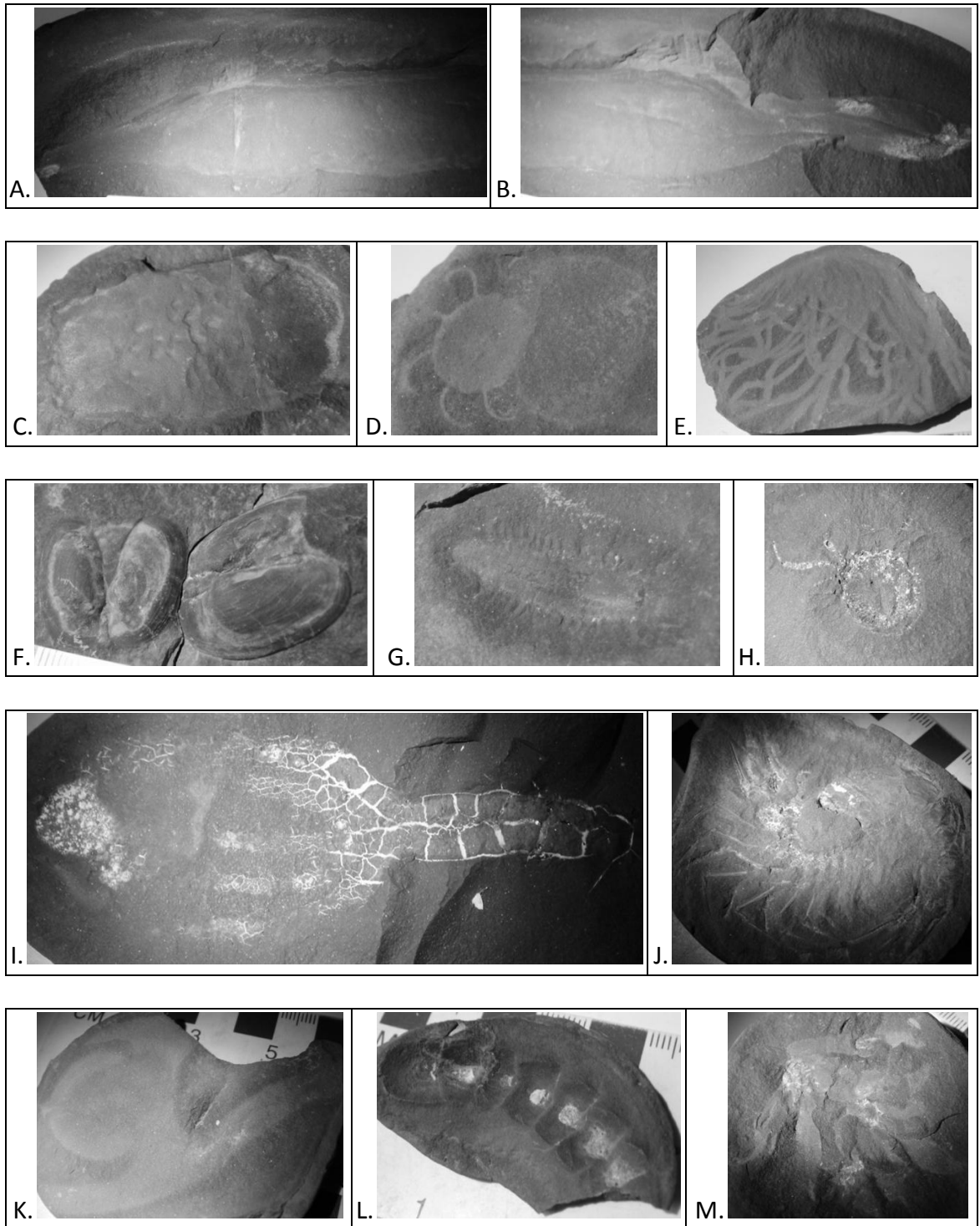


Figure 1.5: The Essex Fauna: A) Anterior of *Tullimonstrum gregarium*. B) Posterior of *Tullimonstrum gregarium*. C) *Essexella asherae*. D) *Octomedusa pieckorum*. E) *Anthracomedusa turnbulli*. F) *Edmondia* sp. G) *Fossundecima konecniorum*. H) *Halicyne max.* I) *Aschistrum* sp. J) *Belotelson magister*. K) *Etacystis communis*. L) *Glaphurochiton concinnus*. M) *Illilepas damrowi*. Pictured specimens are from the invertebrate collection at the Field Museum of Natural History, Chicago, Illinois.

specimens were found in the spoil piles of Pit 13 and Peabody Coal Company Pit 11 (Fig. 1.3) (Baird, 1979).

Plants dominate the Braidwood assemblage, making up 75-90% of specimens (Nitecki, 1979; Baird *et al.*, 1986). The coastal swamp supported an assemblage of ferns (Fig. 1.6A), sphenopsids (Fig. 1.6B), lycopods and other flora that were washed into the Mazon Creek area by distributaries, and are mainly preserved as component organs (*e.g.*, bark, leaves, stems, seeds) (Darrah, 1970; Peppers and Pfefferkorn, 1970). Large, well preserved plant fossils are found at marginal regions of the Francis Creek Shale, next to the limit of the Colchester Coal outcrop. Plant diversity decreases towards the southwest (Baird *et al.*, 1985a). Terrestrial fauna contain mainly insects (Fig. 1.7A,B), arachnids (Fig. 1.7D) (Schram, 1979), and myriapods (Fig. 1.7E,G) (Baird *et al.*, 1985a). Common freshwater fossils are bivalves (*i.e.*, *Permophoris* and *Anthraconaia*) and coprolites (Fig. 1.7C) (Baird and Anderson, 1997). Large coprolites indicate that fresh and brackish water areas supported large nekton, but forms are not present in the fossil record and remain largely a mystery (Baird *et al.*, 1985a). Less frequent freshwater fauna include syncarid shrimps (*e.g.*, *Paleocaris* and *Acanthotelson*), molluscs, lungfish scales, shark teeth, and a possible shark egg capsule (Baird *et al.*, 1985a). Two particularly interesting, less frequent members of the Braidwood fauna were the xiphosuran, *Euproops danae*, a horseshoe crab which may have been partially terrestrial (Fisher, 1979) and the ostracod, *Paraparchites mazonensis*, usually found in brackish water habitats (Sohn, 1977). Rare members of the freshwater fauna were estheriids,

pygocephalomorph shrimp (Fig. 1.7F), insect larvae, fish and amphibians (Fig. 1.7H) (Baird *et al.*, 1985a).

The Essex fauna have varying spatial distribution and consist of diverse marginally marine organisms (Johnson and Richardson, 1966, 1970; Richardson and Johnson, 1971; Schram, 1979). Maximum diversity is found at the southern end of Pit 11, which contains mostly Essex organisms, and gradually decreases to the North, West and South. Essex fauna can be divided into benthic and pelagic subassociations. A region surrounding the upper half of Pit 11 contains mainly benthic invertebrates (Baird *et al.* 1985a). Concretions found in this region show poor preservation, which can be correlated with increased degradation due to scavenging, infaunal feeding and sediment bioturbation (Baird *et al.*, 1986). South of this region, which includes the lower half of Pit 11 and Pit 13, there are mostly pelagic forms (Baird *et al.*, 1985a). These are well preserved and are often found in concretions with interior lamination (Baird *et al.*, 1986). Benthic fossils include the *Edmondia* (Fig. 1.5F) and other marine bivalves, polychaetes (Fig. 1.5G), the echiuroid *Caprinoscolex*, lebensspuren, cycloid crustaceans (Fig. 1.5H), eocarids and holothurians (Fig. 1.5I). Pelagic fauna include shrimp (*e.g.*, *Belotelson* (Fig. 1.5J) and *Kallidecthes*), medusae (*i.e.*, *Essexella* (Fig. 1.5C), *Octomedusa* (Fig. 1.5D) and *Anthracomедusa* (Fig. 1.5E)), and the problematic organisms *Tullimonstrum* and *Etacystis* (Fig. 1.5K). Some benthic fauna are found in regions containing mainly pelagic organisms (*e.g.* *Chitons* (Fig. 1.5L), *Septimyalina* and barnacles (Fig. 1.5M)) (Baird *et al.*, 1985a). The jellyfish, *Essexella*, is ubiquitous and is the most common Essex form (Foster, 1979b).

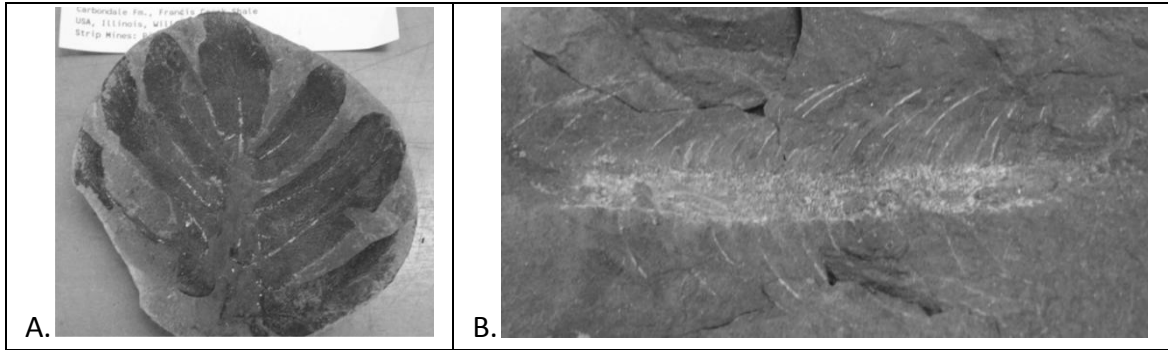


Figure 1.6: Mazon Creek Flora: A) The fern *Neuropteris* with chew damage from an Arthropod Ichnotaxon. B) The sphenopsid *Asterophyllites* sp. Pictured specimens are from the paleobotany collection at the Field Museum of Natural History, Chicago, Illinois.

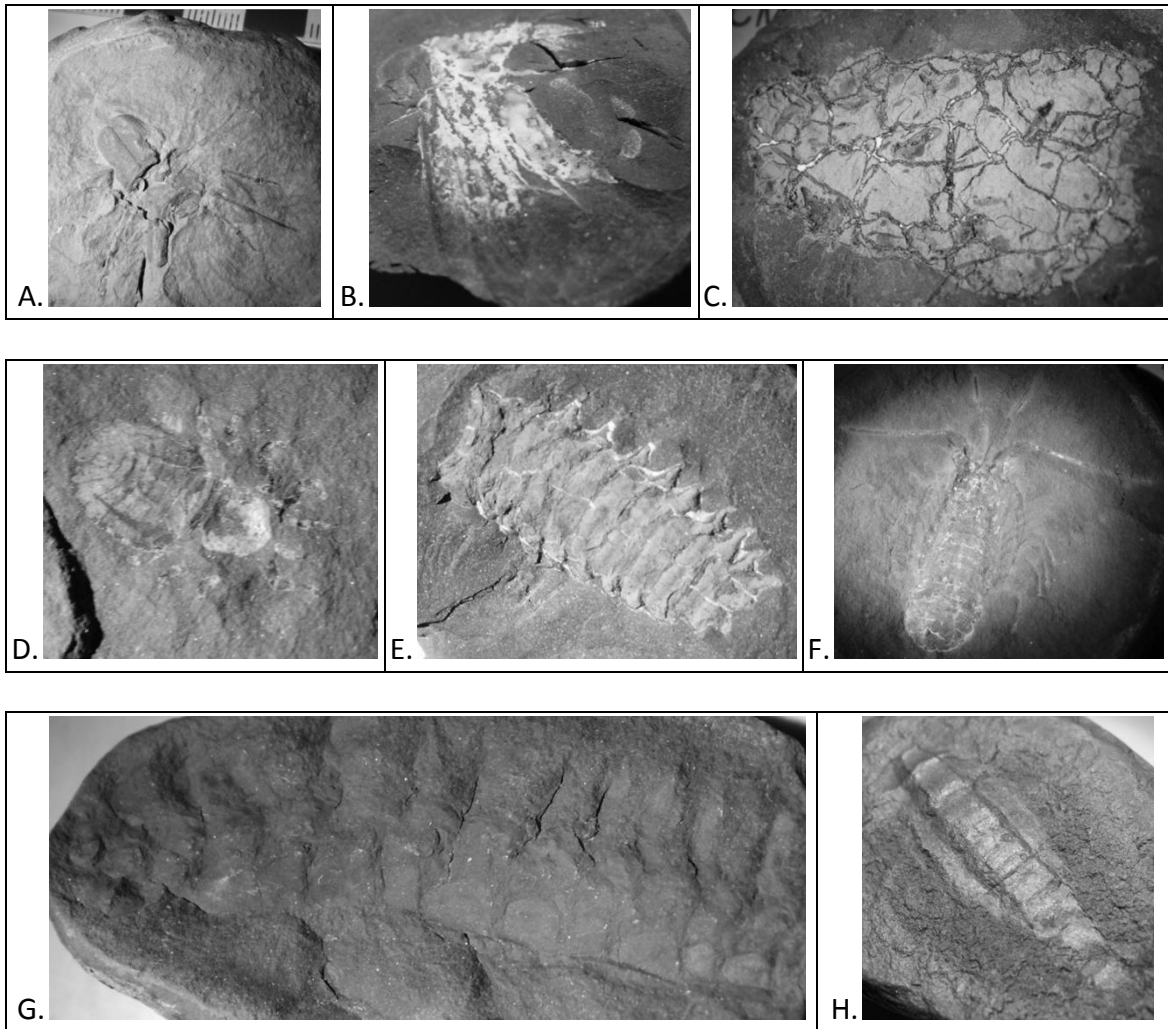


Figure 1.7: The Braidwood Fauna: A) *Curculioides* sp. cast. B) Diaphanopteroidean (cf. Prochoroptera). C) Coprolite. D) Anthracomartid. E) *Aynilyspes* sp. F) Pygocephalomorph (undetermined). G) *Mazoscolopendra richardsoni*. H) *Smithixerxes juliarum*. Pictured specimens are from the invertebrate collection at the Field Museum of Natural History, Chicago, Illinois.

1.4 DIAGENETIC MINERALISATION

1.4.1 Mineralisation

Biomaterials can undergo various transformations after burial. Soft tissue preservation occurs through early authigenic mineralisation mainly by pyrite, calcite, siderite, phosphate or silica (Clarkson, 1998). Replacement minerals vary with environmental geochemistry, and are determined largely by sedimentation rate, oxygen availability, salinity and organic content (Clarkson, 1998). In general, high sediment organic content results in poor preservation, because it is usually accompanied by low background sedimentation rates, low variability between organic matter concentration in sediment and at sites of organism burial, and early carbonate dissolution (Hecht, 1933; Brett and Baird, 1986). Pyritisation requires a combination of moderate background sedimentation and episodic rapid sedimentation, sub- to anoxic conditions, marine to near-marine sulphate concentrations, and low sediment organic content (Curtis, 1980; Hudson, 1982; Berner, 1984; Reaves, 1984; Fisher and Hudson, 1985; Brett *et al.*, 1986; Dick and Brett, 1986). It usually occurs in fine-grained, terrigenous muds, because coarser siliciclastic sediments maintain oxic conditions to depth and are too low in organics to support sulphate reduction, and carbonate sediments do not contain enough iron to allow substantial pyritisation (Berner, 1984). Pyrite fossils are common in black shales, such as at Holzmaden and Arkona (Driscoll *et al.*, 1965; Kauffman, 1977). Carbonate minerals form by rapid burial in sediments with low organic content (Waage, 1964; Berner, 1981a; Brett *et al.*, 1986). Calcite concretions form in marine

environments with bacterial sulphate reduction. Siderite concretions form preferentially in freshwater, where calcium and magnesium concentrations are low. They can form in marine environments if there is an adequate iron supply, and once bacterial sulphate reduction has ceased (Coleman, 1993; Pearson and Nelson, 2005). Dolomite concretions can form in marine environments where iron reduction, methanogenesis and thermal decarboxylation occur simultaneously (Coleman, 1993). Conditions for phosphatisation are created by an interplay between bicarbonate and phosphate concentrations, pH and oxygen availability (Briggs and Kear, 1994). Phosphatisation may be aided by slow sedimentation rates, localised high organic content, particularly if it is phosphate-rich, and low pH (Baturin, 1971; Kennedy and Garrison, 1975; Baird, 1978; Nathan and Sass, 1981; Krajewski, 1984; Briggs and Kear, 1993b). If conditions are alkaline, calcium carbonate will precipitate instead of calcium phosphate (Briggs and Kear, 1993b). It is unclear whether phosphatisation occurs in sub- or anoxic microenvironments (Wetzel, 1975; Baird, 1978; Swirydczuk *et al.*, 1981; Briggs and Kear, 1993b). Formation of calcium phosphate is microbially induced, and can preserve fine anatomical details in soft tissue (Glenn and Arthur, 1988; Martill, 1988; Hirschler *et al.*, 1990; Wilby and Martill, 1992; Briggs and Kear, 1994). Vivianite forms in brackish to freshwater conditions and apatite in marine conditions (Clarkson, 1998). Silicification can occur through passive precipitation on microorganisms in hydrothermal environments or through active biomineralisation processes in some eukaryotes (*e.g.* diatoms, radiolarians) (Konhauser, 2007).

Soft tissues can be preserved by permineralisation, as mineral coats and as tissue

molds (Clarkson, 1998). Permineralisation creates three dimensional replicas of soft tissues by replacing them with minerals. Phosphate is known to do this. Mineral coats forming on soft tissue surfaces can be biologically induced, and can involve pyrite, carbonates, phosphates or silicates (Clarkson, 1998). Tissue casts are formed by stabilisation and eventual lithification of sediments surrounding the organism, such that compaction is limited. Soft tissue fossils are often found within concretions (Clarkson, 1998).

1.4.2 Biomineralisation

Biominerals are produced by organisms in controlled environments and can be organised on a complex organic macromolecular framework, allowing organisms to control their shape, size, chirality, crystallinity and isotopic and trace element compositions (Wilt, 1999; Addadi and Weiner, 2001; Orme *et al.*, 2001; Addadi *et al.*, 2003; De Yoreo and Vekilov, 2003; Weiner and Dove, 2003). An environment with sufficient supersaturation must be created and maintained in order for biomineral nucleation and growth to proceed. Organisms have developed ways of physically isolating biomineralisation sites in order to control their chemistry (Weiner and Dove, 2003). Solutions at biomineralisation sites have high ionic strengths, creating sufficient supersaturation, and stabilizing colloids and amorphous gels by balancing the charges of precursor molecules (Iler, 1979; Perry, 2003). Sclerotised and mineralised skeletal tissues are examples of biominerals (Rucker and Carver, 1969; Lowenstam and Weiner, 1989; Watabe and Kingsley, 1989).

Biom mineralisation processes can be divided into two major groups based on the degree of organism control: 1) biologically induced and 2) biologically controlled (Lowenstam, 1981; Mann 1983). In biologically induced mineralisation, mineral precipitation is secondary to environmental changes mediated by biological activity. Organism metabolic processes and redox conditions determine environmental geochemistry, which indirectly promotes the nucleation of certain minerals (McConnaughey, 1989; Fortin *et al.*, 1997; Tebo *et al.*, 1997; Frankel and Bazylinski, 2003). Anionic groups on cell surfaces can aid in inducing nucleation by adsorbing metals and providing a template for mineral formation or by adsorbing minerals that have precipitated in the extracellular fluid (Marquis *et al.*, 1976; Urrutia *et al.*, 1992; Rancourt *et al.*, 2005). As a result minerals often coat cellular surfaces, and can lead to total encrustation. In biologically controlled mineralisation, organisms use cellular activity to control mineral formation, shape and final location. The final location can be extra-, inter- or intracellular (Weiner and Dove, 2003). Intercellular mineralisation requires clusters of bacterial cells to form diffusion-limited zones, allowing them to control site chemistry through active or passive ion transport processes. In this process, the microbial cell surface acts as the nucleation site and can direct mineral growth (Borowitzka *et al.*, 1974; Borowitzka, 1982), in some cases, leading to total encrustation. Diagenetic mineralisation processes could proceed through biologically induced or biologically controlled intercellular mechanisms.

Biofilms can be a vital component of soft tissue preservation after rapid burial. They prevent erosion of uncompacted watery sediments, serve as a food source during

deep burial or obrution events, protect carcasses against decay by sealing them from the external environment, and change sediment geochemistry to promote the precipitation of authigenic minerals. If no biofilm formed around shallowly buried carcasses, remains would be destroyed by scavenging infauna and aerobic decay. Biofilms can also create the anoxic microenvironment necessary to slow decay long enough for early diagenetic mineralisation of soft body parts (Keupp, 1977; Krumbein, 1983; Martill, 1988; Gall, 1990).

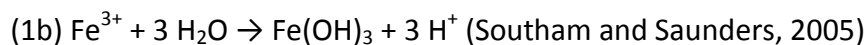
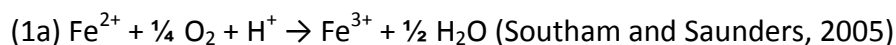
1.5 MICROBIAL METABOLISM

Within the upper centimetres of the sediment column, microbial activity has a major influence on chemistry (Seilacher *et al.*, 1985). Bacteria near the sediment-water interface are usually aerobes or facultative anaerobes, meaning they can survive only in oxygenated or in both oxygenated and non-oxygenated environments respectively (Chapelle, 1993; Ehrlich, 2009). Aerobic and facultative anaerobic bacteria deplete oxygen near the top of the sediment column. Once oxygen is adequately depleted, anaerobes and facultative anaerobes dominate (Southam and Saunders, 2005). Bacteria involved in decay processes are heterotrophic, and use organic compounds as their carbon source. They can couple the oxidation of organic carbon compounds to the reduction of inorganic elements and/or compounds (*e.g.*, oxygen, metal ions, minerals). Chemolithotrophic bacteria produce energy by coupling the oxidation of inorganic compounds to the reduction of organic or inorganic species (Madigan *et al.*, 2012).

Redox zonation occurs with depth in the sediment column, as redox potential decreases (Southam and Saunders, 2005). To produce energy, the redox reactions catalyzed by bacteria must have a negative ΔG_0 (Madigan *et al.*, 2012). Redox pairs between chemical species with a larger electropotential difference can be used to generate more energy (because they have a more negative ΔG_0), giving organisms that use them an advantage over those that use less efficient redox couples; therefore, microbes with less efficient metabolic mechanisms are usually found deeper in the sediment column, at a level where more efficient terminal electron acceptors have been exhausted (Fig. 1.8) (Berner, 1981a; Chapelle, 1993; Lovley and Chapelle, 1995; Southam and Saunders, 2005).

1.5.1 Iron oxidising bacteria

Biotic and abiotic oxidation of ferrous iron (Equation 1a) and subsequent hydrolysis by ferric iron produces iron hydroxide minerals (Equation 1b), which can precipitate on cell surfaces (Beveridge and Fyfe, 1985; Corstjens *et al.*, 1992; Emerson and Revsbech, 1994):



In aerobic conditions, at neutral pH, Fe^{2+} is oxidised to Fe^{3+} abiotically within minutes (Stumm and Morgan, 1996). To compete with this rate of oxidation, aerobic,

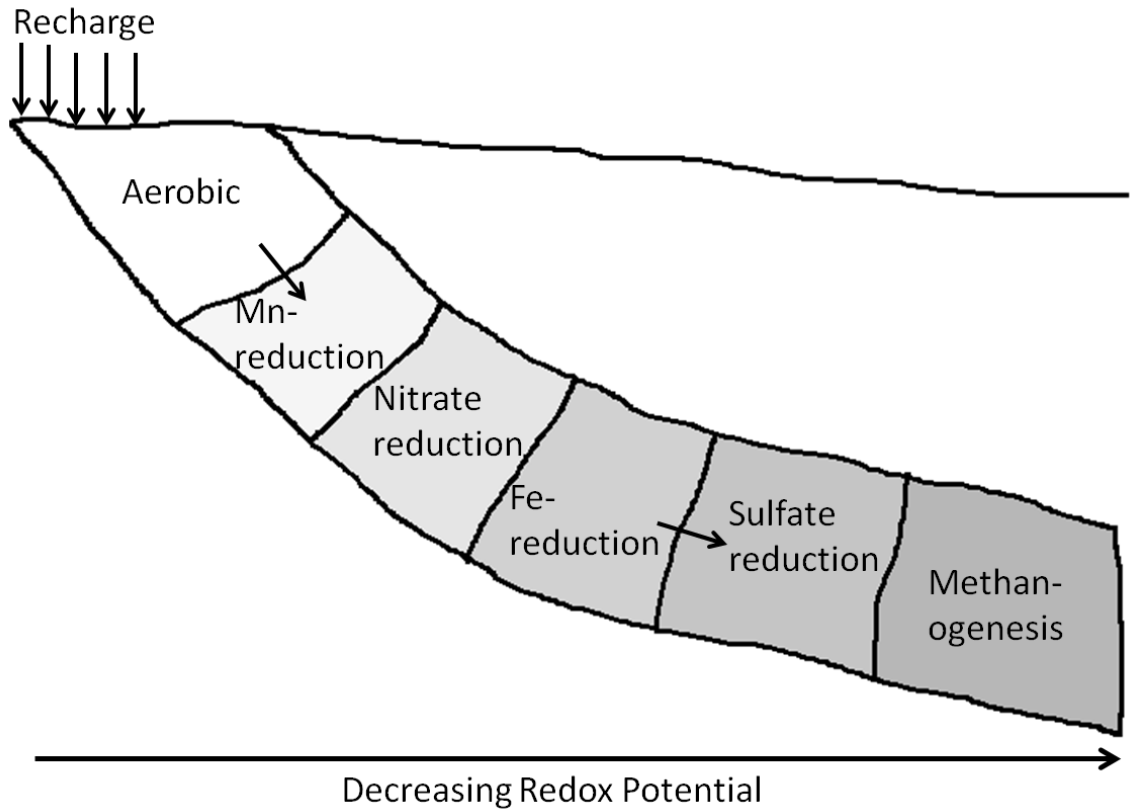
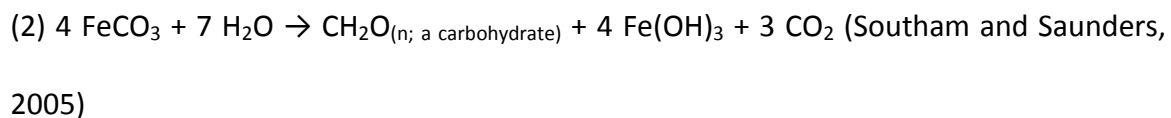


Figure 1.8: Geochemical zones created by microbial redox succession with increasing depth (*i.e.*, decreasing redox potential) below the sediment-water interface. In stagnant environments where bottom water is anoxic, the aerobic zone will not be present; as well, there can be some overlap between zones (modified from Southam and Saunders, 2005).

neutrophilic iron oxidisers often inhabit suboxic niches where abiotic Fe^{2+} oxidation rates are slower (Emerson, 2000). When conditions become acidic, abiotic oxidation of Fe^{2+} slows considerably, and it is available to be oxidised by acidophiles. At pH levels above 2, the Fe^{3+} precipitates to form iron oxides (Kappler and Straub, 2005). Two groups of anaerobic iron-oxidizing bacteria have also been found. One group are phototrophs (Widdel *et al.*, 1993; Kappler and Newman, 2004) and the other are nitrate-reducers (Hafenbradl *et al.*, 1996; Straub *et al.*, 1996). Phototrophs use light energy to transfer electrons from Fe^{2+} to carbon (Equation 2):



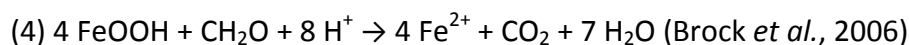
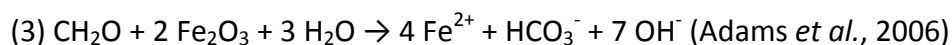
Nitrate-reducers couple oxidation of Fe^{2+} to dissimilatory reduction of nitrate, nitrite, nitric oxide or nitrous oxide, although it is not yet clear whether this provides the energy necessary for cellular metabolism (Straub *et al.*, 1996; Benz *et al.*, 1998; Straub *et al.*, 2004). In acidic and anoxic environments, biotic iron oxidation is the main mechanism converting Fe^{2+} to Fe^{3+} .

Oxidation of iron minerals is faster when minerals are less crystalline and more surface area is available, exposing more active sites for catalysis of transformation reactions (Roden, 2003). This has implications for dissolution kinetics, transformation reactions and adsorption of organic and inorganic compounds (Cornell and Schwertmann, 2003). Exposed hydroxyl functional groups on amorphous iron

oxyhydroxides, that can precipitate on the cell surfaces of iron-oxidizing bacteria, have a high affinity for Fe^{2+} ions. They increase the rate of adsorbed Fe^{2+} oxidation by acting as electron-donor ligands, stabilizing positive charge (Wehrli *et al.*, 1989; Elsner *et al.*, 2004). Stripped electrons are then conducted to the cell surface by the iron oxide (Williams and Scherer, 2004).

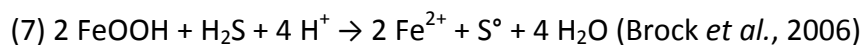
1.5.2 Iron reducing bacteria

In the Fe-Mn reduction zone, under moderately reducing conditions, Fe-reducing bacteria couple the oxidation of organic or inorganic matter to reduction and dissolution of amorphous Fe-oxyhydroxides (Lovley and Phillips, 1988). The bacteria strip electrons from reductants, such as organic matter, and transfer them to Fe^{3+} , reducing it to Fe^{2+} , which goes into solution (Equations 3, 4) (Saunders *et al.*, 1997). Aqueous Fe^{2+} can be used in the formation of biogenic iron minerals (*e.g.*, iron sulphides (Equation 5), siderite (Equation 6), magnetite) (Bubela and McDonald, 1969; Pedersen and Ekendahl, 1990; Saunders and Swann, 1992; Coleman *et al.*, 1993; Saunders *et al.*, 2005):



Iron reducers can be acidophiles or neutrophiles (Johnson and McGinness, 1991; Lovley *et al.*, 2004). Acidophilic iron reducers show the highest reduction rates with dissolved Fe^{3+} as the oxidant. Both acidophiles and neutrophiles prefer to reduce amorphous over crystalline iron oxides (Bridge and Johnson, 2000; Hernandez and Newman, 2001). At least half of the nonsiliceous Fe^{3+} in freshwater and estuarine sediments is considered to be in an amorphous form (Lovley and Phillips, 1986). Iron reducers have developed three main mechanisms for transferring electrons from the cell to iron minerals (Hernandez and Newman, 2001; Lovley *et al.*, 2004): 1) Physical contact between the cell and mineral surface (*e.g.*, through wires or cell surface groups), 2) Release of iron chelators (*e.g.*, siderophores and organic acids) that solubilise Fe^{3+} and 3) Use of extracellular electron shuttles (*e.g.*, phenols and humic substances).

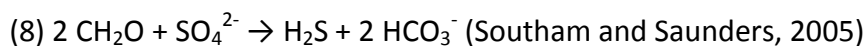
Fe^{2+} can be re-oxidised by iron oxidizing bacteria or oxygen, and precipitate as iron oxyhydroxides in the aerobic zone (Southam and Saunders, 2005). Ferrous ions that are transported from the Fe-Mn reduction zone to the sulphate reduction zone can form iron sulphides (Bubela and McDonald, 1969). Ferric oxides can also be reduced abiotically by hydrogen sulphide, a by-product of sulphate-reduction (Equation 7) (Thamdrup, 2000; Cornell and Schwertmann, 2003):



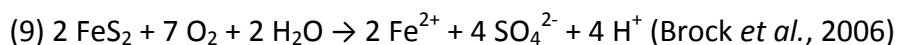
1.5.3 Sulphate reducing bacteria

Sulphate reducing bacteria prefer sub- to anoxic, organic-rich environments.

They couple the oxidation of labile organic matter to the reduction of sulphate, producing hydrogen sulphide and bicarbonate as metabolites (Equation 8) (Skyring, 1988; Donald and Southam, 1999):

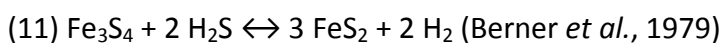
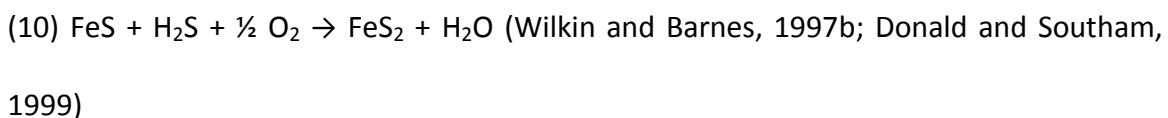


The hydrogen sulphide produced by sulphate reducing bacteria and the interaction between Fe^{2+} and anionic groups on the cell surface can accelerate the precipitation of iron monosulphides (Equation 5) (Tuttle *et al.*, 1969; Lichtner and Biino, 1992; Fortin *et al.*, 1994; Southam *et al.*, 2001). In addition to microbially mediated iron reduction, aqueous Fe^{2+} can be generated by: reaction of hydrogen sulphide with detrital sedimentary iron oxides (Equation 7) (Brock *et al.*, 2006), dissimilatory iron reducing bacteria (Equations 3, 4) (Sørensen, 1982; Lovley and Phillips, 1986), partial oxidation of iron sulphides (Equation 9) (Aller, 1980; Giblin and Howarth, 1984), mackinawite dissolution in acid (Rickard, 2006) and dissociation of aqueous iron sulphide clusters (Druschel *et al.*, 2008).



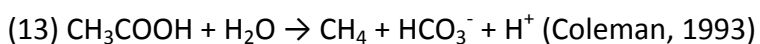
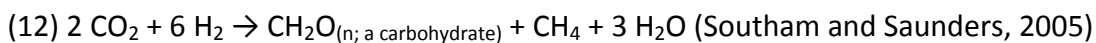
To form pyrite at low temperatures ($\sim 20^\circ\text{C}$), iron monosulphides, such as mackinawite, amorphous FeS and greigite, must overcome a kinetic barrier (Berner, 1970; Rickard, 1997; Southam and Saunders, 2005). This can be done by going through a series of more

soluble intermediates or by partial oxidation with hydrogen sulphide in sub- (Equation 10) to anoxic environments (Equation 11) (Wilkin and Barnes, 1997a; Rickard, 1997):



1.5.4 Methanogens

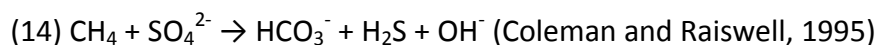
Methanogens produce methane by reducing CO_2 with H_2 , thereby incorporating inorganic carbon back into the organic carbon pool (Equation 12) (Southam and Saunders, 2005; Falkowski *et al.*, 2008):



Methanogens can be heterotrophic, utilizing formate, acetate, methanol or methylamine instead of hydrogen and generating bicarbonate as a by-product (Equation 13) (Balch *et al.*, 1979; Madigan *et al.*, 2012). Methane can diffuse out of the methanogenic zone and act as an organic carbon source for heterotrophic metabolism (Southam and Saunders, 2005).

Methanogens and anaerobic methane oxidisers are closely related members of the Archaea, and use some of the same cellular machinery functioning in reverse, in

their respective pathways (Hallam *et al.*, 2004). If hydrogen tension is sufficiently low, the methanogenesis reaction becomes unfavourable, and anaerobic methane oxidisers take over. This can occur in associations with Sulphate Reducing Bacteria (SRB), which consume H₂ in the production of H₂S (Orphan *et al.*, 2001; Schink, 2002). Anaerobic methane oxidisers can also produce bicarbonate and H₂S, by coupling methane oxidation to sulphate reduction (Equation 14) (Devol and Ahmed, 1981; Reeburgh, 1983):



1.6 MAZON CREEK TYPE FOSSIL DIAGENESIS

1.6.1 Concretions

Concretions can form before, during or after sediment compaction and lithification, or over all three stages, and can be found in shale, mudstone, claystone, siltstone or sandstone strata (Allison and Pye, 1994; Middleton and Nelson, 1996; Hendry *et al.*, 2006). They have been found in modern marsh sediments and sand flats (Allison and Pye, 1994). Concretions can be cemented by a variety of minerals, including: siderite, calcite, dolomite, phosphorite, pyrite and silica (Bromley *et al.*, 1975; Murray and Renard, 1981; Pye, 1984; Coleman, 1993; Coleman and Raiswell, 1995). Sideritic concretions can form in freshwater to marine environments and calcitic or dolomitic concretions form in marine environments (Mozley, 1989; Middleton and Nelson, 1996).

Mn can be incorporated into calcite nodules when they are precipitated in anoxic environments (Pedersen and Price, 1982). Carbonate concretions generally form through passive precipitation of mineral cements in sediment pore spaces, allowing cement volume to be used as an estimate of sediment porosity (Raiswell, 1971; Gautier, 1982). Phosphorite nodules are cemented by apatite and have been found in diatomaceous, organic-rich marine sediments (Burnett, 1977; Birch, 1979). Fluctuations in reduction potential may play a role in their precipitation, as they have been interpreted to form at the oxic-anoxic transition zone (Ogihara, 1999). Though lower pH increases apatite stability relative to calcite (Briggs and Kear, 1993b), Ogihara (1999) suggested that phosphatic nodules were preferentially precipitated in alkaline conditions. Pyritic and siliceous concretions have also been found (Bromley *et al.*, 1975; Borkow and Babcock, 2003). Pyritiferous concretions are often found in marine sediments, and their mechanisms of formation involve microbial sulphate reduction (Driscoll *et al.*, 1965; Raiswell, 1976; Kauffman, 1977; Pye *et al.*, 1990). Concretions form in localised microenvironments, sometimes created by organism decay (Woodland and Stenstrom, 1979; Baird *et al.*, 1986).

There has been a lot of research into the taphonomy of organisms represented in the Mazon Creek biota; however, concretion diagenesis and initial fossilisation processes remain largely a mystery. Mazon Creek fossils are preserved mainly as pyritised molds or impressions at the centre of siderite-cemented mudstone concretions (Schopf, 1979; Baird, 1979, 1997; Woodland and Stenstrom, 1979). Plant parts are locally preserved as three-dimensional molds within concretions or as coalified compression flora within

surrounding mudstone (Schopf, 1979). Three dimensional hard tissues, such as stems, seeds and shells, are mainly preserved as molds (Baird *et al.*, 1986). Molds can contain void precipitates (*i.e.*, calcite, sphalerite, kaolinite, millerite and galena) or remain unfilled, and, in plants, may overlie or mix with coalified residue (Schopf, 1979; Baird *et al.*, 1986; Baird and Sroka, 1990). They preserve the interior or exterior shape and negative surface details of the original organism. Soft bodied marine organisms (*e.g.*, jellyfish, *Tullimonstrum gregarium*) are usually preserved as flattened composite impressions within siderite concretions. Soft tissue impressions can show internal and external anatomical detail (Foster, 1979a,b). In composite impressions of *Essexella asherae* (*i.e.*, “the blob”), the surface can be covered in a thin film of microcrystalline pyrite (Baird *et al.*, 1986). Coatings of sphalerite or kaolinite also occur, but they mask detail. Some *Essexella* fossils show convex down relief. This may be due to underlying sediment displacement on initial organism burial and subsequent infilling of decay voids by overlying sediment. Under- and overlying sediment surfaces are separated by a thin pyrite film, which is all that remains of the organism. The non-mineralised exoskeletons of some organisms, such as polychaetes, can be preserved as organic surficial films (Baird *et al.*, 1986). Borkow and Babcock (2003) suggest that non-mineralised tissues are usually preserved as thin pyrite crusts, whereas skeletal remains are usually preserved in pyrite concretions.

In order to preserve such delicate structures as yolk sacs, colour markings, and jellyfish impressions, sedimentation must have been rapid and concretions must have formed early during diagenesis (Nitecki, 1979). Five main concretion or nodule types

have been identified within the Francis Creek Shale: 1) siderite, 2) siderite with one or more pyrite halos, 3) a mix of siderite and pyrite throughout, 4) siderite with a pyrite centre and 5) pyritic nodules (Baird, 1979; Woodland and Stenstrom, 1979; Allison and Pye, 1994).

Concretion formation begins near the sediment water interface, but can continue to great depths. This is indicated by decreases in the volume of pore filling precipitates outwards from the concretion centre, due to increased sediment compaction (Woodland and Stenstrom, 1979). Modern siderite concretions have been found 1 m below the surface of marsh sediments in Norfolk, England; therefore, concretion formation must have begun <1 m below the surface (Pye, 1984). Concretion precipitation can continue to several hundred metres below the surface (Hendry *et al.*, 2006). Over time, sediment accumulation and compaction cause dewatering of underlying sediments, reducing permeability and creating an upward flow of pore waters due to loading (Woodland and Stenstrom, 1979; Baird *et al.*, 1986). The time required for concretion formation can vary greatly, depending on the sedimentary environment, but most growth is completed over a 100-300 ka period (Middleton and Nelson, 1996).

At Mazon Creek, pyrite usually occurs as halos around fossil nuclei within concretions, and locally occurs as crystalline overgrowths around concretions, fine-grained pyrite throughout concretions or precipitates in septarian fractures (Baird *et al.*, 1986). Most of the pyrite predates siderite, but void filling pyrite and calcite postdate it. Later pyrite may represent a period of seawater influx and subsequent sulphate

reduction after initial onset of siderite formation (Woodland and Stenstrom, 1979). Pyrite halos may have precipitated concurrently with siderite, at a stage when both phases were stable (Woodland and Stenstrom, 1979; Baird *et al.*, 1986).

1.6.2 Pyrite

Iron, sulphur and organic carbon are important in early diagenesis of marine sediments (Froelich *et al.*, 1979; Berner, 1985; Canfield and Raiswell, 1991). Sedimentary iron sulphide formation, and consequent conversion to pyrite, is limited by available organic matter, reactive iron and sulphate concentrations, redox state in sediments and overlying water, sedimentation rate, and the type and availability of oxidant present in the system (Berner, 1970; Berner, 1984; Hurtgen *et al.*, 1999; Neumann *et al.*, 2005). Among these, decay of organic matter is the main control of Eh and pH in sedimentary environments (Allison, 1988b). Initial aerobic decay scavenges oxygen in the upper centimetres of the sediment column. Once oxygen is depleted, iron and sulphate reduction can proceed (Berner, 1981a; Southam and Saunders, 2005). Ferric iron can be reduced to ferrous iron in the same region as bacterial sulphate reduction reduces sulphate to sulphide, or iron and sulphate reduction can occur in different zones and the products can diffuse into the same area (Bubela and McDonald, 1969; Coleman and Raiswell, 1995). Where they meet, Fe(II) and sulphide react to form iron monosulphides (Coleman and Raiswell, 1995). The reaction is slightly different when iron and sulphate reduction occur in the same region (Equation 14) and when the products have to diffuse (Equation 15):

(14) $9 \text{CH}_2\text{O} + 4 \text{SO}_4^{2-} + 4 \text{FeOOH} \rightarrow 9 \text{HCO}_3^- + 4 \text{FeS} + 6 \text{H}_2\text{O} + \text{H}^+$ (Coleman and Raiswell, 1995)

(15) $2 \text{CH}_2\text{O} + \text{SO}_4^{2-} + \text{Fe}^{2+} \rightarrow \text{FeS} + 2 \text{HCO}_3^- + 2 \text{H}^+$ (Coleman and Raiswell, 1995)

Hydrogen sulphide produced by bacterial sulphate reduction can also react with detrital iron to form iron monosulphides (Brock *et al.*, 2006). The iron monosulphides undergo a series of reactions, eventually producing pyrite (Berner, 1971). Sedimentation rate affects use of organic matter by marine SRB. Higher sedimentation rates promote anoxia by inhibiting oxygen diffusion from overlying water and preventing bioturbation (Allison and Briggs, 1993). It also allows more reactive organic matter to reach the sulphate reduction zone without significant aerobic decay, increasing sulphate reduction rates (Berner, 1978; Berner, 1984; Canfield, 1989; Hurtgen *et al.*, 1999). Mineralisation of organic carbon is most likely to occur in the zone of intense sulphate reduction (Hurtgen *et al.*, 1999). Rapid, deltaic sedimentation is not usually conducive to pyritisation, because it dilutes organic matter content and removes organisms from the upper sulphate reduction zone too quickly for significant pyrite formation (Curtis, 1980; Gautier, 1982; Pye, 1984). Layers of pyritic fossils can form if organic matter is rapidly introduced into an area otherwise characterised by moderate background deposition rate and organic-poor sediment (Reaves, 1984; Brett *et al.*, 1986). The sedimentation rate at Mazon Creek may have been as high as 3-4 mm per day during active tidal cycles (Baird *et al.*, 1986). The concentration of sulphate in Mazon Creek sediments would have

been lower than in marine conditions because of significant deltaic input (Woodland and Atenstrom, 1979). Fresh and brackish water sediments do not contain enough sulphate to completely convert acid-volatile iron monosulphides to pyrite (Berner *et al.*, 1979). Consequently, sulphate was rapidly depleted in estuarine Mazon Creek sediments and minimal pyritisation occurred (Berner *et al.*, 1979; Berner, 1981; Pye *et al.*, 1990; Allison and Pye, 1994).

Pyrite surrounding fossils suggests that sulphide is a product of bacterial decay, and that chemical microenvironments created around carcasses favoured pyrite and siderite precipitation (Woodland and Stenstrom, 1979; Baird *et al.*, 1986). Early diagenetic pyrite was a product of bacterial reduction of seawater sulphate (Woodland and Stenstrom, 1979). Pyritisation of organisms is controlled by: sediment anoxia, ratio of sulphide to reactive iron in pore waters and the presence of biofilms around carcasses (Schieber, 2002; Borkow and Babcock, 2003). Pyrite forms within a pH 6-9 range in marine conditions and a pH 5.5-8 range in the lab. Early diagenetic pyritisation occurs in anoxic, nonsulphidic sediments underlying sub- to anoxic waters (Raiswell, 1976; Hudson, 1982; Reaves, 1984; Dick and Brett, 1986). Minimal bioturbation in restricted oxygen environments may aid in diffusion of seawater sulphate into sediment, while maintaining conditions reducing enough for sulphide formation; however, at depths below half a metre, bioturbation can introduce enough oxygen to oxidise monosulphides and cause complete aerobic decay (Goldhaber and Kaplan, 1980; Hudson, 1982). Availability of metabolizable organic matter concentrates pyritisation around nuclei of organism decay (Reaves, 1984; Brett *et al.*, 1986). Sulphate reduction creates a

decomposition microenvironment around the buried organism with outwardly decreasing sulphide concentration gradients. These concentration gradients may help transport Fe(II) to the nucleus of sulphate reduction. The concentration of Fe²⁺ in porewaters determines how far sulphide will diffuse from a decaying carcass before it precipitates as FeS (Canfield and Raiswell, 1991). Biofilms can be in direct contact with organism surfaces or suspended in extracellular polysaccharide substances (EPS) around them. The type of biofilm present determines, in part, the extent of pyritisation, and the formation of pyrite crusts or halos. Bacteria dominated biofilms usually result in crusts, whereas microbial consortia result in halos or nodules (Borkow and Babcock, 2003).

Concretions usually undergo only partial lithification in the sulphate reduction zone (Raiswell and Fisher, 2004; Hendry *et al.*, 2006). Sulphate reduction can be more damaging to carcasses than methanogenic decay (Allison, 1988a,b). This is supported by the observation that, with increasing pyrite content, fossil quality declines, and fully pyritic nodules are non-fossiliferous (Baird, 1979). Once interstitial sulphate has been depleted, methanogenesis reactions take place and siderite precipitation begins (Woodland and Stenstrom, 1979; Berner, 1981).

1.6.3 Siderite

Siderite precipitation must have commenced soon after organism burial in order to preserve soft body detail (Richardson and Johnson, 1971; Shabica, 1971; Woodland and Stenstrom, 1979). Siderite formation requires rapid deposition, organics, low sulphide concentration, reducing conditions, pH between 6 and 8 and higher Fe²⁺

concentrations than are present in seawater (Woodland and Stenstrom, 1979). Modern siderite concretions are found in freshwater to brackish water environments, where there is more iron than calcium (Curtis and Spears, 1968; Pye *et al.*, 1990). In marine settings, pyrite and calcium carbonate are more prevalent than siderite because of higher sulphate and calcium concentrations (Curtis and Spears, 1968; Woodland and Stenstrom, 1979). Thermodynamics and solubility studies indicate that Fe^{2+} preferentially reacts with sulphide whenever it is present (Berner, 1969; Coleman, 1993). In deltaic estuarine environments, river water dilutes sulphate concentrations and supplies enough iron to promote siderite stability (Woodland and Stenstrom, 1979). Siderite formed in low sulphate environments postdates pyrite formation (Adams *et al.*, 2006). When sulphate concentrations are low, for example in areas where reactive organic matter reaches the zone of methanogenesis, Fe^{3+} reduction results in siderite formation (Berner, 1981; Pye, 1984). It is possible for methanogenesis and sulphate reduction to occur simultaneously (Oremland *et al.*, 1982); however, the methane does not accumulate until most of the sulphate has been reduced, because sulphate reducing bacteria can oxidise methane for energy (Martens and Berner, 1974). Siderite can form at shallow depths when pore water sulphate is rapidly reduced in environments with high organic content, high rate of bacterial activity and high sedimentation rate (Pye, 1984). Insulation from seawater sulphate is not always necessary for siderite formation, as it has a small stability field in marine sediments (Maynard, 1983). It can predate pyrite formation despite high sulphate concentrations if reactive organic matter is low or if Fe^{3+} reduction rates exceed sulphate reduction rates (Froelich *et al.*, 1979; Chapelle and

Lovley, 1992; Curtis, 1995). In these environments, iron reducing bacteria can outcompete sulphate reducers for metabolisation of organics, because Fe^{3+} reduction produces more energy than sulphate reduction (Coleman, 1985). Organics are considered recalcitrant when 1) labile organic matter has already been metabolised or 2) they contain mainly proteins and complex carbohydrates (Adams *et al.*, 2006). Early diagenetic siderites from marine environments have higher calcium and magnesium substitution in their outer zones (Mozley, 1989).

Bacterial decay breaks down proteins, increasing ammonia and bicarbonate around carcasses (Woodland and Stenstrom, 1979). Bicarbonate concentrations can be increased by Fe-reduction, and by concomitant sulphate and Fe-reduction (Canfield and Raiswell, 1991; Coleman *et al.*, 1993). Increased bicarbonate and pH, combined with iron from interstitial muds or adjacent swamps and CO_2 from adjacent swamps or underlying peat, promoted formation of siderite concretions around Mazon Creek organisms. The hypothesis that decaying organic matter acted as nuclei for concretion formation is complicated by the fact that there are concretions and sideritic plates and masses that do not contain fossil nuclei (Woodland and Stenstrom, 1979). However, in instances where concretions formed around organisms, their shape is influenced by the shape of the carcass. "Juicy" nuclei, such as coprolites, are often surrounded by larger concretions, but evidence for smaller fossils acting as chemical catalysts is lacking (Baird *et al.*, 1986). It is possible that some of the apparently non-fossiliferous concretions contain pyrite centres, very small fossils, irregular trace fossils, or poorly preserved trace organic material (Woodland and Stenstrom, 1979).

Sources of iron in the Mazon Creek delta may have included acidic pore waters from nearby swamps, water flowing upward from compacted underlying peats and detrital minerals in fluvial sediments (Woodland and Stenstrom, 1979). In swamps and peat, plant decay lowers the oxygen concentration and pH of the water, which increases Fe^{2+} concentrations (Woodland and Stenstrom, 1979). Detrital iron comes from iron oxide or oxyhydroxide coatings on clastic sediments, adsorbed or exchangeable iron in clays or organic particles (Curtis, 1967; Franks, 1969; Allison and Pye, 1994). Preferential formation of siderite concretions in clay-rich horizons supports the theory that clays were a significant source of detrital iron (Middleton and Nelson, 1996). Under highly reducing conditions, the Fe^{3+} fraction in sediments will be reduced to Fe^{2+} (Carroll, 1958; Middleton and Nelson, 1996).

1.6.4 Concretion lithification

Precipitated cements can form 70-80% of concretion volume, suggesting that concretions formed in relatively shallow, uncompacted muds with high water content (Woodland and Stenstrom, 1979). Many fossils from Pit 11 are skewed towards the base of their respective concretions. This may have occurred because shallower muds were more porous, allowing for greater concretion expansion and growth in the upward direction, or because load-induced dewatering of the underlying muds and peat unit caused upward flow of ion-rich pore waters (Baird *et al.*, 1986). As a result, concretions are often subspherical, with the flattened bases oriented parallel to bedding planes.

Once enough siderite was produced, it began to harden, forming a protective

proto-concretion around the organism that resisted compaction. The surrounding muds dewatered and draped around the hardening siderite shell. Surrounding mudstone layers drape around concretions and laminated concretions show thinning of laminae towards the boundary, suggesting that compaction and dewatering occurred after the concretion had begun to solidify (Baird *et al.*, 1986). Accumulation of overlying sediment caused load-induced microfaults in concretions, suggesting that they were not completely hardened prior to sediment dewatering. In some concretions, fossil impressions show faulting, but concretion exteriors do not, suggesting that faulting took place prior to final stages of concretion growth (Baird *et al.*, 1986). Septarian fractures within some concretions formed due to tensional stresses or dewatering of muds during compaction (Woodland and Stenstrom, 1979; Hounslow, 1997). They cut across previously formed pyrite and iron monosulphides, and are filled with post formation precipitates of pyrite, calcite, sphalerite and kaolinite (Woodland and Stenstrom, 1979; Baird *et al.*, 1986). The pyrite and calcite may have been a result of increasingly marine pore waters (Woodland and Stenstrom, 1979). Carbonate for calcite could also have come from anaerobic oxidation of methane in underlying maturing coal seams (Middleton and Nelson, 1996). Septarian cracks usually radiate towards the periphery in all directions from a central, mineral filled void that follows the long axis of the concretion, narrowing and terminating near its boundary (Woodland and Stenstrom, 1979). Hendry *et al.* (2006) propose that septarian cracks form early during concretion lithification, and that bacterially produced extracellular polysaccharide substances are critical in both processes. Water loss caused the concretion to solidify and harden,

encasing the organism. Concretion lithification is essentially complete within shallow sediment layers, and is most intense during depositional hiatus (Hendry *et al.*, 2006). Depositional hiatus allows bacterial metabolites to accumulate in their respective sediment layers, leading to localised supersaturation and mineral precipitation. Alternatively, depositional hiatus may establish geochemical boundaries that promote concretion cementation where upward and downward diffusing solute fronts meet to create favourable conditions for bacterial metabolism (Hendry *et al.*, 2006).

1.7 CHAPTER OUTLINES

Chapter two is an examination of Mazon Creek concretions using a variety of analytical techniques (Scanning Electron Microscopy (SEM), Energy Dispersive Spectroscopy (EDS), and Time of Flight Secondary Ion Mass Spectrometry (ToF-SIMS)), to determine whether primary or secondary organics are preserved, *i.e.*, whether microbial fossils occur along with organism remains in these concretions. Regions of primary and secondary organic preservation, found using SEM in concretions across a range of organisms, were further analyzed for qualitative mineralogy (EDS) and organic compounds (ToF-SIMS). Time of Flight Secondary Ion Mass Spectrometry was used to characterise the organic-mineral relationships within these unique regions of interest.

Chapter three highlights an experimental model of Mazon Creek type preservation in the laboratory, under conditions mimicking those present during initial burial, in an attempt to understand the early diagenesis of these fossils. Microbiological

and geochemical conditions determine the type and extent of mineralisation. Depending on the most labile tissues that can be preserved under given environmental conditions, certain organisms could be lost prior to fossilisation. Taphonomic studies allow us to reconstruct paleoecology and ecosystems more accurately through better understanding of organism decomposition, early mineralisation and post-fossilisation changes to the rock record.

1. REFERENCES

- Adams, L.K., Macquaker, J.H.S., and Marshall, J.D., 2006, Iron(III)-reduction in a low-organic-carbon brackish-marine system: *Journal of Sedimentary Research*, v. 76, no. 5-6, p. 919-925.
- Addadi, L., and Weiner, S., 2001, Biomineralization—crystals, asymmetry and life: *Nature*, v. 411, no. 6839, p. 753-755.
- Addadi, L., Raz, S., and Weiner, S., 2003, Taking advantage of disorder: amorphous calcium carbonate and its roles in biomineralization: *Advanced Materials*, v. 15, no. 12, p. 959-970.
- Allen, J.R.L., 1981, Lower Cretaceous tides revealed by cross-bedding with mud drapes: *Nature*, v. 289, no. 5798, p. 579-581.
- Aller, R.C., 1980, Quantifying solute distributions in the biotubated zone of marine sediments by defining an average microenvironment: *Geochimica et Cosmochimica Acta*, v. 44, no. 12, p. 1955-1965.
- Allison, P.A., 1988a, Konservat-lagestätten: cause and classification: *Paleobiology*, v. 14, no. 4, p. 331-344.
- Allison, P.A., 1988b, The role of anoxia in the decay and mineralization of proteinaceous macro-fossils: *Paleobiology*, v. 14, no. 2, p. 139-154.
- Allison, P.A., and Briggs, D.E.G., eds., 1991, *Taphonomy: releasing the data locked in the fossil record*: New York, NY, Plenum Press, 560 p.
- Allison, P.A., and Briggs, D.E.G., 1993, Exceptional fossil record: distribution of soft-tissue preservation through the Phanerozoic: *Geology*, v. 21, p. 527-530.
- Allison, P.A., and Pye, K., 1994, Early diagenetic mineralization and fossil preservation in modern carbonate concretions: *Palaios*, v. 9, no. 6, p. 561-575.
- Baird, G.C., 1978, Pebbly phosphorites in shale: a key to recognition of a widespread submarine discontinuity: *Journal of Sedimentary Petrology*, v. 48, no. 2, p. 545-555.
- Baird, G.C., 1979, Lithology and fossil distribution, Francis Creek Shale in northeastern Illinois. *in* Nitecki, M.H., ed., *Mazon Creek fossils*: New York, NY, Academic Press, p.41-67.

- Baird, G.C., 1997, Francis Creek Diagenetic Events, *in* Shabica, C.W., and Hay, A.A., eds., *Richardson's Guide to the Fossil Fauna of Mazon Creek: Chicago, Northeastern Illinois University*, p 30-34.
- Baird, G.C., and Anderson, J.L., 1997, Relative abundance of different Mazon Creek organisms, *in* Shabica, C.W., and Hay, A.A., eds., *Richardson's Guide to the Fossil Fauna of Mazon Creek: Chicago, Northeastern Illinois University*, p 27-29.
- Baird, G.C., and Shabica, C.W., 1980, The Mazon Creek depositional event: examination of Francis Creek and analogous facies in the midcontinent region, *in* Langenheim, R.L., and Mann, C.J., eds., *Middle and late Pennsylvanian strata on margin of Illinois Basin: Great Lakes Section, Danville, Society of Economic Paleontologists and Mineralogists, 10th Annual Meeting, Guidebook*, p. 79-92.
- Baird, G.C., and Sroka, S.D., 1990, Geology and geohistory of Mazon Creek area fossil localities, Illinois, *in* Hammer, W.R., and Hess, D.F., eds., *Geology Field Guidebook: Current Perspectives on Illinois Basin and Mississippi Arch Geology: Macomb, IL, Geological Society of America, 24th Annual Meeting of the North-Central Section*, p. C1-C70.
- Baird, G.C., Shabica, C.W., Anderson, J.L., and Richardson, E.S., Jr., 1985a, Biota of a Pennsylvanian muddy coast: habitats within the Mazonian delta complex, northeast Illinois: *Journal of Paleontology*, v. 59, no. 2, p. 253-281.
- Baird, G.C., Sroka, S.D., Shabica, C.W., Beard, T.L., Scott, A.C., and Broadhurst, F.M., 1985b, Mazon Creek-type fossil assemblages in the U.S. midcontinent Pennsylvanian: their recurrent character and palaeoenvironmental significance [and discussion]: *Philosophical Transactions of the Royal Society of London, Series B- Biological Sciences*, v. 311, no. 1148, p. 87-99.
- Baird, G.C., Sroka, S.D., Shabica, C.W., and Kuecher, G.J., 1986, Taphonomy of middle Pennsylvanian Mazon Creek Area fossil localities northeast Illinois, USA: significance of exceptional fossil preservation in syngenetic concretions: *Palaios*, v. 1, no. 3, p. 271-285.
- Balch, W.E., Fox, G.E., Magrum, L.J., Woese, C.R., and Wolfe, R.S., 1979, Methanogens - re-evaluation of a unique biological group: *Microbiological reviews*, v. 43, no. 2, p. 260-296.
- Bartels, C., and Brassel, G., 1990, Fossilien im Hunsrückschiefer: Dokumente des Meereslebens im Devon: *Museum Idar-Oberstein Series 7*, no. 1, 232 p.
- Bartels, C., Briggs, D.E.G., and Brassel, G., 1998, *The fossils of the Hunsrück Slate: marine life in the Devonian*: New York, NY, Cambridge University Press, 309 p.

- Baturin, G.N., 1971, Stages of phosphorite formation on the ocean floor: *Nature-Physical Science*, v. 232, no. 29, p. 61-62.
- Beall, B.S., 1991, The Tully Monster and a new approach to analyzing problematica, *in* Simonetta, A.M., and Morris, S.C., eds., *The Early Evolution of Metazoa and the Significance of Problematic Taxa*: New York, NY, Cambridge University Press, p. 271-285.
- Benz, M., Brune, A., and Schink, B., 1998, Anaerobic and aerobic oxidation of ferrous iron at neutral pH by chemoheterotrophic nitrate-reducing bacteria: *Archives of Microbiology*, v. 169, no. 2, p. 159-165.
- Berner, R.A., 1969, Migration of iron and sulfur within anaerobic sediments during early diagenesis: *American Journal of Science*, v.267, p. 19-42.
- Berner, R.A., 1970, Sedimentary pyrite formation: *American Journal of Science*, v. 268, no. 1, p. 1-23.
- Berner, R.A., 1978, Sulfate reduction and the rate of deposition of marine sediments: *Earth and Planetary Science Letters*, v. 37, p. 492-498.
- Berner, R.A., 1981a, A new geochemical classification of sedimentary environments: *Journal of Sedimentary Petrology*, v. 51, no. 2, p. 359-365.
- Berner, R.A., 1981b, Kinetics of weathering and diagenesis, *in* Lasaga, A.C., and Kirkpatrick, R.J., eds., *Kinetics of Geochemical Processes*: Washington, D.C., Mineralogical Society of America, p. 111-170.
- Berner, R.A., 1984, Sedimentary pyrite formation - an update: *Geochimica et Cosmochimica Acta*, v. 48, no. 4, p. 605-615.
- Berner, R.A., 1985, Sulphate reduction, organic matter decomposition and pyrite formation: *Philosophical Transactions of the Royal Society of London, Series A*, v. 315, no. 1531, p. 25-38.
- Berner, R.A., Baldwin, T., and Holdren, G.R., 1979, Authigenic iron sulfides as paleosalinity indicators: *Journal of Sedimentary Petrology*, v. 49, no. 4, p. 1345-1350.
- Beveridge, T.J., and Fyfe, W.S., 1985, Metal fixation by bacterial cell walls: *Canadian Journal of Earth Sciences*, v. 22, no. 12, p. 1893-1898.
- Birch, G.F., 1979, Phosphatic rocks on the western margin of South Africa: *Journal of Sedimentary Petrology*, v. 49, no. 1, p 93-110.

- Borkow, P.S., and Babcock, L.E., 2003, Turning pyrite concretions outside-in: role of biofilms in pyritization of fossils: *The Sedimentary Record*, v. 1, no. 3, p. 4-7.
- Borowitzka, M.A., 1982, Morphological and cytological aspects of algal calcification: *International Review of Cytology*, v. 74, no. 1, p. 127-162.
- Borowitzka, M.A., Larkum, A.W.D., and Nockolds, C.E., 1974, A scanning electron microscope study of the structure and organization of the calcium carbonate deposits of algae: *Phycologia*, v. 13, no. 3, p. 195-204.
- Bottjer, D.J., 2002, Exceptional fossil preservation: a unique view on the evolution of marine life: New York, NY, Columbia University Press, 403 p.
- Boyd, D.W., and Newell, N.D., 1972, Taphonomy and diagenesis of a Permian fossil assemblage from Wyoming: *Journal of Paleontology*, v. 46, no. 1, p. 1-14.
- Brett, C.E., and Baird, G.C., 1986, Comparative taphonomy: a key to paleoenvironmental interpretation based on fossil preservation: *Palaios*, v. 1, no. 3, p. 207-227.
- Brett, C.E., Speyer, S.E., and Baird, G.C., 1986, Storm-generated sedimentary units: tempestite proximity and event stratification in the Middle Devonian Hamilton Group of New York, *in* Brett, C.E., ed., *Dynamic Stratigraphy and Depositional Environments of the Hamilton Group (Middle Devonian) in New York State, Part 1: New York State Museum Bulletin 457*, p. 129-156.
- Bridge, T.A.M., and Johnson, D.B., 2000, Reductive dissolution of ferric iron minerals by *Acidiphilium* SJH: *Geomicrobiology Journal*, v. 17, no. 3, p. 193-206.
- Briggs, D.E.G., and Kear, A.J., 1993a, Decay and preservation of polychaetes: taphonomic thresholds in soft-bodied organisms: *Paleobiology*, v. 19, no. 1, p. 107-135.
- Briggs, D.E.G., and Kear, A.J., 1993b, Fossilization of soft tissue in the laboratory: *Science*, v. 259, no. 5100, p. 1439-1442.
- Briggs, D.E.G., and Kear, A.J., 1994, Decay and mineralization of shrimps: *Palaios*, v. 9, no. 5, p. 431-456.
- Briggs, D.E.G., Raiswell, R., Bottrell, S.H., Hatfield, D., and Bartels, C., 1996, Controls on the pyritization of exceptionally preserved fossils: analysis of the Lower Devonian Hunsrück Slate of Germany: *American Journal of Science*, v. 296, no. 6, p. 633-663.
- Brock, F., Parkes, R.J., and Briggs, D.E.G., 2006, Experimental pyrite formation associated with decay of plant material: *Palaios*, v. 21, no. 5, p. 499-506.

- Bromley, R.G., Curran, H.A., Frey, R.W., Gutscheck, R.G., and Suttner, L.J., 1975, Problems in interpreting unusually large burrows, *in* Frey, R.W., ed., *The Study of Trace Fossils: A Synthesis of Principles, Problems, and Procedures in Ichnology*: New York, NY, Springer-Verlag, p. 351-376.
- Bubela, B., and McDonald, J.A., 1969, Formation of banded sulphides: metal ion separation and precipitation by inorganic and microbial sulphide sources: *Nature*, v. 221, no. 5179, p. 465-466.
- Burnett, W.C., 1977, Geochemistry and origin of phosphorite deposits from off Peru and Chile: *Geological Society of America Bulletin* 88, p. 813-823.
- Canfield, D.E., 1989, Reactive iron in marine sediments: *Geochimica et Cosmochimica Acta*, v. 53, p. 619-632.
- Canfield, D.E., and Raiswell, R., 1991, Carbonate preservation in modern sediments, *in* Allison, P.A., and Briggs, D.E.G., eds., *Taphonomy: Releasing the Data Locked in the Fossil Record*: New York, NY, Plenum Press, p. 337-387.
- Carroll, D., 1958, Role of clay minerals in the transportation of iron: *Geochimica et Cosmochimica Acta*, v. 14, p. 1-27.
- Chapelle, F.H., 1993, *Groundwater microbiology and geochemistry*: New York, NY, John Wiley, 448 p.
- Chapelle, F.H., and Lovley, D.R., 1992, Competitive exclusion of sulphate reduction by Fe(III)-reducing bacteria: a mechanism for producing discrete zones from high-iron ground water: *Ground Water*, v. 30, p. 29-36.
- Chaloner, W.G., and Creber, G.T., 1973, Growth rings in fossil woods as evidence of past climates, *in* Tarling, D.H., and Runcorn, S.K., eds., *Implications of Continental Drift to the Earth Sciences*, v. 1: New York, NY, Academic Press, p. 425-437.
- Clarkson, E.N.K., 1998, *Invertebrate palaeontology and evolution*: Malden, MA, Blackwell Science, 452 p.
- Coleman, M.L., 1985, Geochemistry of diagenetic non-silicate minerals: kinetic considerations: *Philosophical Transactions of the Royal Society of London, Series A*, v. 315, no. 1531, p. 39-56.
- Coleman, M.L., 1993, Microbial processes - controls on the shape and composition of carbonate concretions: *Marine Geology*, v. 113, no. 1-2, p. 127-140.

- Coleman, M.L., and Raiswell, R., 1995, Source of carbonate and origin of zonation in pyritiferous carbonate concretions - evaluation of a dynamic-model: *American Journal of Science*, v. 295, no. 3, p. 282-308.
- Coleman, M.L., Hedrick, D.B., Lovley, D.R., White, D.C., and Pye, K., 1993, Reduction of Fe(III) in sediments by sulfate-reducing bacteria: *Nature*, v. 361, no. 6411, p. 436-438
- Cornell, R.M., and Schwertmann, U., 2003, *The iron oxides: structures, properties, reactions, occurrences and uses*: Weinheim, Germany, Wiley-VCH, 664 p.
- Corstjens, P.L.A.M., de Vrind, J.P.M., Westbroek, P., and de Vrind-de Jong, E.W., 1992, Enzymatic iron oxidation by *Leptothrix discophora*: identification of an iron-oxidizing protein: *Applied and Environmental Microbiology*, v. 58, no. 2, p. 450-454.
- Curtis, C.D., 1967, Diagenetic iron minerals in some British Carboniferous sediments: *Geochimica et Cosmochimica Acta*, v. 31, p. 2109-2123.
- Curtis, C.D., 1980, Diagenetic alteration in black shales: *Journal of the Geological Society of London*, v. 137, no. 2, p. 189-194.
- Curtis, C.D., 1995, Post-depositional evolution of mudstones 1: early days and parental influences: *Journal of the Geological Society of London*, v. 152, p. 577-586.
- Curtis, C.D., 1980, and Spears, D.A., 1968, The formation of sedimentary iron minerals: *Economic Geology*, v. 63, p. 257-270.
- De Yoreo, J.J., and Vekilov, P.G., 2003, Principles of crystal nucleation and growth: *Reviews in Mineralogy and Geochemistry*, v. 54, no. 1, p. 57-93.
- Darrah, W.C., 1970, A critical review of the upper Pennsylvanian floras of the eastern United States with notes on the Mazon Creek flora of Illinois: Gettysburg, PA, Privately published, 220 p.
- Denny, M.W., Helmuth, B., Leonard, G.H., Harley, C.D.G., Hunt, L.J.H., and Nelson, E.K., 2004, Quantifying scale in ecology: Lessons from a wave-swept shore: *Ecological Monographs*, v. 74, no. 3, p. 513-532.
- Devol, A.H., and Ahmed, S.I., 1981, Are high rates of sulphate reduction associated with anaerobic methane oxidation?: *Nature*, v. 291, no. 5814, p. 407-408.
- Dick, V.B., and Brett, C.E., 1986, Petrology, taphonomy, and sedimentary environments of pyritic fossil beds from the Hamilton Group (Middle Devonian) of western New York USA, in Brett, C.E., ed., *Dynamic Stratigraphy and Depositional Environments*

of the Hamilton Group (Middle Devonian) in New York State, Part 1: New York State Museum Bulletin 457, p. 102-128.

- Donald, R., and Southam, G., 1999, Low Temperature anaerobic bacterial diagenesis of ferrous monosulfide to pyrite: *Geochimica et Cosmochimica Acta*, v. 63, p. 2019-2023.
- Driscoll, E.G., Hall D.D., and Nussmann, D.G., 1965, Morphology and paleoecology of the brachiopod *Leiorhynchus kelloggi* Hall, Middle Devonian, Ohio, Michigan, Ontario: *Journal of Paleontology*, v. 39, no. 5, p. 916-933.
- Druschel, G.K., Emerson, D., Sutka, R., Suchecki, P., and Luther III, G.W., 2008, Low-oxygen and chemical kinetic constraints on the geochemical niche of neutrophilic iron(II) oxidizing microorganisms: *Geochimica et Cosmochimica Acta*, v. 72, no. 14, p. 3358-3370.
- Duan, W.M., Hedrick, D.B., Pye, K., Coleman, M.L., and White, D.C., 1996, A preliminary study of the geochemical and microbiological characteristics of modern sedimentary concretions: *Limnology and Oceanography*, v. 41, no. 7, p. 1404-1414.
- Ehrlich, H.L., 2009, *Geomicrobiology*, 5th ed.: Boca Raton, FL, CRC Press, 606 p.
- Elsner, M., Schwarzenbach, R.P., and Haderlein, S.B., 2004, Reactivity of Fe(II)-bearing minerals towards reductive transformation of organic contaminants: *Environmental Science & Technology*, v. 38, no. 3, p. 799-807.
- Emerson, D., 2000, Microbial oxidation of Fe(II) and Mn(II) at circumneutral pH, in Lovley, D.R., ed., *Environmental Microbe-mineral Interactions*: Washington D.C., ASM Press, p. 53-78.
- Emerson, D., and Revsbech, N.P., 1994, Investigation of an iron-oxidizing microbial mat community located near Aarhus, Denmark: field studies: *Applied and Environmental Microbiology*, v. 60, no. 11, p. 4022-4031.
- Falkowski, P.G., Fenchel, T., and Delong, E.F., 2008, The microbial engines that drive Earth's biogeochemical cycles: *Science*, v. 320, no. 5879, p. 1034-1039.
- Fisher, D.C., 1979, Evidence for subaerial activity of *Euproops danae* (Merostomata, Xiphosurida), in Nitecki, M.H., ed., *Mazon Creek fossils*: New York, NY, Academic Press, p. 379-448.
- Fisher, I. St. J., and Hudson, J.D., 1985, Pyrite geochemistry and fossil preservation in shales: *Philosophical Transactions of the Royal Society of London, Series B-Biological Sciences*, v. 311, no. 1148, p. 167-169.

- Fortin, D., Southam, G., and Beveridge, T.J., 1994, An examination of iron sulfide, iron-nickel sulfide and nickel sulfide precipitation by a *desulfotomaculum* species and its nickel resistance mechanisms: *FEMS Microbiology Ecology*, v. 14, no. 2, p. 121-132.
- Fortin, D., Ferris, F.G., and Beveridge, T.J., 1997, Surface-mediated mineral development by bacteria: *Reviews in Mineralogy*, v. 35, no. 1, p. 161-180.
- Foster, M.W., 1979a, A reappraisal of *Tullimonstrum gregarium*, in Nitecki, M.H., ed., *Mazon Creek Fossils*: New York, NY, Academic Press, p.269-302.
- Foster, M.W., 1979b, Soft-bodied coelenterates in the Pennsylvanian of Illinois, in Nitecki, M.H., ed., *Mazon Creek Fossils*: New York, NY, Academic Press, p.191-267.
- Frankel, R.B., and Bazylinksi, D.A., 2003, Biologically induced mineralization by bacteria: *Reviews in Mineralogy and Geochemistry*, v. 54, no. 1, p. 95-114.
- Franks, P.C., 1969, Synaeresis features and genesis of siderite concretions, Kiowa Formation (early Cretaceous), north-central Kansas: *Journal of Sedimentary Petrology*, v. 39, no. 2, p. 799-803.
- Fritz, W.H., 1971, Geological setting of the Burgess Shale, in Yochelson, E.L., ed., *Proceedings of the North American Paleontological Convention, Volume 2*: Lawrence, KS, Allen Press, p. 1155-1170.
- Froelich, P.N., *et al.*, 1979, Early oxidation of organic matter in pelagic sediments of the eastern equatorial Atlantic: suboxic diagenesis: *Geochimica et Cosmochimica Acta*, v. 43, no. 7, p. 1075-1090.
- Gall, J.-C., 1985, Fluvial depositional environment evolving into deltaic setting with marine influences in the Buntsandstein of northern Vosges (France), in Mader, D., ed., *Aspects of Fluvial Sedimentation in the Lower Triassic Buntsandstein of Europe*: New York, NY, Lecture Notes in Earth Sciences, v. 4, Springer-Verlag, p. 449-477.
- Gall, J.-C., 1990, Microbial veils—their contribution to fossilization of soft-bodied organisms: *Lethaia*, v. 23, no. 1, p. 21-28.
- Gautier, D.L., 1982, Siderite concretions: indications of early diagenesis in the Gammon Shale (Cretaceous): *Journal of Sedimentary Petrology*, v. 52, no. 3, p. 859-871.
- Giblin, A.E., and Howarth, R.W., 1984, Porewater evidence for a dynamic sedimentary iron cycle in salt marshes: *Limnology and Oceanography*, v. 29, no. 1, p. 47-63.

- Glenn, C.R., and Arthur, M.A., 1988, Petrology and major element geochemistry of Peru margin phosphorites and associated diagenetic minerals—authigenesis in modern organic-rich sediments: *Marine Geology*, v. 80, no. 3-4, p. 231-267.
- Goldhaber, M.B., and Kaplan, I.R., 1980, Mechanisms of sulfur incorporation and isotope fractionation during early diagenesis of sediments in the Gulf of California: *Marine Chemistry*, v. 9, p. 95-143.
- Hafenbradl, D., Keller, M., Dirmeier, R., Rachel, R., Rossnagel, P., Burggraf, S., Huber, H., and Stetter, K.O., 1996, *Ferroglobus placidus* gen nov., sp. nov., a novel hyperthermophilic archaeum that oxidizes Fe²⁺ at neutral pH under anoxic conditions: *Archives of Microbiology*, v. 166, no. 5, p. 308-314.
- Hallam, S.J., Putnam, N., Preston, C.M., Detter, J.C., Rokhsar, D., Richardson, P.M., and DeLong, E.F., 2004, Reverse methanogenesis: testing the hypothesis with environmental genomics: *Science*, v. 305, no. 5689, p. 1457-1462.
- Hecht, F., 1933, Der Verbleib der organischer substanz der Tiere bei meerischer Einbettung: *Senckenbergiana*, v. 15, no. 3-4, p. 165-249.
- Heckel, P.H., 1986, Sea-level curve for Pennsylvanian eustatic marine transgressive-regressive depositional cycles along mid-continent outcrop belt, North America: *Geology*, v. 14, no. 4, p. 330-334.
- Hendry, J.P., Pearson, M.J., Trewin, N.H., and Fallick, A.E., 2006, Jurassic septarian concretions from NW Scotland record interdependent bacterial, physical and chemical processes of marine mudrock diagenesis: *Sedimentology*, v. 53, no. 3, p. 537-565.
- Hernandez, M.E., and Newman, D.K., 2001, Extracellular electron transfer: *Cellular and Molecular Life Sciences*, v. 58, no. 11, p. 1562-1571.
- Hirschler, A., Lucas, J., and Hubert, J.-C., 1990, Apatite genesis: a biologically induced or biologically controlled mineral formation process?: *Geomicrobiology Journal*, v. 8, no. 1, p. 47-57.
- Hounslow, M.W., 1997, Significance of localized pore pressures to the genesis of septarian concretions: *Sedimentology*, v. 44, no. 6, p. 1133-1147.
- Hudson, J.D., 1982, Pyrite in ammonite-bearing shales from the Jurassic of England and Germany: *Sedimentology*, v. 29, no. 5, p. 639-667.
- Hurtgen, M.T., Lyons, T.W., Ingall, E.D., and Cruse, A.M., 1999, Anomalous enrichments of iron monosulfide in euxinic marine sediments and the role of H₂S in iron sulfide

- transformations: examples from Effingham inlet, Orca Basin and the Black Sea: *American Journal of Science*, v. 299, p. 556-558.
- Iler, R.K., 1979, *The chemistry of silica: solubility, polymerization, colloid and surface properties, and biochemistry*: New York, NY, John Wiley & Sons, 866 p.
- Irwin, M.L., 1965, General theory of epeiric clear water sedimentation: *Bulletin of the American Association of Petroleum Geologists*, v. 49, no. 4, p. 445-459.
- Jenkyns, H.C., 1980, Cretaceous anoxic events: from continents to oceans: *Journal of the Geological Society of London*, v. 137, no. 2, p. 171-188.
- Johnson, D.B., and McGinness, S., 1991, Ferric iron reduction by acidophilic heterotrophic bacteria: *Applied and Environmental Microbiology*, v. 57, no. 1, p. 207-211.
- Johnson, R.G., and Richardson, E.S., Jr., 1966, A remarkable Pennsylvanian fauna from the Mazon Creek area, Illinois: *Journal of Geology*, v. 74, no. 5, p. 626-631.
- Johnson, R.G., and Richardson, E.S., Jr., 1970, Fauna of the Francis Creek Shale in the Wilmington area, *in* Illinois State Geological Survey Guidebook Series No. 8: Urbana, IL, Illinois State Geological Survey, p. 53-60.
- Kappler, A., and Newman, D.K., 2004, Formation of Fe(III)-minerals by Fe(II)-oxidizing photoautotrophic bacteria: *Geochimica et Cosmochimica Acta*, v. 68, no. 6, p. 1217-1226.
- Kappler, A., and Straub, K., 2005, Geomicrobiological cycling of iron: *Molecular Geomicrobiology*, v. 59, p. 85-108.
- Kauffman, E.G., 1977, Benthic communities in black shales of an anaerobic Jurassic basin—Posidonienschiefer: *Journal of Paleontology*, v. 51, no. 2, p. 16-17.
- Kennedy, W.J., and Garrison, R.E., 1975, Morphology and genesis of nodular phosphates in the Cenomanian Glauconitic Marl of south-east England: *Lethaia*, v. 8, no. 4, p. 339-360.
- Keupp, H., 1977, Ultrafazies und genese der Solnhofener Plattenkalke: Oberer Malm, südliche Frankenalb: *Abhandlungen der Naturhistorischen Gesellschaft Nürnberg* 37, 128 p.
- Klein, G. DeV., 1977, *Clastic tidal facies: Urbana-Champaign, Continuing Education Publication Company, University of Illinois*, 149 p.

- Konhauser, K., 2007, *Introduction to geomicrobiology*: Malden, MA, Blackwell Publishing, 425 p.
- Krajewski, K.P., 1984, Early diagenetic phosphate cements in the Albian condensed glauconitic limestone of the Tatra Mountains, western Carpathians: *Sedimentology*, v. 31, no. 4, p. 443-470.
- Krumbein, W.E., 1983, *Microbial chemistry*: Boston, MA, Blackwell Publishing, 330 p.
- Kuecher, G.J., 1983, Rhythmic sedimentation and stratigraphy of the Middle Pennsylvanian Francis Creek Shale near Braidwood, Illinois [unpubl. M.S. thesis]: Chicago, Northeastern Illinois University, 143 p.
- Kuecher, G.J., Woodland, B.G., and Broadhurst, F.M., 1990, Evidence of deposition from individual tides and of tidal cycles from the Francis Creek Shale (host rock to the Mazon Creek Biota), Westphalian D (Pennsylvanian), northeastern Illinois: *Sedimentary Geology*, v. 68, no. 3, p. 211-221.
- Kumar, N., and Sanders, J.E., Characteristics of shoreface storm deposits: modern and ancient examples: *Journal of Sedimentary Petrology*, v. 46, no. 1, p. 145-162.
- Lichtner, P.C., and Biino, G.G., 1992, A first principles approach to supergene enrichment of a porphyry copper protore: 1. Cu-Fe-S subsystem: *Geochimica et Cosmochimica Acta*, v. 56, no. 11, p. 3987-4013.
- Lovley, D.R., and Chapelle, F.H., 1995, Deep subsurface microbial processes: *Reviews of Geophysics*, v. 33, no. 3, p. 365-381.
- Lovley, D.R., and Phillips, E.J.P., 1986, Organic-matter mineralization with reduction of ferric iron in anaerobic sediments: *Applied and Environmental Microbiology*, v. 51, no. 4, p. 683-689.
- Lovley, D.R., and Phillips, E.J.P., 1988, Novel mode of microbial energy metabolism: organic carbon oxidation coupled to dissimilatory reduction of iron or manganese: *Applied and Environmental Microbiology*, v. 54, no. 6, p. 1472-1480.
- Lovley, D.R., Holmes, D.E., and Nevin, K.P., 2004, Dissimilatory Fe(III) and Mn(IV) reduction: *Advances in Microbial Physiology*, Book Series, v. 49, p. 219-286.
- Lowenstam, H.A., 1981, Minerals formed by organisms: *Science*, v. 211, no. 4487, p. 1126-1131.
- Lowenstam, H.A., and Weiner, S., 1989, *On biomineralization*: New York, NY, Oxford University Press, 324 p.

- Madigan, M.T., Martinko, J.M., Stahl, D.A., and Clark, D.P., 2012, Brock biology of microorganisms, 13th edition: San Francisco, Benjamin Cummings, 1152 p.
- Mann, S., 1983, Mineralization in biological systems: Structure and Bonding, v. 54, p. 125-174.
- Marquis, R.E., Mayzel, K., and Carstensen, E.L., 1976, Cation exchange in cell walls of gram-positive bacteria: Canadian Journal of Microbiology, v. 22, no. 7, p. 975-982.
- Martens, C.S., and Berner, R.A., 1974, Methane production in the interstitial waters of sulfate-depleted sediments: Science, v. 185, p. 1167-1169.
- Martill, D.M., 1988, Preservation of fish in the Cretaceous Santana Formation of Brazil: Palaeontology, v. 31, no. 1, p. 1-18.
- Maynard, J.B., 1983, Geochemistry of sedimentary ore deposits: New York, Springer-Verlag, p. 305.
- McConnaughey, T., 1989, ^{13}C and ^{18}O isotopic disequilibrium in biological carbonates: 1. patterns: Geochimica et Cosmochimica Acta, v. 53, no. 1, p. 151-162.
- McIlreath, I.A., 1977, Accumulation of a Middle Cambrian, deep-water limestone debris apron adjacent to a vertical, submarine carbonate escarpment, southern Rocky Mountains, Canada, in Cook, H.E., and Enos, P., eds., Deep Water Carbonate Environments: Tulsa, OK, Society of Economic Paleontologists and Mineralogists-Special Publication no. 25, p. 113-124.
- Middleton, H.A., and Nelson, C.S., 1996, Origin and timing of siderite and calcite concretions in late Palaeogene non- to marginal-marine facies of the Te Kuiti Group, New Zealand: Sedimentary Geology, v. 103, no. 1-2, p. 93-115.
- Mittmeyer, H.G., 1980, Zur geologie des Hunsrückschiefers, in Stürmer, W., Schaarschmidt, J., and Mittmeyer, H.G., eds., Versteinertes Leben im Röntgenlicht: Kleine Senckenberg-Reihe 11, p. 34-39.
- Morris, K.A., 1979, Classification of Jurassic marine shale sequences - example from the Toarcian (Lower Jurassic) of Great-Britain: Palaeogeography Palaeoclimatology Palaeoecology, v. 26, no. 1-2, p. 117-126.
- Mozley, P.S., 1989, Relation between depositional environment and the elemental composition of early diagenetic siderite: Geology, v. 17, no. 8, p. 704-706.
- Müller, A.H., 1979, Fossilization (taphonomy), in Robison, R.A., and Teichert, C., eds., Treatise on Invertebrate Paleontology: Part A, Introduction, Fossilization

- (Taphonomy), Biogeography, and Biostratigraphy: Lawrence, KS, Geological Society of America and Kansas University Press, p. A2-A78.
- Murray, J., and Renard, A.F., 1981, Report of the scientific results of the voyage of H.M.S. 'Challenger' during the years 1873-1976, Chapter VI, Part III, p. 378-391.
- Nathan, Y., and Sass, E., 1981, Stability relations of apatites and calcium carbonates: *Chemical Geology*, v. 34, no. 1-2, p. 103-111.
- Neumann, T., Rausch, N., Leipe, T., Dellwig, O., Berner, Z., and Böttcher, M.E., 2005, Intense pyrite formation under low-sulfate conditions in the Achterwasser lagoon, SW Baltic Sea: *Geochimica et Cosmochimica Acta*, v. 69, no. 14, p. 3619-3630.
- Nitecki, M.H., 1979, Mazon Creek fauna and flora -- a hundred years of investigation, *in* Nitecki, M.H., ed., *Mazon Creek fossils*: New York, NY, Academic Press, p. 1-11.
- Ogihara, S., 1999, Geochemical characteristics of phosphorite and carbonate nodules from the Miocene Funakawa Formation, western margin of the Yokote Basin, northeast Japan: *Sedimentary Geology*, v. 125, no. 1-2, p. 69-82.
- Ojanuga, A.G., and Lee, G.B., 1973, Characteristics, distribution, and genesis of nodules and concretions in soils of the southwestern Upland of Nigeria: *Soil Science*, v. 116, no. 4, p. 282-291.
- Oremland, R.S., Marsh, L.M., and Polcin, S., 1982, Methane production and simultaneous sulphate reduction in anoxic saltmarsh sediments: *Nature*, v. 296, p. 143-145.
- Orme, C.A., Noy, A., Wierzbicki, A., McBride, M.T., Grantham, M., Teng, H.H., Dove, P.M., and De Yoreo, J.J., 2001, Formation of chiral morphologies through selective binding of amino acids to calcite surface steps: *Nature*, v. 411, no. 6839, p. 775-779.
- Orphan, V.J., House, C.H., Hinrichs, K.U., McKeegan, K.D., and DeLong, E.F., 2001, Methane-consuming archaea revealed by directly coupled isotopic and phylogenetic analysis: *Science*, v. 293, no. 5529, p. 484-487.
- Pedersen, K., and Ekendahl, S., 1990, Distribution and activity of bacteria in deep granitic groundwaters of southeastern Sweden: *Microbial Ecology*, v. 20, no. 1, p. 37-52.
- Pedersen, T.F., and Price, N.B., 1982, The geochemistry of manganese carbonate in Panama basin sediments: *Geochimica et Cosmochimica Acta*, v. 46, no. 1, p. 59-68.
- Peppers, R.A., and Pfefferkorn, H.W., 1970, A comparison of the floras of the Colchester (No. 2) Coal and Francis Creek Shale, *in* Illinois State Geological Survey Guidebook Series No. 8: Urbana, IL, Illinois State Geological Survey, p. 61-72.

- Perry, C.C., 2003, Silicification: the processes by which organisms capture and mineralize silica: *Reviews in Mineralogy and Geochemistry*, v. 54, no. 1, p. 291-327.
- Pfefferkorn, H.W., 1979, High diversity and stratigraphic age of the Mazon Creek flora, *in* Nitecki, M.H., ed., *Mazon Creek fossils*: New York, NY, Academic Press, p. 129-142.
- Phillips, T.L., and Peppers, R.A., 1984, Changing patterns of Pennsylvanian coal-swamp vegetation and implications of climatic control on coal occurrence: *International Journal of Coal Geology*, v. 3, no. 3, p. 205-255.
- Piper, D.J.W., 1972, Sediments of the middle Cambrian Burgess Shale, Canada: *Lethaia*, v. 5, no. 2, p. 169-175.
- Potter, P.E., and Pryor, W.A., 1961, Dispersal centers of Paleozoic and later clastics of the upper Mississippi Valley and adjacent areas: *Geological Society of America Bulletin*, v. 72, no. 8, p. 1195-1249.
- Pye, K., 1984, SEM analysis of siderite cements in intertidal marsh sediments, Norfolk, England: *Marine Geology*, v. 56, no. 1-4, p. 1-12.
- Pye, K., Dickson, J.A.D., Schiavon, N., Coleman, M.L., and Cox, M., 1990, Formation of siderite-Mg calcite-iron sulfide concretions in intertidal marsh and sandflat sediments, north Norfolk, England: *Sedimentology*, v. 37, no. 2, p. 325-343.
- Raiswell, R., 1971, The growth of Cambrian and Liassic concretions: *Sedimentology*, v. 17, no. 3-4, p. 147-171.
- Raiswell, R., 1976, The microbiological formation of carbonate concretions in the Upper Lias of NE England: *Chemical Geology*, v. 18, no. 3, p. 227-244.
- Raiswell, R., and Fisher, Q.J., 2004, Rates of carbonate cementation associated with sulphate reduction in DSDP/ODP sediments: implications for the formation of concretions: *Chemical Geology*, v. 211, p. 71-85.
- Rancourt, D.G., Thibault, P.-J., Mavrocordatos, D., and Lamarche, G., 2005, Hydrous ferric oxide precipitation in the presence of nonmetabolizing bacteria: constraints on the mechanism of a biotic effect: *Geochimica et Cosmochimica Acta*, v. 69, no. 3, p. 553-577.
- Reaves, C.R., 1984, The migration of iron and sulfur during the diagenesis of marine sediments [unpubl. Ph.D. thesis]: New Haven, CT, Yale University, 413 p.
- Reeburgh, W.S., 1983, Rates of biogeochemical processes in anoxic sediments: *Annual Review of Earth and Planetary Sciences*, v. 11, no. 1, p. 269-298.

- Reineck, H.-E., and Singh, I.B., 1973, Depositional sedimentary environments: with reference to terrigenous clastics: New York, NY, Springer-Verlag, 549 p.
- Richardson, E.S., Jr., 1966, Wormlike fossil from the Pennsylvanian of Illinois: *Science*, v. 151, no. 3706, p. 75-76.
- Richardson, E.S., Jr., and Johnson, R.G., 1971, The Mazon Creek faunas, *in* Proceedings of the North American Paleontological Convention: Field Museum of Natural History, Chicago, September 5-7, 1969, Volume 1: Lawrence, KS, Allen Press, p. 1222-1235.
- Rickard, D., 1997, Kinetics of pyrite formation by the H₂S oxidation of iron(II) monosulfide in aqueous solution between 25 and 125°C: the rate equation: *Geochimica et Cosmochimica Acta*, v. 61, no. 1, p. 115-134.
- Roden, E.E., 2003, Fe(III) oxide reactivity toward biological versus chemical reduction: *Environmental Science & Technology*, v. 37, no. 7, p. 1319-1324.
- Rucker, J.B., and Carver, R.E., 1969, A survey of the carbonate mineralogy of cheilostome bryozoa: *Journal of Paleontology*, v. 43, no. 3, p. 791-799.
- Saunders, J.A., and Swann, C.T., 1992, Nature and origin of authigenic rhodocrosite and siderite in the Paleozoic aquifer, northeast Mississippi: *Applied Geochemistry*, v. 7, no. 4, p. 375-387.
- Saunders, J.A., Duke, L., and Roden, E.E., 1997, Effects of anaerobic bacterial respiration on the geochemistry of silica: evidence from the Holocene diagenetic alteration of logs: *Geological Society of America Abstracts with Programs*, v. 29, no. 15037, p. 295.
- Saunders, J.A., Mohammad, S., Korte, N.E., Lee, M.-K., Fayek, M., Castle, D., and Barnett, M.O., 2005, Groundwater geochemistry, microbiology, and mineralogy of two arsenic-bearing Holocene alluvial aquifers from the USA: *American Chemical Society Symposium Series 915*, p. 191-205.
- Schellenberg, S.A., 2002, Mazon Creek: preservation in late Paleozoic deltaic and marginal marine environments, *in* Bottjer, D.J., Etter, W., Hagadorn, J.W. and Tang, C.M., eds., *Exceptional fossil preservation: a unique view on the evolution of marine life*: New York, Columbia University Press, p. 185-203.
- Schieber, J., 2002, Sedimentary pyrite: a window into the microbial past: *Geology*, v. 30, p. 531-534.

- Schink, B., 2002, Synergistic interactions in the microbial world: Antonie Van Leeuwenhoek International Journal of General and Molecular Microbiology, v. 81, no. 1-4, p. 257-261.
- Schopf, J.M., 1979, Evidence of soft-sediment cementation enclosing Mazon plant fossils, *in* Nitecki, M.H., ed., Mazon Creek fossils: New York, NY, Academic Press, p. 105-128.
- Schram, F.R., 1979, The Mazon Creek biotas in the context of a Carboniferous faunal continuum, *in* Nitecki, M.H., ed., Mazon Creek fossils: New York, NY, Academic Press, p. 159-190.
- Scotese, C.R., Bambach, R.K., Barton, C., Van der Voo, R., and Ziegler, A.M., 1979, Paleozoic base maps: Journal of Geology, v. 87, no. 3, p. 217-277.
- Seilacher, A., 1964, Biogenic sedimentary structures, *in* Imbrie, J., and Newell, N.D., eds., Approaches to Paleocology: New York, NY, Wiley, p. 296-316.
- Seilacher, A., 1970, Begriff und bedeutung der fossil-lagerstätten: Neues Jahrbuch für Geologie und Paläontologie Monatshefte, v. 7, p. 34-39.
- Seilacher, A., 1971, Preservational history of ceratite shells: Palaeontology, v. 14, no. 1, p. 16-21.
- Seilacher, A., 1982a, General remarks about event deposits, *in* Einsele, G., and Seilacher, A., eds., Cyclic and Event Stratification: New York, NY, Springer-Verlag, p. 161-174.
- Seilacher, A., 1982b, Posidonia Shales (Toarcian, S. Germany) – stagnant basin model revalidated, *in* Montanaro-Gallitelli, E., ed., Palaeontology, Essential of Historical Geology: Proceedings of the First International Meeting on "Palaeontology, Essential of Historical Geology," held in Venice, Fondazione Giorgio Cini, 2-4 June 1981: Modena, Italy, S.T.E.M.-Mucchi, p. 25-55.
- Seilacher, A., and Westphal, F., 1971, Fossil-lagerstätten, *in* Sedimentology of Parts of Central Europe, Guidebook 8: Heidelberg, International Sedimentological Congress, 344 p.
- Seilacher, A., Reif, W.E., and Westphal, F., 1985, Sedimentological, ecological and temporal patterns of fossil lagerstätten [and discussion]: Philosophical Transactions of the Royal Society of London, Series B: Biological Sciences, v. 311, no. 1148, p. 5-24.

- Shabica, C.W., 1970, Depositional environments in the Francis Creek Shale, *in* Illinois State Geological Survey Guidebook Series No. 8: Urbana, IL, Illinois State Geological Survey, p. 43-52.
- Shabica, C.W., 1971, Depositional environments in the Francis Creek Shale and associated strata [unpubl. Ph.D. thesis]: Chicago, University of Chicago, 206 p.
- Shabica, C.W., 1979, Pennsylvanian sedimentation in northern Illinois: examination of delta models, *in* Nitecki, M.H., ed., Mazon Creek Fossils: New York, NY, Academic Press, p. 13-40.
- Shabica, C.W., and Hay, A.A., editors, 1997, Richardson's guide to the fossil fauna of Mazon Creek: Chicago, Northeastern Illinois University, 308 p.
- Skyring, C.W., 1988, Acetate as the main substrate for the sulfate-reducing bacteria in Lake Eliza (South Australia) hypersaline sediments: *FEMS Microbiology Ecology*, v. 53., no. 2, p. 87-93.
- Smith, W.H., 1970, Lithology and distribution of the Francis Creek Shale in Illinois, *in* Illinois State Geological Survey Guidebook Series No. 8: Urbana, IL, Illinois State Geological Survey, p. 34-42.
- Smith, W.H., Nance, R.B., Hopkins, M.E., Johnson, R.G., and Shabica, C.W., 1970, Field trip log, *in* Illinois State Geological Survey Guidebook Series No. 8: Urbana, IL, Illinois State Geological Survey, p. 1-33.
- Sohn, I.G., 1977, *Paraparchites mazonensis* n. sp. (Ostracoda) from Middle Pennsylvanian ironstone concretions of Illinois: *Fieldiana, Geology*, v. 32, no. 2, p. 43-60.
- Sørensen, J., 1982, Reduction of ferric iron in anaerobic, marine sediment and interaction with reduction of nitrate and sulfate: *Applied and Environmental Microbiology*, v. 43, no. 2, p. 319-324.
- Southam, G., and Saunders, J.A., 2005, The geomicrobiology of ore deposits: *Economic Geology*, v. 100, no. 6, p. 1067-1084.
- Southam, G., Brock, C., Donald, R., and Røstad, A., 2001, Pyrite discs in coal: evidence for fossilized bacterial colonies: *Geology*, v. 29, no. 1, p. 47-50.
- Speyer, S.E., and Brett, C.E., 1991, Taphofacies controls: background and episodic processes in fossil assemblage preservation, *in* Allison, P.A., and Briggs, D.E.G., eds., *Taphonomy: Releasing the Data Locked in the Fossil Record*: New York, NY, Plenum Press, p. 501-545.

- Straub, K.L., Benz, M., Schink, B., and Widdel, F., 1996, Anaerobic, nitrate-dependent microbial oxidation of ferrous iron: *Applied and Environmental Microbiology*, v. 62, no. 4, p. 1458-1460.
- Straub, K.L., Schönhuber, W.A., Buchholz-Cleven, B.E.E., and Schink, B., 2004, Diversity of ferrous iron-oxidizing nitrate-reducing bacteria and their involvement in oxygen-independent iron cycling: *Geomicrobiology Journal*, v. 21, no. 6, p. 371-378.
- Stumm, W., and Morgan, J.J., 1996, *Aquatic chemistry: chemical equilibria and rates in natural waters*, 3rd ed.: New York, NY, John Wiley & Sons, 1022 p.
- Swirydczuk, K., Wilkinson, B.H., and Smith, G.R., 1981, Synsedimentary lacustrine phosphorites from the Pliocene Glens Ferry Formation of southwestern Idaho: *Journal of Sedimentary Petrology*, v. 51, no. 4, p. 1205-1214.
- Tebo, B.M., Ghiorse, W.C., van Waasbergen, L.G., Siering, P.L., and Caspi, R., 1997, Bacterially mediated mineral formation: insights into manganese(II) oxidation from molecular genetic and biochemical studies: *Reviews in Mineralogy*, v. 35, no. 1, p. 225-266.
- Thamdrup, B., 2000, Bacterial manganese and iron reduction in aquatic sediments, *in* Schink, B., ed., *Advances in Microbial Ecology*: New York, NY, Kluwer Academic/Plenum Publishers, p. 41-84.
- Tuttle, J.H., Dugan, C.B., and Randles, C.I., 1969, Microbial sulfate reduction and its potential utility as an acid mine water pollution abatement procedure: *Applied Microbiology*, v. 17, no. 2, p. 297-302.
- Urrutia, M., Kemper, M., Doyle, R., and Beveridge, T.J., 1992, The membrane-induced proton motive force influences the metal binding ability of *Bacillus subtilis* cell walls: *Applied and Environmental Microbiology*, v. 58, no. 12, p. 3837-3844.
- Viohl, G., 1985, Geology of the Solnhofen lithographic limestone and the habitat of *Archaeopteryx*, *in* Hecht, M.K., Ostrom, J.H., Viohl, G., and Wellnhofer, P., eds., *The beginnings of birds*, Proceedings of the international *Archaeopteryx* conference, 1984: Eichstätt, Freunde des Jura-Museums, p. 31-44.
- Viohl, G., 1996, The paleoenvironment of the Late Jurassic fishes from the southern Franconian Alb (Bavaria, Germany), *in* Arratia, G., and Viohl, G., eds., *Mesozoic Fishes—Systematics and Paleoecology*: Munich, Verlag Pfeil, p. 513-528.
- Waage, K.W., 1964, Origin of repeated fossiliferous concretion layers in the Fox Hills Formation, *in* Merriam, D.F., ed., *Symposium on Cyclic Sedimentation*, v. 2: Kansas Geological Survey Bulletin 169, p. 541-563.

- Wanless, H.R., 1939, Pennsylvanian correlations in the eastern interior and Appalachian coal fields: Geological Society of America Special Paper 17, 130 p.
- Wanless, H.R., and Weller, J.M., 1932, Correlation and extent of Pennsylvanian cyclothems: Geological Society of America Bulletin, v. 43, no. 4, p. 1003-1016.
- Watabe, N., and Kingsley, R.J., 1989, Extra-, inter-, and intracellular mineralization in invertebrates and algae, *in* Crick, R.E., ed., Origin, Evolution, and Modern Aspects of Biomineralization in Plants and Animals: New York, NY, Plenum Publishing Corporation, p. 209-223.
- Wegener, A., 1929, The origin of continents and oceans [English translation]: New York, NY, Dover Publications (1966), 246 p.
- Wehrli, B., Sulzberger, B., and Stumm, W., 1989, Redox processes catalyzed by hydrous oxide surfaces: Chemical Geology, v. 78, no. 3-4, p. 167-179.
- Weiner, S., and Dove, P.M., 2003, An overview of biomineralization processes and the problem of the vital effect: Biomineralization, v. 54, p. 1-29.
- Wetzel, R.G., 1975, Limnology: Philadelphia, W.B. Saunders Company, 743 p.
- Widdel, F., Schnell, S., Heising, S., Ehrenreich, A., Assmus, B., and Schink, B., 1993, Ferrous iron oxidation by anoxygenic phototrophic bacteria: Nature, v. 362, no. 6423, p. 834-835.
- Wilby, P.R., and Martill, D.M., 1992, Fossil fish stomachs: a microenvironment for exceptional preservation: Historical Biology, v. 6, no. 1, p. 25-36.
- Wilkin, R.T., and Barnes, H.L., 1997a, Formation processes of framboidal pyrite: Geochimica et Cosmochimica Acta, v. 61, no. 2, p. 323-339
- Wilkin, R.T., and Barnes, H.L., 1997b, Pyrite formation in an anoxic estuarine basin: American Journal of Science, v. 297, p. 620-650.
- Williams, A.G.B., and Scherer, M.M., 2004, Spectroscopic evidence for Fe(II)-Fe(III) electron transfer at the iron oxide-water interface: Environmental Science & Technology, v. 38, no. 18, p. 4782-4790.
- Wilt, F.H., 1999, Matrix and mineral in the sea urchin larval skeleton: Journal of Structural Biology, v. 126, no. 3, p. 216-226.

- Winston, R.B., 1986, Characteristic features and compaction of plant tissues traced from permineralized peat to coal in Pennsylvanian coals (Desmoinesian) from the Illinois Basin: *International Journal of Coal Geology*, v. 6, no. 1, p. 21-41.
- Woodland, B.G., and Stenstrom, R.C., 1979, The occurrence and origin of siderite concretions in the Francis Creek Shale (Pennsylvanian) of northeastern Illinois, *in* Nitecki, M.H., ed., *Mazon Creek fossils*: New York, NY, Academic Press, p.69-103.
- Wright, C.R., 1965, Environmental mapping of the beds of the Liverpool Cyclothem in the Illinois Basin and equivalent strata in the northern midcontinent region: Unpublished Ph.D. thesis, University of Illinois, Urbana, 100 p.
- Wright, C.R., 1979, Depositional history of the Pennsylvanian system in the Illinois Basin – a summary of work by Dr. Harold R. Wanless and associates, *in* Palmer, J.E., and Dutcher, R.R., eds., *Depositional and Structural History of the Pennsylvanian System of the Illinois Basin. Part 2: Invited Papers: Illinois State Geological Survey Guidebook 15a*, p. 21-26.
- Zangerl, R., 1971, On the geologic significance of perfectly preserved fossils, *in* *Proceedings, North American Paleontological Convention I, Chicago, 1969, Volume 2, Part 1*: Lawrence, KS, Allen Press, p. 1207-1222.
- Zangerl, R., and Richardson, E.S., Jr., 1975, Die paläoökologische bedeutung der Mazon Creek und Mecca faunen im zentralen Nordamerika, *in* *Compte Rendu, 7th International Congress on Carboniferous Stratigraphy and Geology, Krefeld, Germany, August 1971*, v. 4, p. 385-391.
- Zeigler, A.M., Scotese, C.R., McKerrow, W.S., Johnson, M.E., and Bambach, R.K., 1979, Paleozoic paleogeography: *Annual Review of Earth and Planetary Sciences*, v. 7, p. 473-502.

CHAPTER 2

MINERALOGY AND BIOGEOCHEMISTRY OF MAZON CREEK CONCRETIONS

2.1 INTRODUCTION

The Mazon Creek fossil biota of Illinois, U.S.A., represents one of the world's best known *Konservat Lagerstätte*, preserving diverse assemblages of terrestrial, marine and freshwater flora and fauna (Richardson and Johnson, 1971). Hard and soft tissue fossils of these organisms, the latter typically pyritised, are found entombed in siderite-cemented mudstone concretions (Woodland and Stenstrom, 1979; Baird *et al.*, 1986). The concretions formed in a deltaic-estuarine environment, within 10° of the paleoequator, during the mid-Pennsylvanian subperiod of the Carboniferous, a time when most of Illinois was covered by an epeiric sea that had encroached the region from the southwest (Wright, 1965; Scotese *et al.*, 1979; Shabica, 1970, 1979; Zeigler *et al.*, 1979; Baird *et al.*, 1985b).

At times of heavy rainfall and flooding, major fluvial systems flushed siliciclastic sediment, derived from upland areas in the northeast, into the Illinois Basin (Potter and Pryor, 1961; Shabica, 1971). During such events, the remains of resident estuarine biota, together with terrestrial/freshwater aquatic biota flushed from upstream areas of the drainage system, were rapidly buried in mud (Schopf, 1979). This was immediately followed by microbial decay of disseminated labile organic matter, which quickly rendered sediment porewaters anoxic (Allison, 1988). The combination of rapid burial and anoxia is thought to have been largely responsible for the exceptional fidelity of preservation observed in the concretion-hosted fossil remains of the Mazon Creek biota (Nitecki, 1979; Zangerl, 1971).

The Mazon Creek concretions occur in the lower 3-5 m of the Francis Creek Shale, a member of the Carbondale Formation that is locally underlain by the Colchester No. 2 Coal Member (Wanless and Weller, 1932; Wanless, 1939; Smith, 1970; Baird and Sroka, 1990). They were collected, mostly by amateur collectors, from the spoil heaps of coal mines in the Mazon Creek area (Shabica and Hay, 1997).

Some Mazon Creek organisms are the only known occurrences of ancestral-forms and/or early representatives of their taxonomic groups, and others, such as *Tullimonstrum gregarium*, remain enigmatic with respect to taxonomic affinities (Richardson, 1966; Foster, 1979; Beall, 1991). The fossil remains investigated in this study, *i.e.*, a polychaete worm, the jellyfish *Essexella asherae* and a holothurian are preserved in concretions collected from Francis Creek Shale spoil piles of Peabody Coal Company Pit 11 – currently the main source of “Essex-type” (predominantly marine) fossils collected from the Mazon Creek area (Baird, 1979).

Significant attention has been focussed on the remarkable level of detail preserved in fossilised soft parts of the concretion-encapsulated Mazon Creek biota (Nitecki, 1979; Baird *et al.*, 1985a; Baird *et al.*, 1986). While it is now well-understood that this exceptional preservation required both rapid burial and the development of unusual geochemical conditions in direct association with fossil remains, the details of the initial fossilisation process and, even more so, the factors that led to subsequent concretion growth in the Francis Creek Shale remain somewhat ambiguous.

The current level of understanding of Mazon Creek-type preservation draws primarily from studies of Baird *et al.* (1985a, 1986) and Shabica and Hay (1997). Baird *et*

al. (1985a) deduced that very soon after rapid burial and initial (aerobic) soft tissue decomposition, a carcass begins emitting body fluids in an upward-rising plume, creating a decomposition microenvironment characterised by sulphate reduction. Shabica and Hay (1997) surmised that once interstitial sulphate was depleted, methanogenesis reactions would have proceeded, leading to the precipitation of siderite from sediment porewaters and the development of a protective proto-concretion around the organism and associated products of early decay (*e.g.*, iron monosulphide and pyrite). Dewatering within the proto-concretion could then have produced septarian fractures that cut through all previously formed diagenetic features, and would eventually have led to hardening of the cement-indurated body into a rigid concretion. That the remains preserved within the concretions retain at least some degree of three-dimensional relief and that, when observed *in situ*, the concretions are draped above and below by sediment layers, indicates that the process of concretion growth must have occurred fairly quickly (*i.e.* while the sediment was still soft) (Baird *et al.*, 1986).

Microorganisms are thought to have played a major role in the precipitation of authigenic minerals that appears essential for exceptional fossil preservation. It is thus conceivable that microbial biomarkers or other evidence for microbial activity may still be present within such mineralised remains. Concretions, in particular, might be good candidates for the search for such evidence owing to their presumed early diagenetic origin (Woodland and Stenstrom, 1979; Pye, 1984) and their apparently close association with microbial activity (Baird *et al.*, 1986; Hendry *et al.*, 2006).

As part of the present thesis project, Mazon Creek concretions were studied using multiple analytical techniques, *i.e.*, scanning electron microscopy (SEM), energy dispersive spectroscopy (EDS), micro-x-ray diffraction (μ XRD) and time-of-flight secondary ion mass spectrometry (ToF-SIMS), to help clarify the role microbes play in concretion formation, with the aim of gaining a better understanding of the fossilisation process and types of tissues preserved. All of these techniques allow for non-destructive, in situ sample analysis, which is particularly useful for determination of spatial relationships between and among concretion sediment clasts, diagenetic minerals, microbial textures and organic remnants. Such relationships may hold important clues to mechanisms of both exceptional fossil preservation and subsequent concretion formation.

As knowledge of organism preservation potential and the mechanisms of fossilisation and concretion formation improve, reconstructions of ancient ecosystems will become more accurate. As well, being able to identify organic remains within concretions is a necessary step prior to further analysis for specific biomarkers and the microbes that mediate siderite concretion formation.

2.2 METHODS

2.2.1 Sample preparation

The Mazon Creek concretions studied herein were found by amateur fossil collectors in the spoil piles of Peabody Coal Company Pit 11 (Mazon Creek Area,

northeastern Illinois), and were donated to the University of Western Ontario (UWO) by the Royal Ontario Museum (ROM). At the ROM, the concretions were stored outdoors (on the museum roof), submerged in water and were exposed to annual freeze-thaw cycles for several years. This caused some of them to crack along planes of weakness and exposed their contained fossils. Fossilised remains of a polychaete worm (species uncertain), a jellyfish (presumed to be *Essexella asherae*) and a holothurian (species uncertain), each preserved in an individual concretion, were analyzed in this study.

Polished sections were prepared from concretion slices cut along the fossil plane of the polychaete (3 mm thickness) and holothurian (5 mm thickness), and normal to the fossil plane of the jellyfish (3 mm thickness). A petrographic thin section was also made for the polychaete (cut along the fossil plane). Epoxy was not used in the preparation of polished sections. Thin and polished sections were prepared in the Thin Section Laboratory of the Department of Earth Sciences (UWO) by Mr. Stephen Wood.

2.2.2 Micro-X-ray diffraction

The polychaete thin section was analyzed with a 500 μm beam, on the Bruker D8 DISCOVER micro-X-ray Diffractometer (Dr. Roberta Flemming, Laboratory for X-ray Diffraction and Microdiffraction, UWO). Four spots were analyzed on MC1 (Fig. 1d). Diffraction patterns were analyzed for major mineral phases using Bruker DIFFRAC.EVA software.

2.2.3 Scanning electron microscopy (SEM) and energy dispersive spectroscopy (EDS)

Thin and polished sections were viewed using a Nikon Eclipse LV100POL reflected-light microscope with UV-fluorescence and imaged using a Nikon Digital Sight DS-Ri1 camera.

Polished sections were Pt-coated using a Denton Vacuum Desk II sputter coater (12 mA, 150 sec) or Os-coated (5 nm) using a Filgen Osmium Plasma Coater 80T to reduce charging during examination on a LEO (Zeiss) 1540XB FIB/SEM (Nanofabrication Facility, UWO), operated at 1 kV to produce high-resolution images using a secondary electron detector, and at 10 kV to examine atomic mass contrast using a quadrant backscattered electron detector. The FIB/SEM was equipped with an Oxford Instruments INCAx-sight energy dispersive spectrophotometer (EDS) for qualitative elemental analysis. The voltage for EDS analyses was 10 kV, and spectra were analyzed using Oxford INCA Analytical Software.

2.2.4 Time of flight - secondary ion mass spectrometry (ToF-SIMS)

ToF-SIMS, a technique that can separate molecules and ions based on their mass to charge ratio, is a strong, relatively new, tool for biomarker analysis (Orphan *et al.*, 2001; Thiel *et al.*, 2007). The sample surface is bombarded with a pulsed primary ion beam (*e.g.*, Bi, Cs or Ga) that liberates secondary ions (Cotter, 1997). The secondary ions are accelerated into a flight tube and the time taken for them to reach the detector is used to determine their mass (Cotter, 1997). The heavier the ion, the longer it will take to reach the detector (Cotter, 1997). The ToF-SIMS instrument can reach micron to sub-

micron scale spatial resolutions and mass resolutions (mass, in daltons, over difference in mass) up to 10,000 (Cliff *et al.*, 2002; Orphan and House, 2009).

A region of interest (ROI) (approximately 200 x 200 μm) on each polished section, showing either carbon-enrichment or biological texture, was analyzed further on an Ion-ToF (GMBH) ToF-SIMS IV reflectron type mass spectrometer using a pulsed Bi^+ primary beam (Surface Science Western, UWO). Analyses were conducted in high current bunched mode, and a pulsed electron flood gun was used to neutralise surface charging. A Cs ion beam was used to clean sample surfaces by sputtering, providing a fresh surface for analysis. Data were analyzed using the Ion-ToF (GMBH) Ion-Spec™ and Ion-Image™ software suite. The polychaete worm was scanned 70 times at 2 shots per pixel (1.56 x 1.56 μm). The jellyfish was scanned 100 times at 5 shots per pixel. The holothurian was scanned 100 and 70 times at 2 shots per pixel for the positive and negative spectrum respectively.

2.3 RESULTS

2.3.1 Polychaete worm (PW)

The PW concretion was cut to expose the fossil seen in the polished section (Fig. 2.1A). Macroscopic and hand-lens observations of the pyritised annelid worm revealed the presence of multiple pyrite halos arranged concentrically around the central fossil. The halos are more diffuse with increasing distance from the pyritised worm, and there

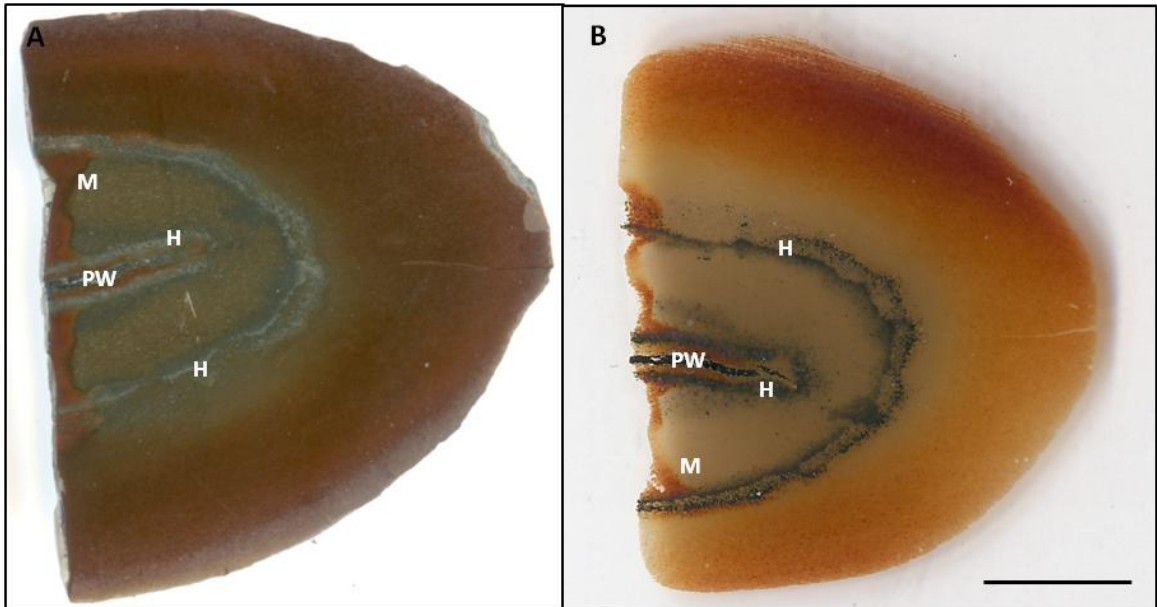


Figure 2.1: Photographs showing A) a polished section and B) a petrographic thin section, scale bar = 5 mm, of the pyritised polychaete worm. The fossil (PW), concentric pyrite halos (H) and matrix (M) are indicated.

is a noticeable gap between the densest pyrite halo, closest to the pyritised worm, and the two closely spaced, more diffuse outer halos.

Micro-X-ray diffraction analyses of the petrographic thin section (Fig. 2.1B) showed the major phase within the fossil region to be pyrite with minor siderite (Fig. 2.2). The major mineral phases within the halos are pyrite, siderite and quartz and within the matrix is siderite and quartz (Fig. 2.2). Minor aluminosilicates were also detected in the matrix (data not shown). The mineral compositions of the detrital grains, matrix and fossil regions respectively, are similar across all pyritised specimens.

Pyrite in the fossilised worm appeared massive in hand-sample (Fig. 2.1A) and under backscattered secondary electron – scanning electron microscopy (BSE-SEM) (Fig. 2.3), and was found to occur as either monocrystalline or polycrystalline pyrite using μ XRD (data not shown). The pyrite in the halos was more diffuse in hand-sample and appeared polycrystalline under BSE-SEM (Fig. 2.3A). In addition to being more disseminated, the pyrite in the halos contained more clay and quartz grains than the fossil region, which may account for its slightly darker colour in BSE micrographs (Fig. 2.3A). The innermost halo appeared polycrystalline and the outer two halos appeared microcrystalline in μ XRD (data not shown). μ XRD scans showed microcrystalline siderite and monocrystalline quartz in the halos. EDS analyses of the worm and halos confirmed that they are composed of Fe and S (Fig. 2.4C).

High resolution imaging of the PW polished section using BSE-SEM confirmed the macroscopic observations, and also revealed the presence of sedimentary materials throughout the siderite matrix (Fig. 2.4A). XRD analysis of the petrographic thin section

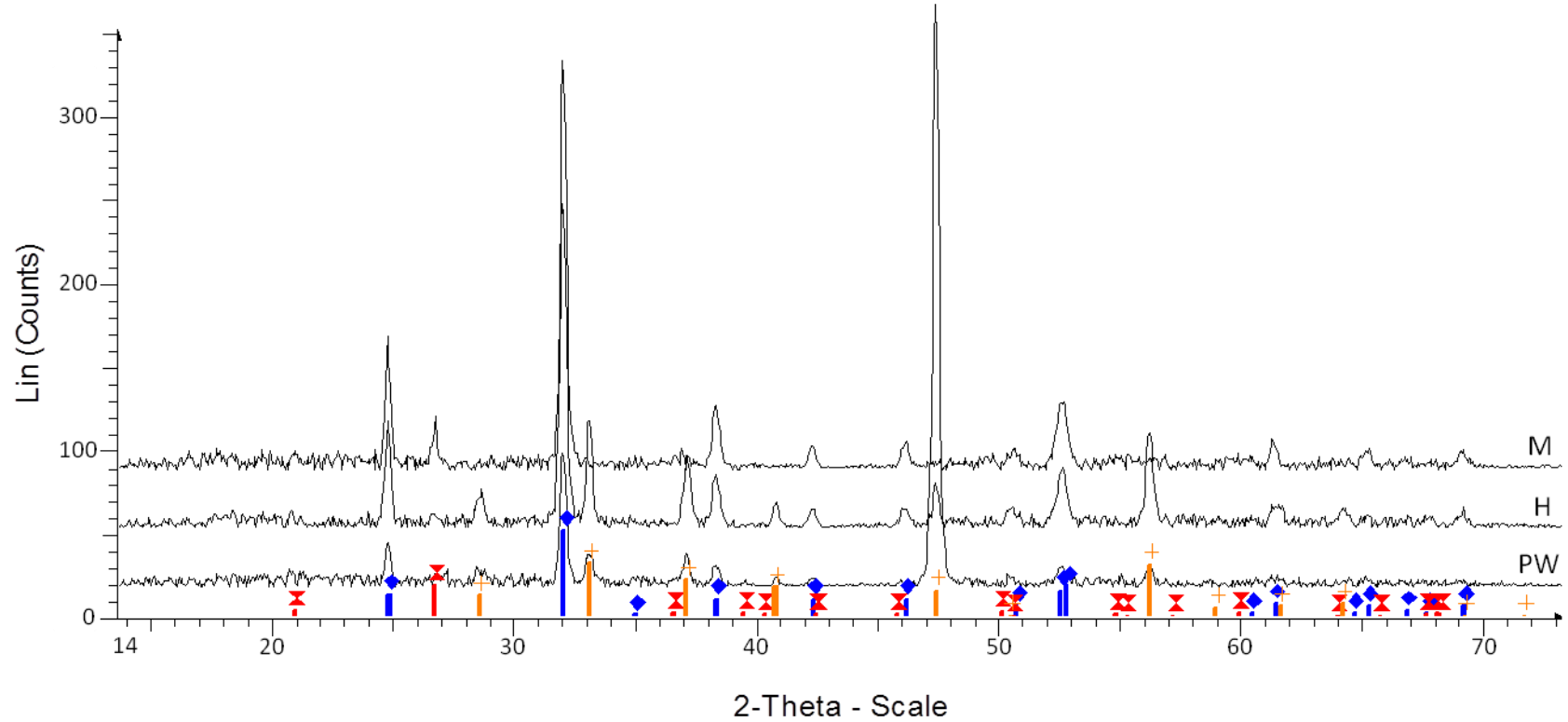


Figure 2.2: XRD scans showing major mineral phases in the PW, halos (H), and matrix (M). Legend: pyrite = +, siderite = \blacklozenge , quartz = X. Scans were taken on the spots indicated in figure 2.1B. Beam size was 500 μm .

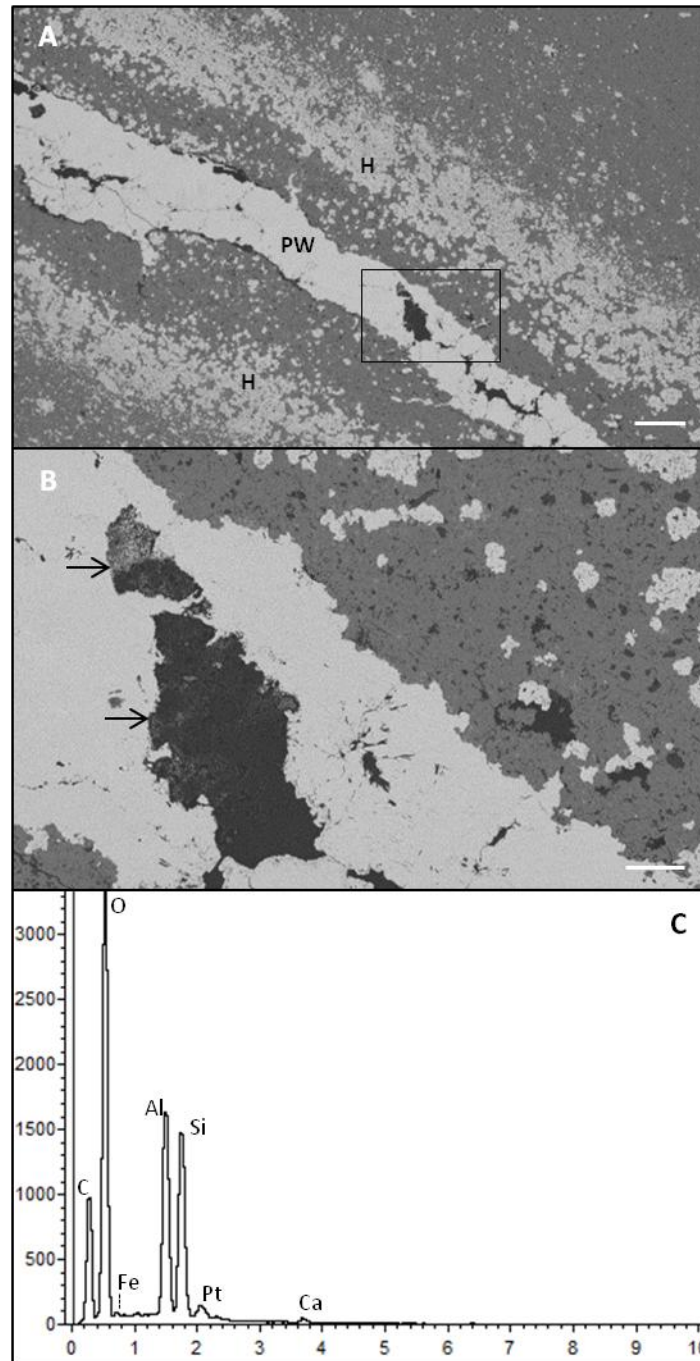


Figure 2.3: Backscattered SEM micrographs showing A) the PW and dense pyrite halo (H), scale bar = 200 μm and B) a magnified view of the fossil inclusions (arrows) from the boxed region in A, scale bar = 40 μm . C) EDS spectrum (x-axis = keV, y-axis = counts) of the fossil inclusions. Pt is from the conductive coating used to prevent sample charging.

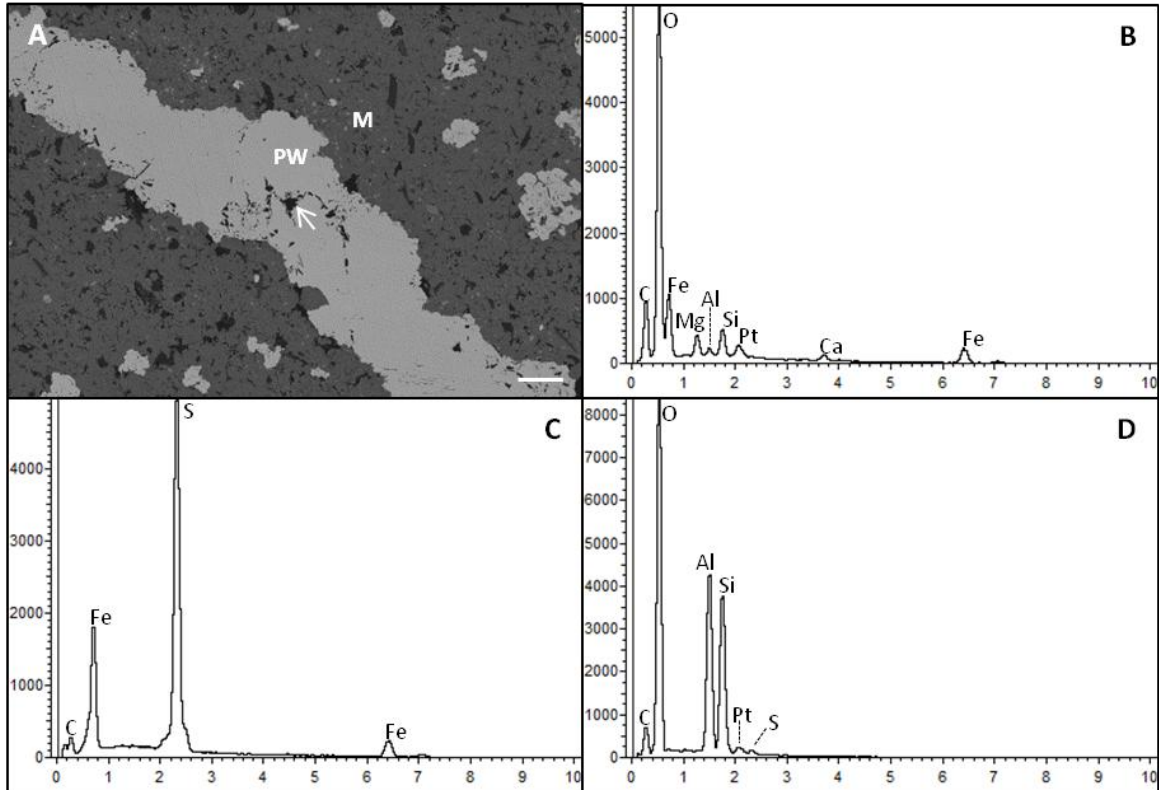


Figure 2.4: A) Backscattered SEM micrograph showing the PW and surrounding matrix with sedimentary inclusions and pyrite flakes, scale bar = 20 μm. EDS spectra (x-axis = keV, y-axis = counts) showing the elemental compositions of: B) the matrix (M); C) the PW; and D) the fossil inclusion (arrow) indicated in A. Pt is from the conductive coating used to prevent sample charging.

showed microcrystalline siderite as the dominant mineral phase comprising the matrix of the concretion, with minor mono- to polycrystalline quartz. SEM, EDS and XRD analyses of the matrix, fossil and sedimentary inclusions revealed that they are composed mainly of siderite, pyrite and aluminosilicate and quartz debris respectively (Fig. 2.4).

BSE-SEM imaging revealed dark inclusions, some with diffuse pyrite, within the fossilised worm (Fig. 2.3B). EDS analysis of one of the inclusions showed increased carbon (Fig. 2.3C). ToF-SIMS spectra (Fig. 2.5) of the carbon-rich inclusion showed a large number of ions with repetitive clusters of peaks, especially above 200 Da.

2.3.2 Jellyfish: *Essexella asherae*

The jellyfish concretion was opened by weathering, which caused it to crack along the fossil plane, exposing the pyritised *Essexella asherae* specimen within (Fig. 2.6A). Macroscopic and hand-lens observations of the concretion surface revealed the presence of grainy pyrite within the fossil dome, surrounded by a circular, diffuse grainy pyrite halo. The white mineral seen around the pyrite grains is gypsum or anhydrite (data not shown). The polished section (Fig. 2.6B) was cut normal to the fossil plane. Diffuse pyrite was visible in the fossil region as well as in the halo. The pyrite in the halo continued below the fossil plane, as can be seen by diffuse pyrite present within the polished section.

In high-resolution BSE-SEM images, the pyrite in the halo appears polycrystalline and disaggregated, and sedimentary inclusions are present throughout the concretion

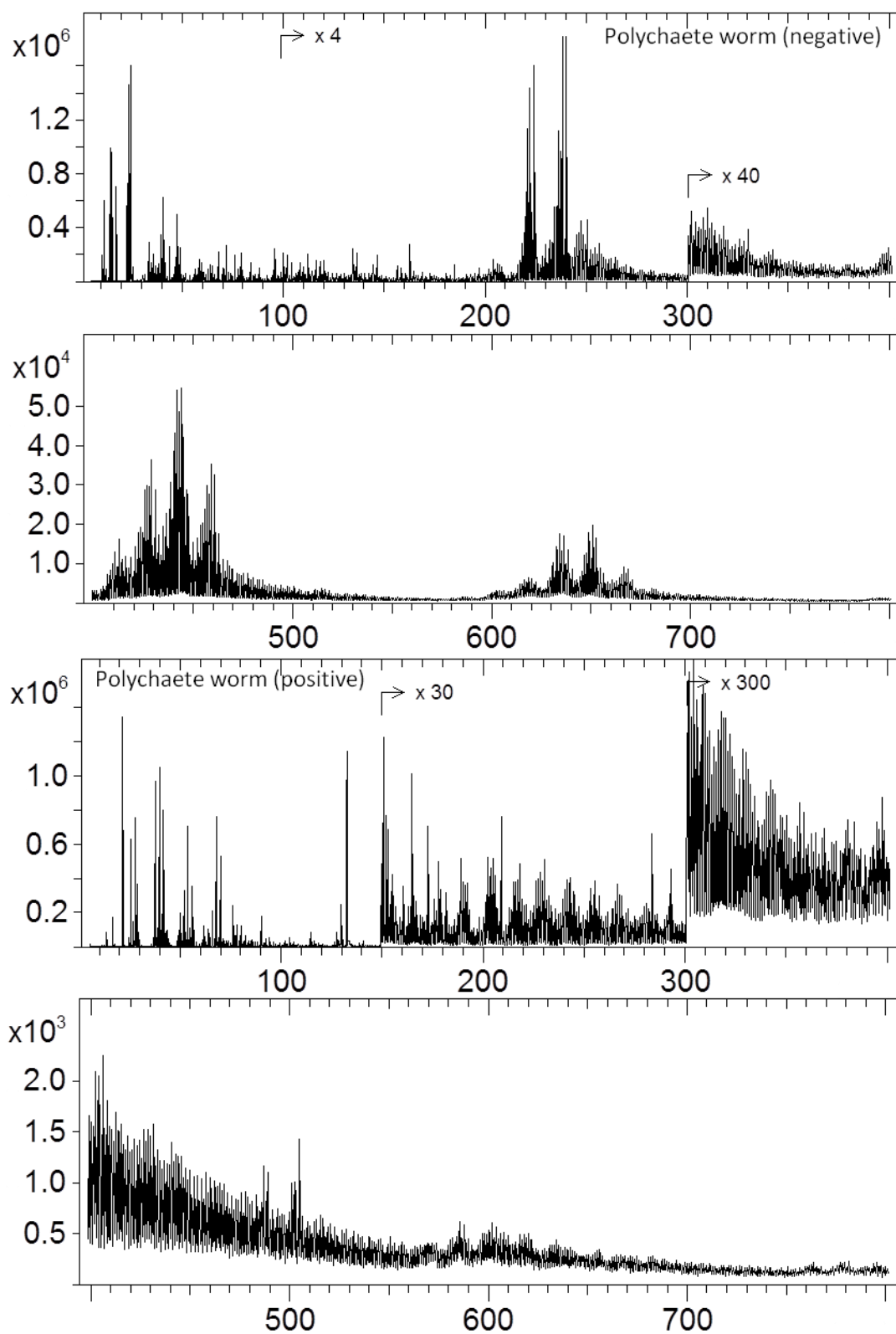


Figure 2.5: Negative- and positive-ion ToF-SIMS spectra (x-axis = mass in Da, y-axis = intensity) of the region indicated in Fig. 2.3A. The ion intensities of peaks beyond the multipliers have been exaggerated for visualisation purposes.

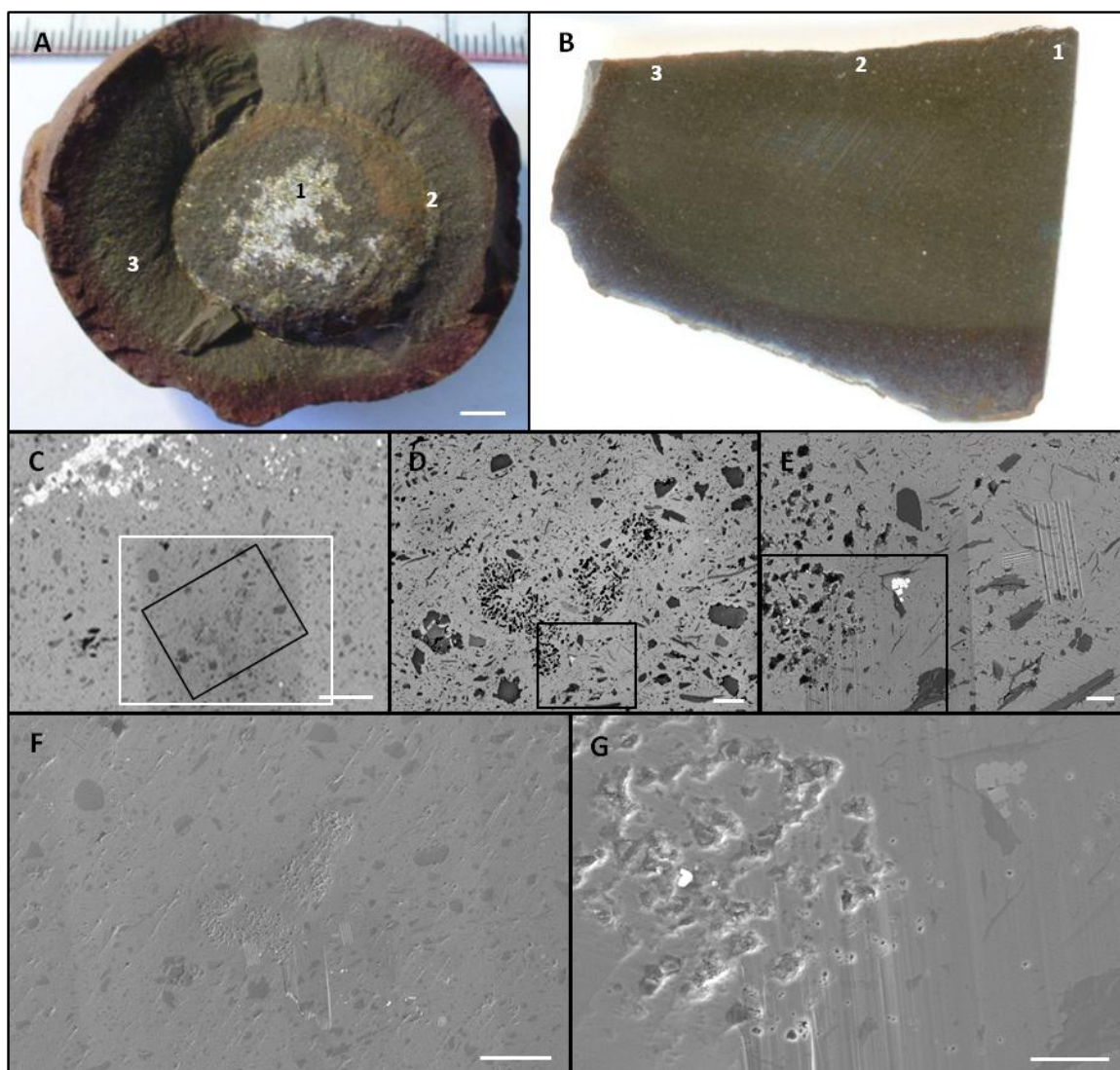


Figure 2.6: Photographs showing A) a jellyfish (*Essexella asherae*) concretion cracked open along the fossil plane, scale bar = 5 mm and B) a polished section cut perpendicular to the fossil plane, which lies along the top edge. The fossil (1), pyrite halo (2) and matrix (3) are indicated in A and B. High-resolution backscattered SEM micrographs showing: C) the polished section in B with the fossil plane at the top edge, scale bar = 200 μm ; D) a magnified view of the region indicated by the black box in C, scale bar = 40 μm ; and E) a magnified view of the region indicated in D (the lines on the right were FIB-milled to mark the ROI), scale bar = 10 μm . High-resolution secondary SEM micrographs showing: F) a magnified view of the region indicated by the white box in C, scale bar = 100 μm ; and G) a magnified view of the region indicated in E, scale bar = 10 μm .

matrix (Fig. 2.6C). EDS analysis confirmed that the halo and fossil consist of Fe and S, the matrix of Fe, C and O, with some Mg and Ca, and the sedimentary inclusions of Fe, K, Mg, Al, Si and O (Fig. 2.7).

A magnified view of the region indicated in figure 2.6C showed an area with spongy texture within the halo (Fig. 2.6D,E, Fig. 2.7). Secondary electron micrographs of the region confirmed that the dark spots seen in backscattered electron images were not holes in the polished section (Fig. 2.6 F,G). EDS analysis of the aggregated structures showed carbon enrichment (Fig. 2.8) and ToF-SIMS spectra once again revealed a large number of ions above 200 Da (Fig. 2.9).

2.3.3 Holothurian

The holothurian was exposed by weathering that caused the concretion to crack along the fossil plane (Fig. 2.10A). Unlike the PW and jellyfish fossils, the holothurian did not possess significant pyrite and did not have a mineralised halo. Macroscopic and hand-lens observations of the concretion surface, showed a network of cracks running throughout the fossil, filled with a white mineral.

The polished section (Fig. 2.10B) was cut from the region indicated in the fossil plane. A small amount of mineral containing Fe and S (Fig. 2.11E), and resembling pyrite in brightness under BSE-SEM (Fig. 2.11A) was seen in the cracks; however, its occurrence is not widespread.

High-resolution BSE-SEM imaging of the fossil region showed that the cracks running throughout the fossil are darker than the matrix material, and consist of C, O, Al

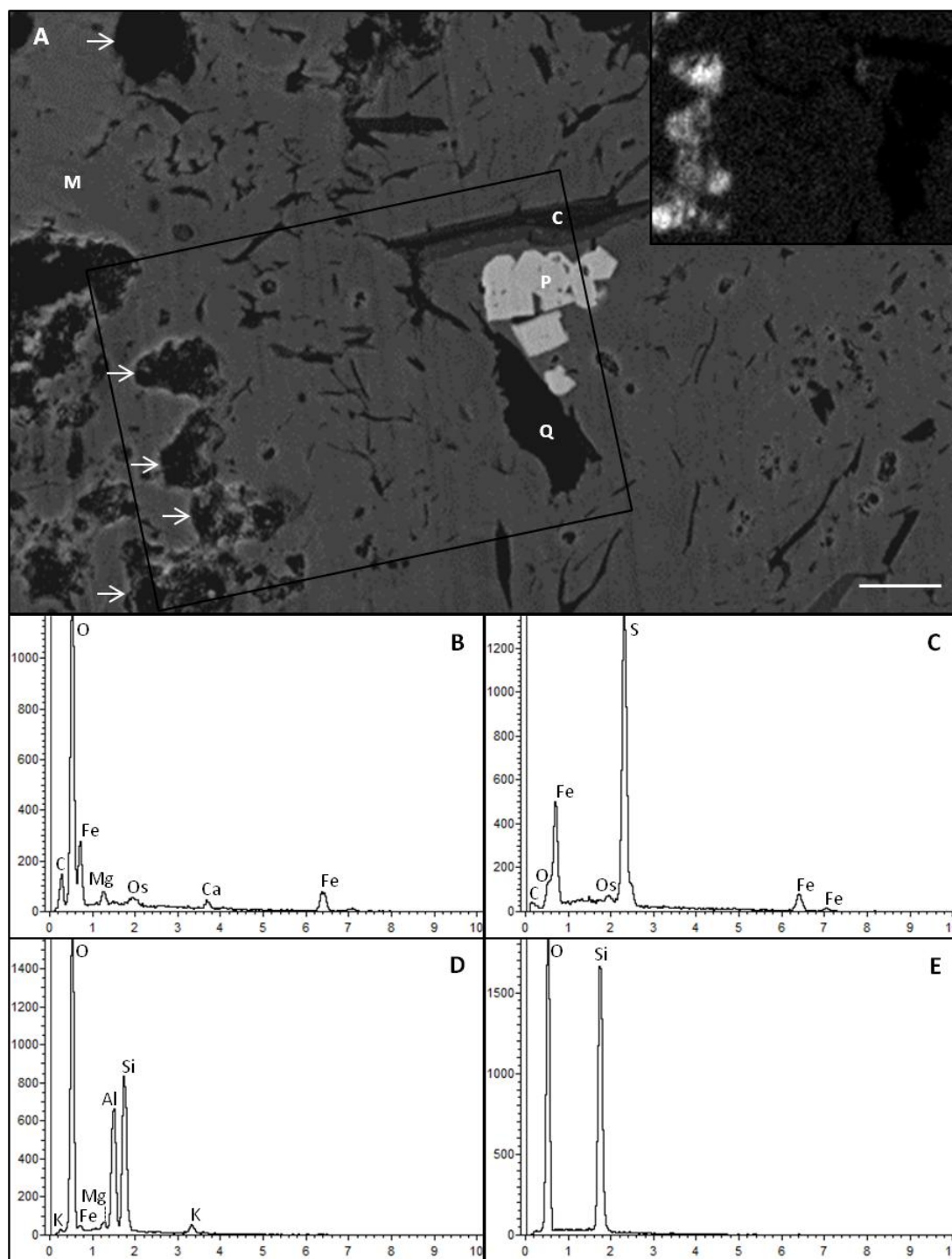


Figure 2.7: A) Backscattered SEM micrograph showing a magnified view of the pyrite grains and C-rich aggregates (arrows) within the region of interest shown in Fig. 2.6E, scale bar = 4 μm. Inset shows an EDS elemental map of carbon in the region indicated, with higher carbon areas appearing brighter. EDS spectra (x-axis = keV, y-axis = counts) showing the elemental compositions of: B) the matrix (M); C) the pyrite grains (P); D) the clay (C); and E) the quartz (Q) indicated. Os is from the conductive coating used to prevent sample charging.

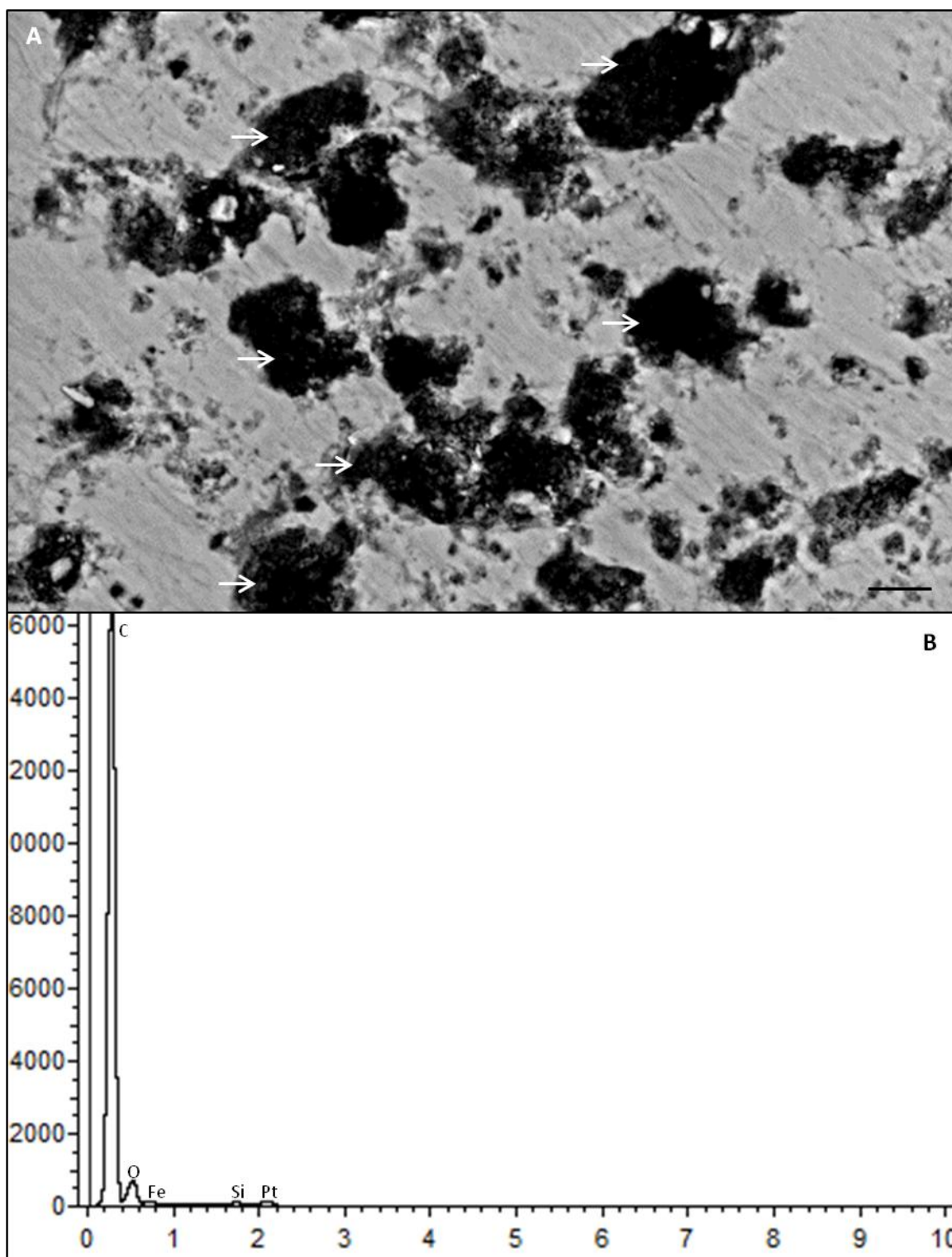


Figure 2.8: A) Backscattered SEM micrograph showing a magnified view of the C-rich aggregates (arrows) in Fig. 2.6E, scale bar = 2 μm . B) EDS spectrum of an aggregate (x-axis = keV, y-axis = counts). Pt is from the conductive coating used to prevent sample charging.

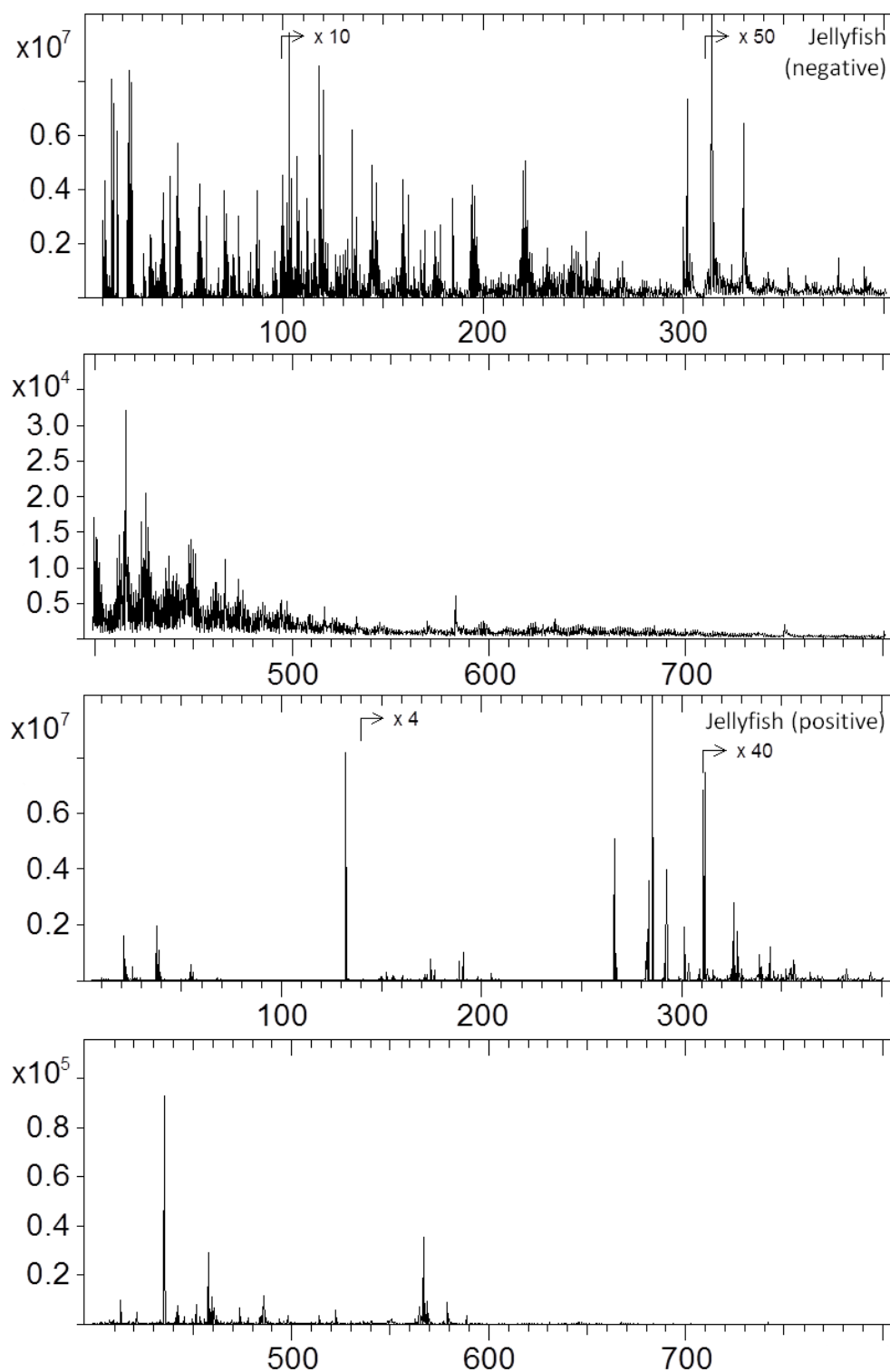


Figure 2.9: Negative- and positive-ion ToF-SIMS spectra (x-axis = mass in Da, y-axis = intensity) of the region containing carbon-enriched aggregated structures and pyrite (indicated in Fig. 2.6E). The ion intensities of peaks beyond the multipliers have been exaggerated for visualisation purposes.

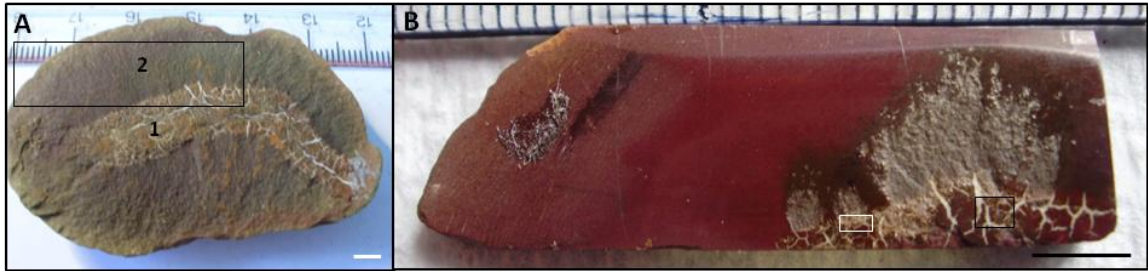


Figure 2.10: Photographs showing A) a holothurian concretion cracked open along the fossil plane and B) a polished section cut from the boxed region in A, scale bars = 5 mm. The fossil (1) and matrix (2) are indicated in A. High-resolution BSE-SEM images of the white and black boxes are found in figures 2.12 and 2.11 respectively.

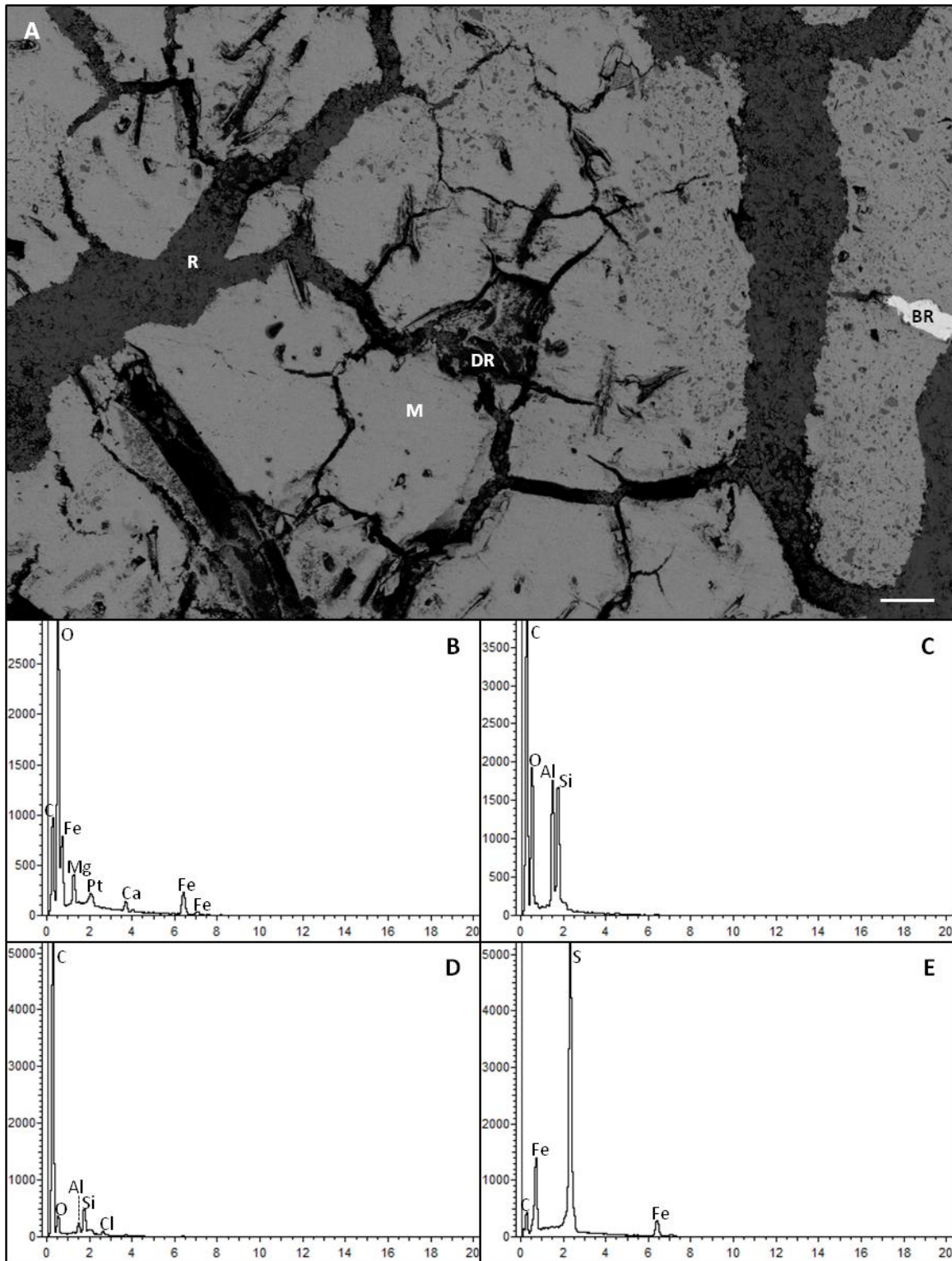


Figure 2.11: A) Backscattered SEM micrograph showing a magnified view of the fossil region indicated in the black box in Fig. 2.10B, scale bar = 100 μm. EDS spectra (x-axis = keV, y-axis = counts) showing the elemental composition of: B) the matrix (M), C) the reticulate cracks (R), D) the dark region (DR), and E) the bright region (BR) indicated in A. Pt is from the conductive coating used to prevent sample charging.

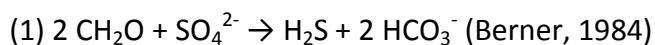
and Si (Fig. 2.11C). The dark regions within the cracks are enriched in carbon and contain some Al, Si, O and Cl (Fig. 2.11D).

The remainder of the fossil and the matrix consist of C, O, Fe, Mg and Ca (Fig. 2.11A) and a weathered rust-coloured mineral in some regions. Sedimentary inclusions were seen dispersed throughout the matrix. A region of interest (Fig. 2.12) containing carbonaceous features was selected for ToF-SIMS analysis. As in the PW and jellyfish samples, ToF-SIMS mass spectra showed several peaks above 200 Da (Fig. 2.13).

2.4 DISCUSSION

2.4.1 Sulphate reduction and pyritisation

XRD and EDS results show that some soft bodied Mazon Creek organisms are preserved as pyrite films surrounded by pyrite halos. Pyrite, which appears bright under BSE-SEM, must have formed soon after the initial anoxic decomposition of buried organisms by sulphate reducing bacteria (SRB) (Woodland and Stenstrom, 1979). These bacteria oxidise organics for energy, reducing seawater sulphate to hydrogen sulphide in the process (Equation 1). The hydrogen sulphide reacts with available Fe^{2+} ions to produce metastable iron monosulphides (Equation 2), such as mackinawite and greigite (Berner, 1984; Allison, 1988). Mackinawite (Equations 3 and 4) and greigite can react with remnant H_2S or S^0 , if available, to form authigenic pyrite (Allison, 1988).



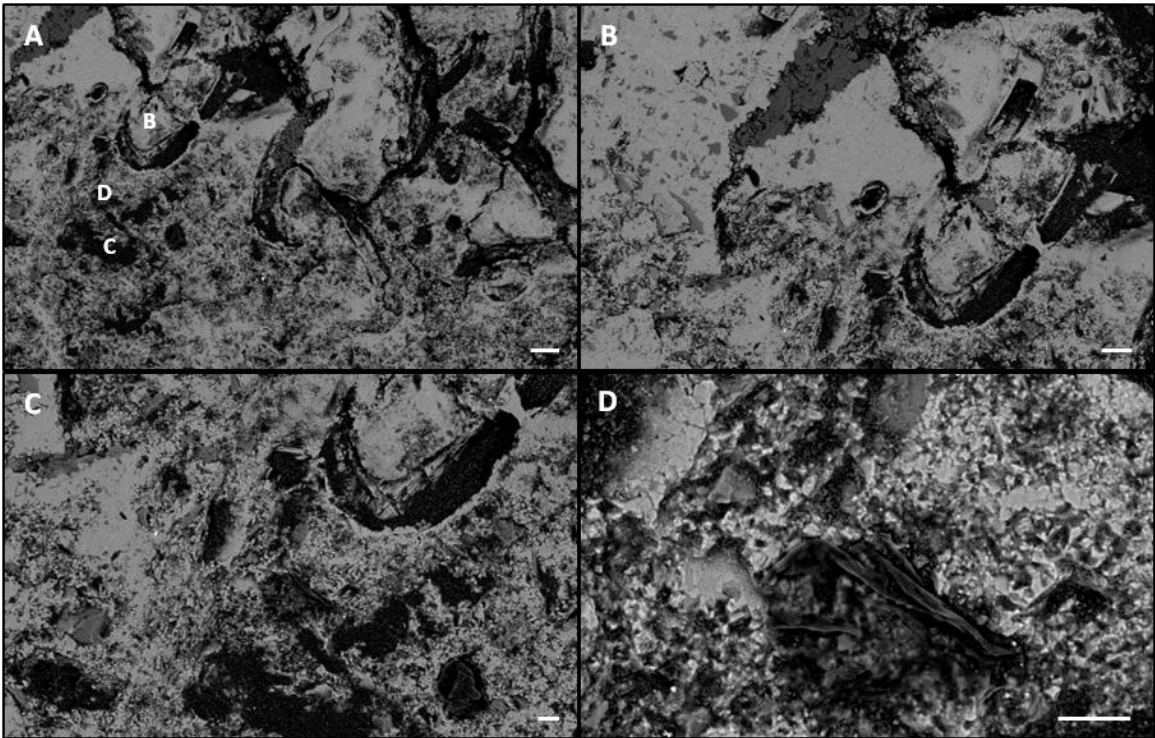


Figure 2.12: Backscattered SEM micrographs showing a magnified view: A) of the fossil region indicated by the white box in Fig. 2.10B, scale bar = 30 μm ; B), C) and D) the features indicated in A, scale bars = 20, 10 and 10 μm respectively.

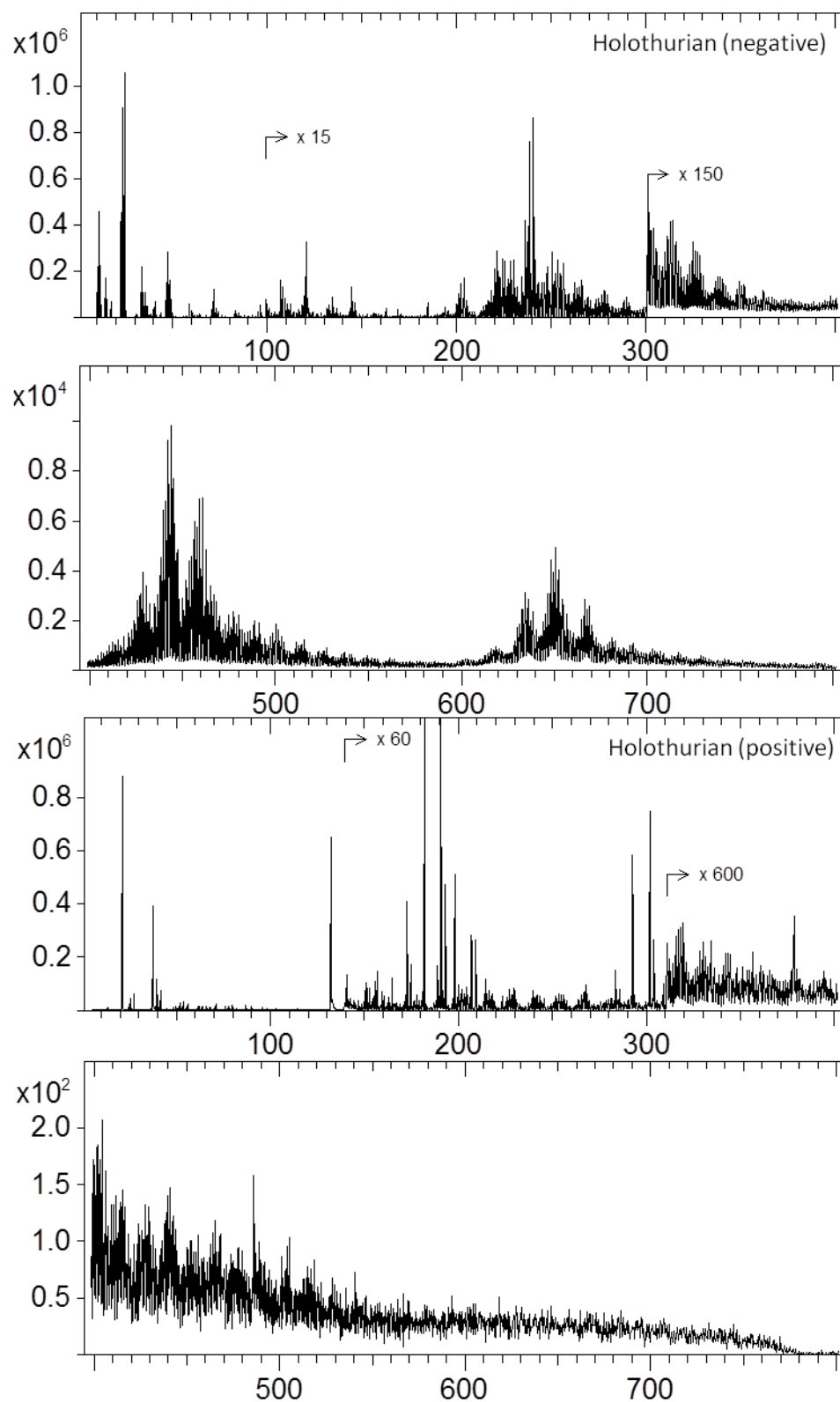
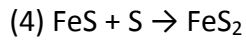
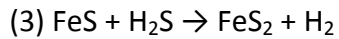
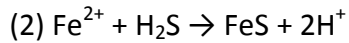


Figure 2.13: Negative- and positive-ion ToF-SIMS spectra (x-axis = mass in Da, y-axis = intensity) of the region indicated in Fig. 2.12A. The ion intensities of peaks beyond the multipliers have been exaggerated for visualisation purposes.



The major controls on pyrite formation in brackish environments are porewater sulphate concentration, presence of organics and presence of reactive detrital iron minerals (Berner, 1984). In the Mazon Creek area, the organics came from decomposing native organisms and other organic detritus in sediments brought in during tidal cycles and delta progradation events (Baird *et al.*, 1985a). There were several possible sources of reactive iron in Mazon Creek sediments: 1) iron oxyhydroxide coatings on clastic sediments; 2) exchangeable cations in clays; 3) dissolved iron in river water; or 4) upwelling interstitial waters expelled during compression of the underlying Colchester peat (Woodland and Stenstrom, 1979). This suggests that sulphate was the limiting reagent for pyritisation in Mazon Creek fossils.

Concretion pyrite can vary from massive, as in the polychaete worm, to disseminated, as in the jellyfish and halos. Pyrite could be more crystalline closer to the fossil region because this is the zone of major SO_4^{2-} reduction, and therefore H_2S production (Woodland and Stenstrom, 1979). As ferrous iron is believed to have been non-limiting in the Mazon Creek area, the H_2S presumably did not diffuse far from decomposing organisms before precipitating as FeS (Woodland and Stenstrom, 1979). Through diagenesis, this FeS produced pyritised replicates of soft-bodied organisms. The pyrite halos surrounding some fossils may represent multiple decomposition fronts

created by the differing degradation rates of various biological tissues (*i.e.*, soft tissue vs. chitin vs. bone) (Allison, 1988; Briggs and Kear, 1993). Halos appear to be three-dimensional, which supports the idea of decomposition fronts; additionally, in the PW, they become increasingly diffuse as you move away from the fossil, suggesting the dilution of easily degradable organics and decomposition products with increasing distance from the carcass.

Remnants resembling framboidal pyrite are visible in some concretions, especially in regions with diffuse pyrite. Neumann *et al.* (2005) found framboidal pyrite in Achterwasser lagoon surface sediments. Achterwasser sediments are reducing and sulphidic, but the sediment-water interface is oxidizing and estuarine with low sulphate concentrations. These conditions can promote longer framboid nucleation and growth times than euxinic basins (Neumann *et al.*, 2005). The brackish conditions at Mazon Creek presumably provided a similar environment, with anoxic sediments underlying a shallow, oxic water column; however, pyrite formation in the Achterwasser lagoon is limited by the availability of aqueous Fe^{2+} and oxidants to convert FeS to pyrite, whereas in Mazon Creek sulphate was limiting (Neumann *et al.*, 2005). Framboidal pyrite forms preferentially over euhedral pyrite in anoxic FeS_2 supersaturated environments, where the pyrite nucleation rate exceeds its crystal growth rate (Neumann *et al.*, 2005; MacLean *et al.*, 2008). Dellwig *et al.* (2001) discovered framboidal pyrite in a Holocene coastal peat environment, where marine transgressive and regressive cycles created intermittent brackish conditions. Pyrite within the more limnic peat layers was polyframboidal, whereas pyrite within the more marine lagoonal sediment layers was

framboidal adjacent to an organic matrix and euhedral in diatom frustule infillings (Dellwig *et al.*, 2001). The exact mechanism of framboid formation has not yet been fully resolved, but it is likely to proceed through an Fe_3S_4 intermediate in an environment that is supersaturated with respect to FeS and FeS_2 (Dellwig *et al.*, 2001; MacLean *et al.*, 2008). High pore water concentrations of Fe^{2+} , proximity to organics and high rates of sulphate reduction are also important. Polyframboid formation requires strictly anoxic conditions, which were presumably present at Mazon Creek during pyritisation. This may explain the polycrystalline pyrite aggregates present within the halos and carbon rich fossil inclusions. Euhedral pyrite forms when iron monosulphides react with S^0 and H_2S (Dellwig *et al.*, 2001). If porewaters are undersaturated with respect to FeS, euhedral pyrite can form by direct precipitation, and it has been suggested that pyrite morphology changes from spherulitic to cubic with decreasing pyrite supersaturation. FeS and FeS_2 saturation would have been lower during initial stages of sulphate reduction, which may explain why pyrite in the PW is massive. Pyrite in the jellyfish does not appear massive; however, this may be obscured by the weathering mineral present in the fossil region. A possible explanation for the grainier pyrite is more rapid anaerobic decay, leading to faster FeS and FeS_2 saturation. Sparse euhedral pyrite grains found at the outer edge of pyritised regions can also be attributed to decreased FeS and FeS_2 saturation. Depletion of porewater Fe can contribute to euhedral pyrite formation (Dellwig *et al.*, 2001); however, this is unlikely in Mazon Creek sediments based on the occurrence of siderite as the matrix material in these concretions.

2.4.2 Fossil impressions and weathering minerals

Pyrite is not the sole mineral in all of the Mazon Creek fossils investigated, as demonstrated by the holothurian specimen. Recalcitrant tissues in Mazon Creek fossils can be preserved as molds of sphalerite, kaolinite, calcite, quartz or galena (Schellenberg, 2002). Soft-bodied organisms, such as sea cucumbers, can also be preserved as two-dimensional light-on-dark impressions (Schellenberg, 2002). The reticulate cracks on the holothurian may be due to brittle deformation of the mineralised crust during early sediment compaction. The white mineral infilling the cracks is likely kaolinite (Schellenberg, 2002), as supported by EDS results (Fig. 2.11C). The Cl (Fig. 2.11D) may have been incorporated from seawater.

The white powder in the pyritised region of the jellyfish, on the other hand, is probably a weathering product formed during the freeze-thaw cycles used to break open the concretion. Pyrite oxidises on exposure to surface weathering conditions, producing an acidic solution and freeing Fe^{2+} and SO_4^{2-} ions (Tuttle and Breit, 2009). The acidic solution reacts with calcite, freeing Ca^{2+} , which can then react with the sulphate to form gypsum (Tuttle and Breit, 2009). Jarosite can also be produced from the weathering products; however, with slight increases in pH and exposure to oxygen, the jarosite is weathered to goethite and amorphous Fe(III) oxides (Tuttle and Breit, 2009). The rust-coloured mineral present on exposed jellyfish and holothurian surfaces, and on the outer edges of concretions suggests weathering to amorphous Fe(III) oxides.

2.4.3 Extracellular polysaccharide substances in protoconcretions

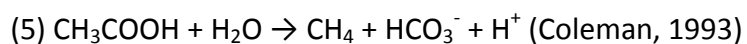
The microbial consortium (SRB, iron-reducers, methanogens etc.) present around a decomposing organism secretes extracellular polysaccharide substances (EPS) (Hendry *et al.*, 2006). This would have reinforced the sediments around decaying Mazon Creek organisms and increased the volume of pore space. The increased pore volume protected the sediments from compaction and syneresis, aiding in the preservation of fossil structures (Hendry *et al.*, 2006). EPS also acts as a nucleation site for mineral precipitation and growth, and was likely the template for subsequent pyritisation and concretion growth (Hendry *et al.*, 2006). The formation of pyrite crusts versus pyrite halos or concretions may depend on the microbes present around a carcass. An SRB dominated biofilm is more likely to produce a pyrite crust, whereas a more physically and metabolically diverse microbial consortium is more likely to produce a concretion (Myrow, 1995; Borkow and Babcock, 2003). In both cases, the EPS promotes mineral precipitation and pyrite nucleation can begin at multiple points within the protoconcretion (Borkow and Babcock, 2003). Metal adsorption would serve to stabilise the EPS in a three-dimensional arrangement (Myrow, 1995; Borkow and Babcock, 2003). SRB dominated biofilms form preferentially on labile tissues and more microbially diverse biofilms form around biomineralised tissues (Woodland and Stenstrom, 1979; Borkow and Babcock, 2003). Intuitively this makes sense, as SRB are only competitive when there is a labile source of organics. When the primary organics are more recalcitrant, SRB would depend on the degradation products of more competitive heterotrophs for their metabolism. The formation of a pyrite crust in the jellyfish

concretion and pyrite halos around the polychaete worm support this theory; however, it fails to explain the formation of a pyrite halo around the jellyfish concretion and multiple pyrite halos around the polychaete worm without the formation of a pyrite concretion.

2.4.4 Iron reduction and siderite precipitation

Iron-reducers convert detrital, secondary Fe^{3+} minerals to soluble Fe^{2+} and produce HCO_3^- in the process (Duan *et al.*, 1996). They have been found in modern salt-marsh siderite concretions, and were presumably present in Mazon Creek sediments (Duan *et al.*, 1996; Romanek *et al.*, 2009). In the presence of H_2S , the ferrous iron precipitated as iron monosulphides, which are more stable than iron carbonates (Duan *et al.*, 1996); however, once the limited sulphate supply was exhausted, iron-reduction would have contributed to the precipitation of protective siderite concretions (Woodland and Stenstrom, 1979; Schellenberg, 2002). Methanogens may also have played a role in the decomposition process (Equation 5) (Woodland and Stenstrom, 1979). Sulphate reduction and anaerobic decay of protein increase the pH around organisms through production of bicarbonate and ammonia respectively (Allison, 1988; Coleman, 1993). Increased pH in association with high concentrations of Fe^{2+} would have resulted in precipitation of siderite in the pore spaces of proto-concretions (Berner *et al.*, 1979). Siderite is the major mineral phase in the matrix of Mazon Creek concretions, and in light-on-dark fossil impressions. Siderite was found to be microcrystalline in μXRD analyses of the PW, and previous studies have shown that siderite crystals can be under

10 μm in several environments of formation. Siderite concretions from an intertidal marsh in Norfolk, England were found to contain spherules approximately 5 μm in size (Pye, 1984). Siderite precipitated by *Shewanella putrefaciens* during reduction of hydrous ferric oxide and oxidation of pyruvate was composed of spherules up to 10 μm in size (Salas *et al.*, 2009). An inorganic siderite precipitation experiment produced 8 μm siderite rhombohedra after one year of incubation (Jimenez-Lopez and Romanek, 2004). Varying colour in the siderite matrix between different concretions is the result of a combination of factors, including: minor phase minerals, such as clays and quartz; secondary weathering minerals; and intuitively, microbial activity during formation (Duan *et al.*, 1996).



2.4.5 Detrital grains

Quartz and clays comprise the main sedimentary inclusions within the siderite matrix, with quartz occurring in both polycrystalline and monocrystalline forms. Both poly- and monocrystalline quartz could have come from immature clastic sediments deposited in the Illinois basin by a large southwestward-flowing river system, which delivered the majority of Pennsylvanian sedimentation to the Illinois Basin from the southeastern flanks of the Appalachian geosynclinal belt (Potter and Pryor, 1961). Monocrystalline quartz may also have been authigenic. μXRD did not reveal the presence of aluminosilicates in the PW concretion; however, they were apparent in all

concretions under SEM and EDS. Previous XRD analyses of Mazon Creek concretions have revealed illite, chlorite, kaolinite and mixed-layer clays (Woodland and Stenstrom, 1979). Detrital clays were also introduced to the coastal estuary as fluvial sediment influx from tectonic uplift of the Appalachian geosynclinal belt between the middle Pennsylvanian and early Cretaceous (Potter and Pryor, 1961; Baird *et al.*, 1985a; Neumann *et al.*, 2005). This uplift supplied immature sediments and some crystalline rocks to the coastal plain and shallow marine shelf of the Illinois basin (Potter and Pryor, 1961). The Pennsylvanian subgraywacke sandstones of the Illinois basin were high in polycrystalline quartz and contained the same clays found in Mazon Creek concretions (Potter and Pryor, 1961).

2.4.6 Organic preservation

Several features within the concretions were enriched in carbon, which appeared black under BSE-SEM. The carbon-rich aggregates in the jellyfish halo (Fig. 2.7) were 2 μm to 4 μm in diameter, and may represent cellular remains. The high C-content, as well as the dark grain colour under BSE-SEM, may be due to preservation of organics. An array of peaks above 100 Da is indicative of organics because organic macromolecules are large, and can produce a range of light to heavy molecular fragments when exposed to a ToF-SIMS beam (Wanger, 2008). Inorganic compounds are usually composed of smaller molecules that fragment in predictable ways and repeatedly produce peaks at specific mass numbers, as opposed to the diverse range of peaks seen in this study. As well, inorganic molecular fragments are usually concentrated in the region below 100

Da. The ToF-SIMS spectra observed resembled those seen in experiments done by Wanger (2008), on samples of *Plectonema boryanum* that were exposed to different temperatures and pressures for varying times.

Fatty acids have been found preserved in Cretaceous cemented mudstone concretions (Pearson and Nelson, 2005). Biomarkers may also be preserved in Mazon Creek concretions, as determined from C content, cell-like aggregates and ToF-SIMS spectra; however, further analysis is needed to determine what these might be. The observed diversity in organic structures within concretions combined with the detection of nitrogen, which is rare in sedimentary systems, during a ToF-SIMS study by Alaina Hills (2006, personal communication), suggests that intact cells may have become entombed, *i.e.*, permineralised (Preston *et al.*, 2011), within the concretion. The weathering of the holothurian concretion may have contaminated the organics preserved on the fossil surface; however, the sampling regions on the polychaete worm and jellyfish were cut from areas that were not exposed to weathering.

2. REFERENCES

- Allison, P.A., 1988, The role of anoxia in the decay and mineralisation of proteinaceous macro-fossils: *Paleobiology*, v. 14, no. 2, p. 139-154.
- Baird, G.C., 1979, Lithology and fossil distribution, Francis Creek Shale in northeastern Illinois. *in* Nitecki, M.H., ed., *Mazon Creek fossils: New York, NY, Academic Press*, p.41-67.
- Baird, G.C., and Sroka, S.D., 1990, Geology and geohistory of Mazon Creek area fossil localities, Illinois, *in* Hammer, W.R., and Hess, D.F., eds., *Geology Field Guidebook: Current Perspectives on Illinois Basin and Mississippi Arch Geology: Macomb, IL, Geological Society of America, 24th Annual Meeting of the North-Central Section*, p. C1-C70.
- Baird, G.C., Shabica, C.W., Anderson, J.L., and Richardson, E.S., Jr., 1985a, Biota of a Pennsylvanian muddy coast: habitats within the Mazonian delta complex, northeast Illinois: *Journal of Paleontology*, v. 59, no. 2, p. 253-281.
- Baird, G.C., Sroka, S.D., Shabica, C.W., Beard, T.L., Scott, A.C., and Broadhurst, F.M., 1985b, Mazon Creek-type fossil assemblages in the U.S. midcontinent Pennsylvanian: their recurrent character and palaeoenvironmental significance [and discussion]: *Philosophical Transactions of the Royal Society of London. Series B, Biological Sciences*, v. 311, no. 1148, *Extraordinary Fossil Biotas: Their Ecological and Evolutionary Significance*, p. 87-99.
- Baird, G.C., Sroka, S.D., Shabica, C.W., and Kuecher, G.J., 1986, Taphonomy of middle Pennsylvanian Mazon Creek Area fossil localities northeast Illinois, USA : significance of exceptional fossil preservation in syngenetic concretions: *Palaios*, v. 1, no. 3, p. 271-285.
- Beall, B.S., 1991, The Tully Monster and a new approach to analyzing problematica, *in* Simonetta, A.M., and Morris, S.C., eds., *The Early Evolution of Metazoa and the Significance of Problematic Taxa: New York, NY, Cambridge University Press*, p. 271-285.
- Berner, R.A., 1984, Sedimentary pyrite formation - an update: *Geochimica et Cosmochimica Acta*, v. 48, no. 4, p. 605-615.
- Berner, R.A., Baldwin, T., and Holdren, G.R., 1979, Authigenic iron sulfides as paleosalinity indicators: *Journal of Sedimentary Petrology*, v. 49, no. 4, p. 1345-1350.

- Borkow, P.S., and Babcock, L.E., 2003, Turning pyrite concretions outside-in: role of biofilms in pyritisation of fossils: *The Sedimentary Record*, v. 1, no. 3, p. 4-7.
- Briggs, D.E.G., and Kear, A.J., 1993, Decay and preservation of polychaetes: taphonomic thresholds in soft-bodied organisms: *Paleobiology*, v. 19, no. 1, p. 107-135.
- Cliff, J.B., Gaspar, D.J., Bottomley, P.J., and Myrold, D.D., 2002, Exploration of inorganic C and N assimilation by soil microbes with time-of-flight secondary ion mass spectrometry: *Applied and Environmental Microbiology*, v. 68, no. 8, p. 4067-4073.
- Coleman, M.L., 1993, Microbial processes - controls on the shape and composition of carbonate concretions: *Marine Geology*, v. 113, no. 1-2, p. 127-140.
- Cotter, R.J., 1997, Time-of-flight mass spectrometry: instrumentation and applications in biological research: Washington, DC, American Chemical Society, 326 p.
- Dellwig, O., Watermann, F., Brumsack, H.J., Gerdes, G., and Krumbein, W.E., 2001, Sulphur and iron geochemistry of Holocene coastal peats (NW Germany): a tool for palaeoenvironmental reconstruction: *Palaeogeography Palaeoclimatology Palaeoecology*, v. 167, no. 3-4, p. 359-379.
- Duan, W.M., Hedrick, D.B., Pye, K., Coleman, M.L., and White, D.C., 1996, A preliminary study of the geochemical and microbiological characteristics of modern sedimentary concretions: *Limnology and Oceanography*, v. 41, no. 7, p. 1404-1414.
- Foster, M.W., 1979, A reappraisal of *Tullimonstrum gregarium*, in Nitecki, M.H., ed., *Mazon Creek Fossils*: New York, NY, Academic Press, p.269-302.
- Hendry, J.P., Pearson, M.J., Trewin, N.H., and Fallick, A.E., 2006, Jurassic septarian concretions from NW Scotland record interdependent bacterial, physical and chemical processes of marine mudrock diagenesis: *Sedimentology*, v. 53, no. 3, p. 537-565.
- Jimenez-Lopez, C., and Romanek, C.S., 2004, Precipitation kinetics and carbon isotope partitioning of inorganic siderite at 25 degrees C and 1 atm: *Geochimica et Cosmochimica Acta*, v. 68, no. 3, p. 557-571.
- MacLean, L.C.W., Tyliczszak, T., Gilbert, P.U.P.A., Zhou, D., Pray, T.J., Onstott, T.C., and Southam, G., 2008, A high-resolution chemical and structural study of framboidal pyrite formed within a low-temperature bacterial biofilm: *Geobiology*, v. 6, no. 5, p. 471-480.
- Myrow, P.M., 1995, Thalassinoides and the enigma of early paleozoic open-framework burrow systems: *Palaios*, v. 10, no. 1, p. 58-74.

- Neumann, T., Rausch, N., Leipe, T., Dellwig, O., Berner, Z., and Bottcher, M.E., 2005, Intense pyrite formation under low-sulfate conditions in the Achterwasser Lagoon, SW Baltic Sea: *Geochimica et Cosmochimica Acta*, v. 69, no. 14, p. 3619-3630.
- Nitecki, M.H., 1979, Mazon Creek fauna and flora -- a hundred years of investigation, *in* Nitecki, M.H., ed., *Mazon Creek fossils*: New York, NY, Academic Press, p. 1-11.
- Orphan, V.J., and House, C.H., 2009, Geobiological investigations using secondary ion mass spectrometry: microanalysis of extant and paleo-microbial processes: *Geobiology*, v. 7, no. 3, p. 360-372.
- Orphan, V.J., House, C.H., Hinrichs, K.U., McKeegan, K.D., and DeLong, E.F., 2001, Methane-consuming archaea revealed by directly coupled isotopic and phylogenetic analysis: *Science*, v. 293, no. 5529, p. 484-487.
- Pearson, M.J., and Nelson, C.S., 2005, Organic geochemistry and stable isotope composition of New Zealand carbonate concretions and calcite fracture fills: *New Zealand Journal of Geology and Geophysics*, v. 48, no. 3, p. 395-414.
- Potter, P.E., and Pryor, W.A., 1961, Dispersal centers of Paleozoic and later clastics of the Upper Mississippi Valley and adjacent areas: *Geological Society of America Bulletin*, v. 72, no. 8, p. 1195-1249.
- Preston, L.J., Shuster, J., Fernandez-Remolar, D., Banerjee, N.R., Osinski, G.R., and Southam, G., 2011, The preservation and degradation of filamentous bacteria and biomolecules within iron oxide deposits at Rio Tinto, Spain: *Geobiology*, v. 9, no. 3, p. 233-249.
- Pye, K., 1984, SEM analysis of siderite cements in intertidal marsh sediments, Norfolk, England: *Marine Geology*, v. 56, no. 1-4, p. 1-12.
- Rao, V.P., Kessarkar, P.M., Nagendra, R., and Babu, E.V.S.S.K., 2007, Origin of Cretaceous phosphorites from the onshore of Tamil Nadu, India: *Journal of Earth System Science*, v. 116, no. 6, p. 525-536.
- Richardson, E.S., Jr., 1966, Wormlike fossil from the Pennsylvanian of Illinois: *Science*, v. 151, no. 3706, p. 75-76.
- Richardson, E.S., Jr., and Johnson, R.G., 1971, The Mazon Creek faunas, *in* *Proceedings of the North American Paleontological Convention: Field Museum of Natural History, Chicago, September 5-7, 1969, Volume 1*: Lawrence, KS, Allen Press, p. 1222-1235.
- Romanek, C.S., Jimenez-Lopez, C., Rodriguez-Navarro, A., Sanchez-Roman, M., Sahai, N., and Coleman, M., 2009, Inorganic synthesis of Fe-Ca-Mg carbonates at low temperature: *Geochimica et Cosmochimica Acta*, v. 73, no. 18, p. 5361-5376.

- Salas, E.C., Berelson, W.M., Hammond, D.E., Kampf, A.R., and Nealson, K.H., 2009, The influence of carbon source on the products of dissimilatory iron reduction: *Geomicrobiology Journal*, v. 26, no. 7, p. 451-462.
- Schellenberg, S.A., 2002, Mazon Creek: preservation in late Paleozoic deltaic and marginal marine environments, *in* Bottjer, D.J., Etter, W., Hagadorn, J.W. and Tang, C.M., eds., *Exceptional fossil preservation: a unique view on the evolution of marine life*: New York, Columbia University Press, p.185-203.
- Schopf, J.M., 1979, Evidence of soft-sediment cementation enclosing Mazon plant fossils, *in* Nitecki, M.H., ed., *Mazon Creek fossils*: New York, NY, Academic Press, p. 105-128.
- Scotese, C.R., Bambach, R.K., Barton, C., Van der Voo, R., and Ziegler, A.M., 1979, Paleozoic base maps: *Journal of Geology*, v. 87, no. 3, p. 217-277.
- Shabica, C.W., 1970, Depositional environments in the Francis Creek Shale, *in* Illinois State Geological Survey Guidebook Series No. 8: Urbana, IL, Illinois State Geological Survey, p. 43-52.
- Shabica, C.W., 1971, Depositional environments in the Francis Creek Shale and associated strata [unpubl. Ph.D. thesis]: Chicago, University of Chicago, 206 p.
- Shabica, C.W., 1979, Pennsylvanian sedimentation in northern Illinois: examination of delta models, *in* Nitecki, M.H., ed., *Mazon Creek Fossils*: New York, NY, Academic Press, p. 13-40.
- Shabica, C.W., and Hay, A.A., editors, 1997, *Richardson's guide to the fossil fauna of Mazon Creek*: Chicago, Northeastern Illinois University, 308 p.
- Smith, W.H., 1970, Lithology and distribution of the Francis Creek Shale in Illinois, *in* Illinois State Geological Survey Guidebook Series No. 8: Urbana, IL, Illinois State Geological Survey, p. 34-42.
- Thiel, V., Heim, C., Arp, G., Hahmann, U., Sjøvall, P., and Lausmaa, J., 2007, Biomarkers at the microscopic range: ToF-SIMS molecular imaging of Archaea-derived lipids in a microbial mat: *Geobiology*, v. 5, no. 4, p. 413-421.
- Tuttle, M.L.W., and Breit, G.N., 2009, Weathering of the New Albany Shale, Kentucky, USA: 1. weathering zones defined by mineralogy and major-element composition: *Applied Geochemistry*, v. 24, no. 8, p. 1549-1564.
- Wanger, G., 2008, The deep biosphere of the Witwatersrand basin, Republic of South Africa [Doctor of Philosophy]: University of Western Ontario, p.1-98

- Wanless, H.R., 1939, Pennsylvanian correlations in the eastern interior and Appalachian coal fields: Geological Society of America Special Paper 17, 130 p.
- Wanless, H.R., and Weller, J.M., 1932, Correlation and extent of Pennsylvanian cyclothems: Geological Society of America Bulletin, v. 43, no. 4, p. 1003-1016.
- Woodland, B.G., and Stenstrom, R.C., 1979, The occurrence and origin of siderite concretions in the Francis Creek Shale (Pennsylvanian) of northeastern Illinois, *in* Nitecki, M.H., ed., Mazon Creek fossils: New York, NY, Academic Press, p.69-103.
- Wright, C.R., 1965, Environmental mapping of the beds of the Liverpool Cyclothem in the Illinois Basin and equivalent strata in the northern midcontinent region: Unpublished Ph.D. thesis, University of Illinois, Urbana, 100 p.
- Zangerl, R., 1971, On the geologic significance of perfectly preserved fossils, *in* Proceedings, North American Paleontological Convention I, Chicago, 1969, Volume 2, Part 1: Lawrence, KS, Allen Press, p. 1207-1222.
- Zeigler, A.M., Scotese, C.R., McKerrow, W.S., Johnson, M.E., and Bambach, R.K., 1979, Paleozoic paleogeography: Annual Review of Earth and Planetary Sciences, v. 7, p. 473-502.

CHAPTER 3

A LABORATORY MODEL FOR THE INITIAL STAGES OF SOFT BODY FOSSIL DIAGENESIS

3.1 INTRODUCTION

Mineralised biological tissues are more recalcitrant than non-mineralised tissues, and therefore more likely to be preserved in the fossil record. Tissue preservation potential, in order of decreasing likelihood of preservation, falls along the continuum (Allison, 1988; Briggs and Kear, 1993a,b): 1) shells and bone; 2) sclerotised structures; 3) non-sclerotised structures; and 4) soft tissue (Briggs and Kear, 1993a,b; Bottjer, 2002).

The term *lagerstätten* is applied to fossil deposits of exceptional character. *Konservat* (conservation) *Lagerstätten* are fossil deposits characterised by exceptional preservational fidelity, commonly retaining evidence of tissues with a normally low preservation potential, including soft tissues. Such preservation generally requires the coating or replacement of originally non-mineralised tissue by (more stable) diagenetic minerals (Seilacher *et al.*, 1985; Allison, 1988; Bottjer, 2002). In contrast, *Konzentrat* (concentration) *Lagerstätten* are fossil deposits with exceptional quantity of preservation (Seilacher *et al.*, 1985; Allison, 1988). The famous Pennsylvanian- (Carboniferous-) age fossil deposit of the Francis Creek Shale, in the Mazon Creek area of northeastern Illinois falls into both of these categories (Baird *et al.*, 1985a; Allison, 1988).

The exceptionally preserved fossils that constitute the Mazon Creek biota in the mid-Pennsylvanian Francis Creek Shale are typically found entombed within siderite-cemented concretions. These hard masses of iron carbonate-indurated (and in some cases, pyritiferous) mudrock, typically measuring a few centimetres in diameter, range in

shape from oblate spheroids to elongate ellipsoids and commonly resemble the overall shapes of their contained fossils (Woodland and Stenstrom, 1979; Allison and Pye, 1994). As they commonly preserve soft bodied structures that retain some degree of three-dimensional relief, protoconcretions (gel-like precursors to concretions) are diagenetic bodies that must have formed before significant sediment compaction occurred (Allison and Pye, 1994).

Concretion formation appears to have begun close to the sediment water interface where the water content of host sediment was still high, as indicated by up to 70% cement volume at the center of some concretions; however, their development could have continued to greater depth with continued sedimentation, as indicated by a decreasing volume of pore filling precipitates outwards from the concretion centre, and hence, an implied increase in sediment compaction with time (Woodland and Stenstrom, 1979). Over time, sediment accumulation and compaction cause dewatering of underlying sediments, reducing permeability and creating an upward flow of pore waters due to loading (Baird *et al.*, 1986). Dewatering and final cementation of protoconcretions presumably continued through sediment compaction and lithification (Middleton and Nelson, 1996).

The paleoenvironmental conditions that characterised the Mazon Creek area during the mid-Pennsylvanian have been well-studied, as are the principal taphonomic factors that promoted the exceptional preservation of the Mazon Creek biota (Potter and Pryor, 1961; Nitecki, 1979; Baird *et al.*, 1985a,b; Phillips *et al.*, 1985; Baird *et al.*, 1986; Kuecher *et al.*, 1990); however, many of the details of concretion diagenesis and

initial fossilisation processes that operated after the burial of remains remain obscure. The fossils are preserved mainly as pyritised molds or impressions at the centres of siderite-cemented mudstone concretions (Schopf, 1979; Baird, 1979, 1997; Woodland and Stenstrom, 1979). Some molds contain void precipitates (*e.g.*, calcite, sphalerite, kaolinite, millerite and galena), whereas others remain unfilled (Schopf, 1979; Baird *et al.*, 1986; Baird and Sroka, 1990). Soft-bodied marine organisms (*e.g.*, jellyfish, *Tullimonstrum gregarium*) are usually preserved as flattened composite impressions. Soft tissue impressions can show internal and external anatomical details (Foster, 1979a,b). For example, in composite impressions of the jellyfish *Essexella asherae*, the surface can be covered in a thin film of microcrystalline pyrite. Where coatings of sphalerite or kaolinite occur instead of pyrite, anatomical details are masked (Baird *et al.*, 1986). Some *Essexella* fossils show convex down relief, suggesting that underlying sediment was displaced on initial organism burial and decay voids were infilled by overlying sediment. Under- and overlying sediment surfaces are separated by a thin pyrite film, which is all that remains of the organism. The non-mineralised exoskeletons of some organisms, such as polychaetes, can be preserved as organic surficial films (Baird *et al.*, 1986).

The interaction of several environmental factors, *e.g.*, oxygen concentration, Eh and pH, determines how well organisms will be preserved in the fossil record (Allison, 1988; Briggs and Kear, 1993b; Allison and Pye, 1994). Organisms' indigenous microbiota, along with bacteria in the surrounding sediments, contribute to organism decomposition

and presumably mineralisation and concretion formation (Allison, 1988; Briggs and Kear, 1993a, 1994).

On initial burial, aerobes and facultative anaerobes deplete porewater oxygen near the sediment surface (Berner, 1984; Southam and Saunders, 2005). Once dissolved oxygen in sediment porewaters is depleted to dysaerobic levels, anaerobes or facultative anaerobes become competitive. Redox zonation occurs with depth in the sediment column. Decreasing sediment reduction potential with depth favours the successive replacement of dominant microbes beginning with Fe- and Mn-reducing bacteria, and followed by dissimilatory sulphate reducing bacteria and methanogens (Southam and Saunders, 2005). In an attempt to better understand the progression of microbial processes that may have dominated early diagenetic stages of Mazon Creek type preservation, an experimental laboratory model was designed to mimic the conditions thought to have been present in the Francis Creek sediments of the Mazon Creek area soon after initial burial.

3.2 METHODS

3.2.1 Bacteria and Culture Conditions

All culturing was done at the Geomicrobiology Laboratory (Dr. Gordon Southam), UWO.

3.2.1.1 Iron reducing bacterium - Shewanella oneidensis MR-1

Shewanella oneidensis MR-1 was grown aerobically on tryptic soy broth (TSB) at room temperature. The TSB media was made in a 2 L Erlenmeyer flask by dissolving 30 g of TSB powder in 1 L of E-pure water. The Erlenmeyer was then covered with aluminum foil and the TSB media was autoclaved. After the media had cooled to room temperature, it was inoculated using aseptic technique, from *Shewanella* samples stored under liquid N₂. The Erlenmeyer with inoculated media was re-covered with the sterile aluminum foil, parafilm and statically incubated for 2-3 days.

3.2.1.2 Sulphate Reducing Bacteria

A consortium of sulphate reducing bacteria (Foster, 2009) were grown at ½-marine salinity media in butyl rubber stopper-Al crimp sealed serum bottles incubated at room temperature (21°C). The salt solution (900 mL) was made by combining the following in E-pure water (all weights in g): tryptone 10, FeSO₄•7H₂O 0.5, MgSO₄•7H₂O 2, 60% Na-lactate 6 mL, yeast extract 1, NaCl 17.5. The pH was adjusted to 7.5 with NaOH. The solution was filter sterilised (0.45-µm filter) and dispensed aseptically into serum or screw top vials. Reducing Agent Supplement (RAS) (100 mL) was made by dissolving 1.5 g of L-ascorbic acid in E-pure water. The pH was adjusted to 7.5 with NaOH. The RAS was filter sterilised (0.45-µm filter) and added to the salt solution using aseptic technique, at a 0.1% (vol./vol.) concentration. Vials were sealed. Aseptic technique was used in the handling of all media and cultures.

3.2.1.3 Methanogenic archaea

Methanococcus voltae was grown in Balch medium, in 155 mL serum bottles (sealed as above), in the dark, at room temperature (21°C). Balch medium (Balch *et al.*, 1979) (1 L) was made by combining the following in E-pure water (all weights in g): KCl 0.335, MgCl₂•6H₂O 5.87, MgSO₄•7H₂O 3.45, NH₄Cl 0.25, CaCl₂ 0.07, K₂HPO₄ 0.18, NaCl 18, mineral elixir (see below) 10 mL, vitamin mixture (see below) 10 mL, sodium acetate 1, yeast extract 2, trypticase/pepticase/peptone 2, FeSO₄ stock (see below) 6 mL, NiCl₂ stock (see below) 0.1 mL, 1% (wt./vol.) resazurin 1 mL (turned media pink on oxygen exposure). The solution was boiled under 80% H₂-20% CO₂ to remove dissolved O₂, and allowed to stand for 15 min, being flushed with 80% H₂-20% CO₂ at approx. 1cc/sec. Na₂CO₃ (8%, 4.8 mL) and aqueous cysteine-sulphide (1.25%, 8 mL), a reducing agent, were added. The solution was heated, becoming anaerobic, and allowed to stand for 10 min. while gassing. Aqueous cysteine-sulphide (1.25%, 8 mL) was added and the solution was boiled to remove remnant dissolved O₂ and dispensed anaerobically into serum vials flushed with 80% H₂-20% CO₂. Sealed serum vials were autoclaved at 121°C for 20 min. Aseptic technique was used in all handling of media.

Mineral Elixir (1 L) was made by combining the following ingredients in E-pure water (all weights in g): nitrilotriacetic acid 1.5, MgSO₄•7H₂O 1.46, MnSO₄•H₂O 0.5, NaCl 1.0, CoCl₂•6H₂O 0.1, CaCl₂ 0.075, ZnSO₄•7H₂O 0.1, CuSO₄•5H₂O 0.01, AlK(SO₄)₂•12H₂O 0.01, H₃BO₃ 0.01, Na₂MoO₄•2H₂O 0.01. The nitrilotriacetic acid was dissolved with 3N NaOH as the pH was brought to 6.5, and then the other ingredients were added. The solution was stored refrigerated (4°C).

The Vitamin Mixture (1 L) was made by combining the following in E-pure water (all weights in g): biotin 0.002, folic acid 0.002, pyridoxine hydrochloride 0.01, thiamine hydrochloride 0.005, riboflavin 0.005, nicotinic acid 0.005, cobalamin 0.005, PABA 0.005, lipoic acid 0.005, pantothenic acid 0.005. The solution was filter sterilised (0.45- μ m filter) and stored refrigerated (4°C).

The Na_2CO_3 solution (8%) was made by dissolving 8 g of Na_2CO_3 in 100 mL of E-pure H_2O , and boiling the mixture under 80% H_2 -20% CO_2 . The heat was turned off and the solution was equilibrated by bubbling in 80% H_2 -20% CO_2 for 30 min. The solution was transferred anaerobically into serum vials flushed with 80% H_2 -20% CO_2 . Vials were sealed (as above) and autoclaved for 20 min at 121°C.

The aqueous cysteine-sulphide reducing solution (1.25%) was made by dissolving 2.5 g of cysteine-HCl in 50 mL of E-pure water. The pH was brought to 10 with 3N NaOH (freshly prepared NaOH was used, pH adjustment was done rapidly). pH adjusted cysteine-HCl solution was flushed with N_2 and 2.5 g of $\text{Na}_2\text{S}\cdot 9\text{H}_2\text{O}$ was added. The total volume was brought to 200 mL with E-pure water, and boiled under N_2 . The solution was dispensed anaerobically into serum vials, sealed with butyl rubber stoppers and aluminum crimp seals and autoclaved at 121°C for 20 min. The autoclaved solution was stored refrigerated (4°C).

FeSO_4 stock solution (100 mL) was made by dissolving 0.2 g $\text{FeSO}_4\cdot 7\text{H}_2\text{O}$ in distilled water and adding 3 drops of concentrated HCl. NiCl_2 stock solution (100 mL) was made by dissolving 1.2 g NiCl_2 in distilled water.

Methanogen cultures were transferred into new media weekly. Vials containing week-old cultures were pressurised with a thin stream of 80% H₂-20% CO₂ until the stopper bulged (approx. 1 min.). The culture was transferred anaerobically into new media. Inoculum volume was calculated to give a 10⁻³ dilution. Aseptic technique was used in all handling of media.

Gases used in preparation of media and transfer of cultures were not scrubbed of O₂. Methanogen viability was confirmed by the presence of methane in serum vial headspaces as determined by gas chromatography/mass spectrometry (GC/MS) on an Agilent 5890A gas chromatograph attached to an Agilent 5975C mass spectrometer (Earth Sciences Module, Biotron Institute, UWO).

3.2.2 Column set-up

3.2.2.1 Arkona Shale sampling and characterisation

Dry, grab samples of Arkona Shale (Middle Devonian) were collected using a shovel from the north clay quarry at Hungry Hollow (Arkona area), Ontario, Canada, and stored in 20 L plastic buckets with lids. Powdered Arkona Shale was freeze-dried for 48 hr using a Labconco FreeZone Triad System (shelf at -2°C, coils at -85°C), and analyzed for major mineral phases on a Rigaku RTP 300RC X-ray diffractometer using Cu K α radiation. The main minerals found were quartz, calcium carbonate and clays (data not shown). For the diagenesis model, the dry Arkona Shale was broken up using a mortar and pestle and suspended in half-strength (brackish) seawater (see below).

3.2.2.2 Diagenesis model

Columns, set-up in sterile 60 cc plastic syringes, were used as a laboratory model to mimic Mazon Creek type fossilisation conditions (Fig. 3.1A). Plungers were removed, needle hubs were capped with sealed 200 μ L pipette tips, and the bottom of each syringe was layered with 10 cc of silica wool to prevent sediment loss. Brine shrimp were used as a model organism and buried in sediment slurry, made by suspending powdered (mortar and pestle) Arkona Shale in a $\frac{1}{2}$ marine-Fe³⁺ solution.

The final slurry contained 0.7 g/mL Arkona Shale, and was approximately 70% (vol./vol.) $\frac{1}{2}$ marine-Fe³⁺ solution. To make the $\frac{1}{2}$ marine-Fe³⁺ solution, $\frac{1}{2}$ -marine synthetic seawater medium (SSM) salt solution (see below; 623.125 mL), SSM trace element solution (see below; 0.625 mL), SSM vitamin solution (see below; 1.25 mL), and Balch medium-mineral elixir (6.25 mL) and -vitamin mix (6.25 mL) were combined and filter sterilised (0.45- μ m filter). Fe³⁺-stock solution (see below, 62.5 mL) was added, along with 110 μ g/L ascorbic acid to make the solution anaerobic, and the pH was brought to 8.5 with NaOH. Bacterial cultures, *i.e.*, *Shewanella oneidensis* MR-1, the sulphate reducing bacterial consortium, and *Methanococcus voltae* (100 mL each) were added to complete the aqueous phase. The aqueous phase and Arkona Shale (700 g) were combined in a capped, autoclaved plastic bottle (4 L), and the slurry was shaken to produce a 'homogenous' mixture with a target microbial count of 10⁶/g. Columns were filled with slurry to the 15 cc mark. An additional 10 mL layer of slurry containing 5 brine shrimp was added to each column, and then they were topped off with additional slurry to the 60 cc mark. Columns were sealed with double parafilm, wrapped in aluminum foil

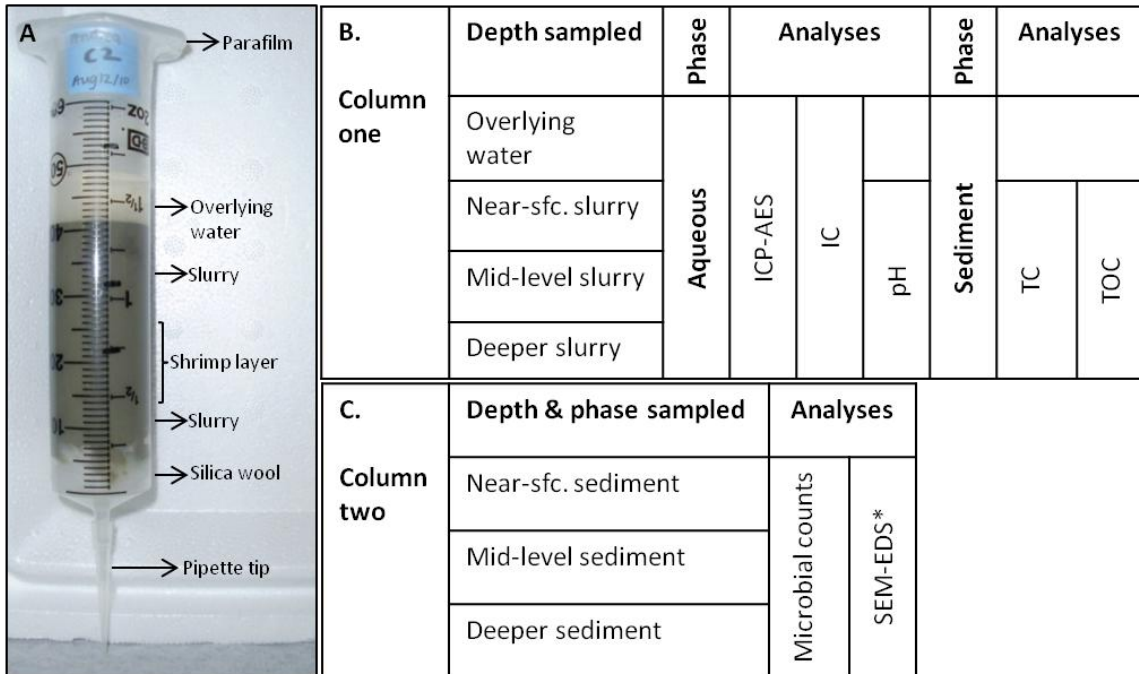


Figure 3.1: A) Photograph highlighting column set-up. B) and C) Outlines of column sampling and analyses showing depths and phases (aqueous or sediment) analyzed for each technique. *Column was cut open to get SEM-EDS samples.

and left to incubate at room-temperature (21°C) in a dark cupboard until analyzed. The slurry settled to the 50 cc mark by day three (Fig. 3.1A).

Control columns, prepared with E-pure water replacing the microbial cultures were analysed at T=0 and after incubation at RT for 9 months. These incubated control columns were observed periodically to determine whether Arkona Shale and *Artemia salina's* indigenous microbiota produced the decomposition phenotypes observed in experimental columns.

3.2.2.3 Half-marine synthetic seawater medium (modified from Schut et al, 1993)

The following were combined in E-pure water to 1 L final volume (all weights in g): NaCl 15, MgCl•6H₂O 1, MgSO₄•7H₂O 1.695, KCl 0.7, CaCl₂•2H₂O 0.15, NH₄Cl 0.5, NaHCO₃ 0.2, KBr 0.1, SrCl₂•6H₂O 0.04, H₃BO₃ 0.025, KF 0.001, MOPS 2.09, KH₂PO₄ 0.27, trace element solution (see below) 1 mL and vitamin solution (see below) 2 mL. The pH was brought to 8 with NaOH and the solution was filter sterilised (0.45-µm filter).

Trace element solution (1 L) was made by combining the following in E-pure water (all weights in mg): Na₂EDTA 1000, FeCl₃•6H₂O 2000, LiCl 1000, AlK(SO₄)₂•2H₂O 178, NaVO₃•14H₂O 5, K₂Cr₂O₇ 0.15, MnCl₂•4H₂O 80, CoCl₂•6H₂O 5, NiCl₂•6H₂O 20, CuCl₂•2H₂O 25.36, ZnSO₄•7H₂O 126.6, Na₂O₄Se 10.77, RbCl 150, Na₂MoO₄•2H₂O 75, SnCl₂•2H₂O 1.5, KI 80, BaCl₂•2H₂O 50, Na₂WO₄•2H₂O 15. The solution was filter sterilised (0.45-µm filter) and stored at 4°C.

Vitamin solution (1 L) was made by combining the following in E-pure water (all weights in mg): PABA 100, biotin 20, folic acid 50, α-lipoic acid 50, riboflavin 100,

thiamine 200, nicotinic acid amide 200, pyridoxamine 500, pantothenic acid 100, cobalamin 100. The solution was filter-sterilised (0.45- μm filter) and stored frozen (-20°C).

3.2.2.4 Fe^{3+} -stock solution (Leah Curtis, personal communication)

$\text{FeCl}_3 \cdot 6\text{H}_2\text{O}$ (22 g) was added to 100 mL of E-pure water, using aseptic technique. The solution was titrated with NaOH to a pH of 8.5, centrifuged (5125 X g, 5 min) and the supernatant was discarded. E-pure water was added, the solution was vortexed and centrifuged (5125 x g, 5 min), and the supernatant again discarded. This was repeated 5 times until the pH was neutral. The final volume was made up to 100 mL with E-pure water. Aseptic technique was used in all handling of stock solutions.

3.2.3 Column Analysis

After incubation for approx. 9 months, the columns developed heterogeneous macroscopic zonation versus the $T = 0$, control columns (Fig. 3.2). Two columns were processed for each diagenetic phenotype: control ($T = 0$); death of shrimp at the water-sediment interface; shrimp dispersed throughout the column; and death of shrimp below the water-sediment interface. Columns were photographed prior to analysis. The overlying water was removed using a sterile pipette and stored (4°C) in a scintillation vial prior to analysis. For each diagenetic phenotype, reaction systems were assigned as column one, for inductively coupled plasma-atomic emission spectroscopy (ICP), ion-exchange chromatography (IC), dry weight (DW), pH, total carbon (TC) and total organic

carbon (TOC) analyses, or as column two, for microbial counts, scanning electron microscopy (SEM) and energy dispersive spectroscopy (EDS) analyses (Fig. 3.1B,C).

Plungers were cleaned with ethanol and reinserted into syringes to prevent slurry movement during the drilling of sampling holes. To reinsert the plunger, the syringe was kept vertical while a small hole was drilled into the barrel, 2-3 mm above the sediment surface, using an ethanol rinsed 7/64" drill bit. The tip of a glass pipette was inserted into the hole, and the pipette was connected to the vacuum line. The vacuum was used to draw the plunger down to the sediment surface. Three sampling holes were drilled in each column, at varying depths below the plunger. The near-surface, middle and deepest sampling zones ranged from 9-19.8, 20.7-36 and 39.6-55.8 mm below the water-sediment interface, respectively. In columns with visible redox zonation, sampling holes corresponded with black, orange or grey coloured zones (see Fig. 3.2). The three drilling spots were marked with tape and permanent marker. The column was held in place horizontally, and sampling holes were drilled using an ethanol rinsed 15/64" drill bit. Drilled surfaces were wiped with ethanol, and columns were immediately covered with cling wrap to minimise oxygen exposure. Columns were sampled in an N₂ flushed workspace. Contaminated surface mud was removed from sampling holes using a sterile transfer pipette.

Column two was cut open to allow better access to sediments and buried shrimp. All sample handling was done in the N₂ flushed workspace using aseptic technique. The column was laid horizontally with the sampling holes facing up and wiped with ethanol prior to cutting. An ethanol rinsed electric diamond-edge knife was used to cut open the

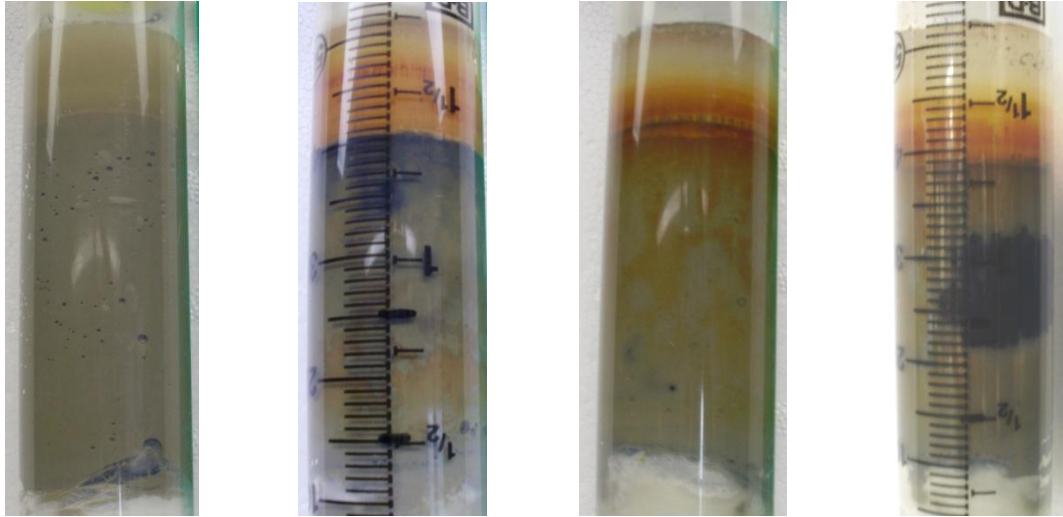
1: Control**2: Upper sulphidic****3: Diffuse sulphidic****4: 'Middle' sulphidic**

Figure 3.2: Column photographs showing the heterogeneous diagenetic phenotypes: 1) Control phenotype (C), 2) death of shrimp at the water-sediment interface (US), 3) shrimp dispersed throughout the column (DS) and 4) death of shrimp below the water-sediment interface (MS).

top half of the column. The slurry was poured into petri plates, and anaerobic sterile saline rinses were used to separate shrimp carcasses from sediment. Shrimp (3-4 per column) and sediment samples (3-4 per column) were placed in vials of anaerobic glutaraldehyde (1-2%, 2 mL) flushed with N₂, vials were capped and samples were fixed overnight on a Markson Heavy Duty Rotator (speed 6, 20° angle).

Anaerobic saline (1.75% NaCl, 0.075% ascorbic acid, 1 L) was made by adding 17.5 g NaCl and 0.75 g ascorbic acid to E-pure water. The pH was rapidly adjusted to 7.5 using NaOH and the solution was filter sterilised (0.45-µm filter). Sterile solution was used immediately or dispensed into autoclaved serum vials and sealed as above.

Anaerobic glutaraldehyde (2% (vol./vol.), 100 mL) was made by combining buffered saline (3.5% (wt./vol.) NaCl in 40 mM HEPES, 48 mL), RAS (0.05% (wt./vol.) ascorbic acid, 48 mL) and glutaraldehyde (50%, 4 mL). To make 48 mL buffered saline 1.68 g NaCl and 0.458 g HEPES were dissolved in E-pure water. To make 48 mL of RAS, 0.024 g ascorbic acid was dissolved in E-pure water. The pH of both solutions was adjusted to 8 with NaOH and they were filter sterilised (0.45-µm filter). The three solutions were combined, dispensed into autoclaved serum vials and sealed.

A sample of slurry (ranging from 0.6-1.9 mL) from each zone of Column two was pipetted into pre-weighed, autoclaved serum vials containing 12 mL anaerobic saline; these vials were sealed and set aside for microbial counts.

A sample of slurry from each zone of Column one was pipetted into 50 mL serum vials for inductively coupled plasma-atomic emission spectroscopy (ICP-AES) preparation. Vials were capped with butyl rubber stoppers fitted with 20G cannulas and

aluminum crimp seals were placed on top. Samples of 'slurry' from each depth zone of Column one were also pipetted into pre-weighed microtubes: approx. 1.5 mL into a total carbon (TC) microtube, 2 X 1.5 mL into an ion-exchange chromatography and total organic carbon (IC + TOC) microtube, and 1 mL into a dry weight and pH (DW + pH) microtube. All samples were weighed and set aside for further analysis.

3.2.3.1 Inductively coupled plasma-atomic emission spectrometry (ICP-AES)

Inductively coupled plasma-atomic emission spectrometric analysis was conducted on the overlying water from all columns and on weak-leach extractions from three slurry samples from Column one. Sodium acetate (1 M, 20 mL, pH 8.2) was added to each slurry sample, serum vials were sealed (as described in 3.2.1.2) and 20G cannulas inserted to relieve gas pressure. Vials were placed on a Barnstead Lab-Line Lab Rotator (max. speed) for 1 hr at room temperature to extract adsorbed ions into the soluble fraction. Shaken samples were centrifuged (5125 X g, 15 min) and the supernatant was used for ICP-AES. Surface (1 mL) and pore water samples (5 mL) were filtered through 0.1 μm before analysis. Blank samples contained 5 mL E-pure water, and the final volume of the surface water samples were brought to 5 mL with E-pure water. All samples were acidified with concentrated HNO_3 (0.2%), and weighed before and after the addition of E-pure water and HNO_3 .

Cations were analyzed using a Perkin-Elmer Optima 3300DV inductively coupled plasma-atomic emission spectrometer (ICP-AES) (Dr. Charles Wu, Earth Sciences Module, Biotron Institute, UWO). Final concentrations were adjusted based on sample

dilution to reflect the 'soluble' components in the column. Concentrations of elements and compounds were converted to mM and blanks were subtracted. Concentrations below the detection limit (DL) were scored as $\frac{1}{2}$ DL. The overlying water chemistry was plotted at the sediment-water interface (0 mm depth).

3.2.3.2 Ion-exchange chromatography (IC)

Ion-exchange chromatography was conducted on the overlying water from all columns and the porewater collected from the IC+TOC slurry samples. The IC+TOC microtubes were centrifuged (12,000 X g, 5 min) and the supernatants were used for IC. Surface (1 mL) and sediment pore water samples (0.3-1 mL per zone) were filtered through 0.1 μ m pore space syringe filters, into sample tubes. Blank samples contained 5 mL E-pure water, and the final volume of overlying water, control and supernatant samples was brought to 5 mL with E-pure water. All samples were weighed, before and after the addition of E-pure water.

Anions were analyzed using a Dionex IC-3000 ion chromatograph (IC) (Dr. Charles Wu, Earth Sciences Module, Biotron Institute, UWO). Samples were diluted to reduce interference on NO_3^- and NO_2^- peaks by Cl^- and on PO_4^{3-} peaks by SO_4^{2-} . Final concentrations were adjusted based on dilutions to soluble constituents in the overlying water and in the sediment void volume and processed as above. Blanks of deionised water were below detection limits for all ions except SO_4^{2-} .

3.2.3.3 Dry weight (DW), pH, total carbon (TC) and total organic carbon (TOC)

The DW + pH sediment samples from Column one were centrifuged (2000 X g, 5 min). The supernatant was used in litmus tests to determine the porewater pH (+/- 0.2). Excess supernatant was discarded.

E-pure water (1 mL) was added to the DW pellets, which were vortexed to rinse away salts, centrifuged (2000 X g, 5 min) and the supernatant discarded. This was repeated. The TC microtubes were processed in the same manner as the DW tubes.

The TOC microtubes were reacted with HCl (1 M, 1 mL) for 5 min to dissolve the CaCO₃ fraction. Microtubes were opened periodically during the incubation period between vortexing to degas. The remaining solids were centrifuged (2000 X g, 5 min) and the supernatant discarded. HCl treatments were repeated until the supernatant pH was acidic when tested. Samples were washed using centrifugation and rinsing as above to remove dissolved ions.

Samples were rinsed into crucibles, one per sampling zone for DW and TC, and two per sampling zone for TOC, respectively, and dried at 110°C for 48 hr. Samples were weighed. Control samples of Arkona Shale treated as above were also analyzed for TC and TOC. All TC and TOC samples were ground finely and analyzed on a LECO-CNS 2000 induction furnace analyzer (Dr. Charles Wu, Earth Sciences Module, Biotron Institute, UWO). Results were normalised to 1 g of sediment DW.

3.2.3.4 Microbial counts

Limiting dilutions of sediment were inoculated into media to obtain MPN counts (USDA, 2008) for iron reducing bacteria, *i.e.*, *Shewanella oneidensis* MR-1, and for

sulphate reducing bacteria. MPN counts were not done for methanogens because they were not viable in columns after $T = 0$, as determined by GC/MS methane analysis (See section 3.2.1.3). The three slurry samples from Column one, diluted in 12 mL anaerobic saline, were vortexed, and a sterile needle was used to transfer 1.3 mL from the first vial into a second vial of 12 mL anaerobic saline, creating a 1:10 dilution. This was repeated 8 more times, resulting in a series of 10 dilutions for each sampling zone. All septa were flamed with 70%_(aq) ethanol before and after transfers.

Iron reducers were cultured in screw cap vials containing 3 mL of TSB media (section 3.2.1.1) spiked with 0.2 mL Fe^{3+} -stock solution (section 3.2.1.3), inoculated with 0.3 mL of slurry solution. *Shewanella oneidensis* MR-1 growth was verified by a colour change in the media from rust to clear, brown or black (*i.e.*, production of iron oxyhydroxide minerals). Screw cap vials containing 8 mL of SRB media (section 3.2.1.2) were inoculated with 0.9 mL of slurry solution. Sulphate reducing bacterial growth was verified by a colour change in the media from clear to black.

Columns were divided into two zones (upper and lower) for MPN determination, with replicates from the middle zone being split between the two. In $T = 0$ control columns, upper and lower zone values were averaged to give baseline microbial counts.

3.2.3.5 Critical point drying (CPD) for scanning electron microscopy (SEM)

Glutaraldehyde fixed shrimp carcasses and sediment samples were processed through an ethanol dehydration series (25%, 50%, 75%, 100% X 3) in 1 hr increments. Shrimp were dehydrated in capped vials and sediment was dehydrated on 0.1- μm pore-

size membrane filters in syringe filter kits. Dehydrated samples were placed in BEAM capsules and CPD using a Samdri PVT 3B critical point drier (Tousimis Research Corp.). Critical point dried samples were placed on carbon-sticky tabs mounted on SEM stubs, Os-coated (5 nm) using a Filgen Osmium Plasma Coater 80T and analyzed at 1 kV using a LEO (Zeiss) 1540XB FIB/SEM (Nanofabrication Facility, UWO). The FIB/SEM was equipped with an Oxford Instruments INCAx-sight energy dispersive spectrophotometer (EDS) for qualitative elemental analysis. The voltage was increased to 5 kV for imaging and EDS analyses. Spectra were analyzed using Oxford INCA Analytical Software.

3.2.3.6 LR-white embedding for scanning electron microscope (SEM)

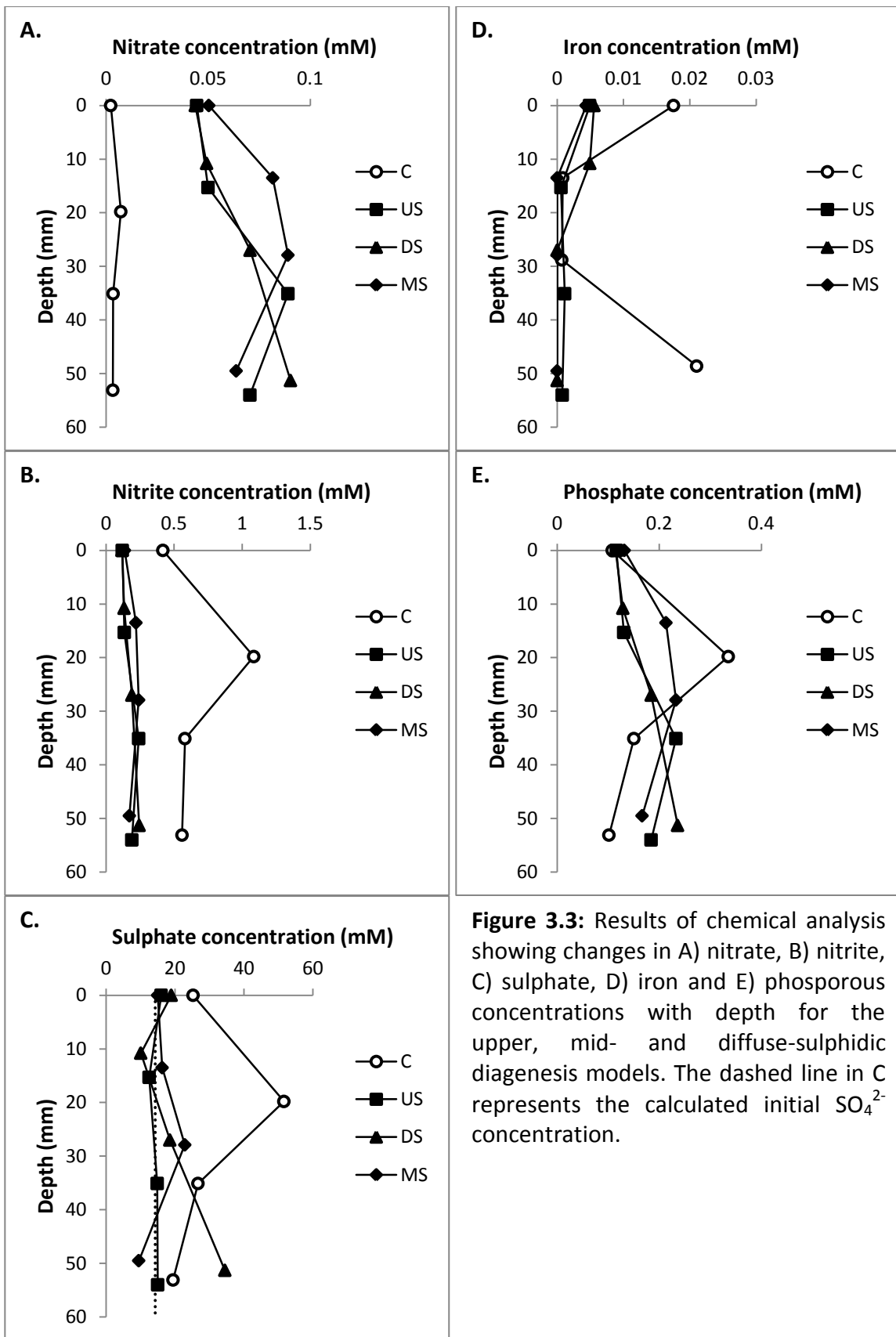
Glutaraldehyde fixed shrimp carcasses and sediment samples were rinsed twice in 20 mM HEPES buffer (pH 8.2) for 30 min each. Samples were stained with 1% osmium tetroxide in 100 mM Na-cacodylate buffer for 1 hr, rinsed twice in 100 mM Na-cacodylate buffer and processed through an ethanol dehydration series (50%, 75%, 100% X 2) in 30 min increments. Ethanol was replaced with LR white resin (medium grade) in three stages: 50% EtOH:50% LR (30 min), 100% LR X 3 (30 min each), 100% LR X 2 (1 hr each). Dehydrations and infiltrations were performed in capped glass vials. Air was evacuated from vial headspaces; vials were sealed and baked under vacuum at 60°C for 48 hours. Embedded samples were removed from glass vials and surfaces were ground to flatten. Samples were Os-coated (5 nm) and analyzed at 10 or 15 kV using the SEM and EDS equipment mentioned above.

3.3 RESULTS

While the different diagenetic phenotypes, *i.e.*, upper-, mid- and diffuse-sulphidic zones produced these obvious macroscopic differences, the chemistry of the overlying water and of the pore water within the sediment were remarkably consistent. Note, the large cm-scale peripheral sulphidic zones resulted from an edge-effect. During sampling, they were confined to the column wall and did not extend into the sediments.

3.3.1 Ion-exchange chromatography (IC), inductively couple plasma-atomic emission spectroscopy (ICP-AES), pH and total carbon (TC) results

Nitrate concentrations were low at $T = 0$, but increased in all systems during diagenesis, and perhaps increased slightly with depth (Fig. 3.3A). In contrast, the nitrite concentrations decreased during diagenesis, relative to the starting concentrations (Fig. 3.3B). Sulphate concentrations were higher at time zero, versus the diagenesis (Fig. 3.3C), but were surprisingly heterogeneous with depth. Note the calculated sulphate concentration indicated by the vertical dashed line. Overall, the dissolved iron concentrations in the columns were very low, though they did vary with depth at $T = 0$ (Fig. 3.3D). They dropped with diagenesis in the overlying water, and especially within the sediment, *i.e.*, typically below the detection limit. The phosphate concentration was highest in the near-surface sediment zone at time zero, but varied surprisingly with depth (Fig. 3.3E). It decreased from this highest level during diagenesis, but remained above $T = 0$ concentrations at lower levels.



Calcium concentrations were consistently lower in the overlying water than in the sediment (Fig. 3.4A); however, sediment concentrations did not produce any consistent pattern related to diagenetic phenotype. At 9 months, Ca^{2+} levels were at (diffuse-sulphidic), above (mid-sulphidic) or below (upper-sulphidic) the T = 0 control concentrations. Magnesium concentrations in the sediment increased slightly with diagenesis relative to T = 0 (Fig. 3.4B). Relative to time zero, the pH increased by one pH unit over the course of the 9 month incubation (Fig. 3.4C). At T = 0, organic carbon (OC) (Fig. 3.4D) was higher in the middle of the column than inorganic carbon (Fig. 3.4E). Organic carbon within the columns either remained the same or decreased over the 9 month incubation period (Fig. 3.4D). In the middle-sulphidic column, the decrease corresponded with the zone of sulphide formation; however, this trend was not apparent in the other phenotypes, with upper- and diffuse-sulphidic columns showing similar organic carbon levels throughout. Inorganic carbon remained the same or increased over the course of the incubation (Fig. 3.4E). In upper- and middle-sulphidic columns, the highest level of inorganic carbon corresponded with the zone of sulphide formation. In the diffuse-sulphidic column this trend was not apparent, with the inorganic carbon levels increasing with depth.

3.3.2 Most probable number (MPN) results

Shewanella oneidensis MR-1 populations increased after 9 months in all diagenetic phenotypes (Table 3.1). Their numbers were highest in diffuse sulphidic columns. The population decreased by three orders of magnitude in the lower zone of

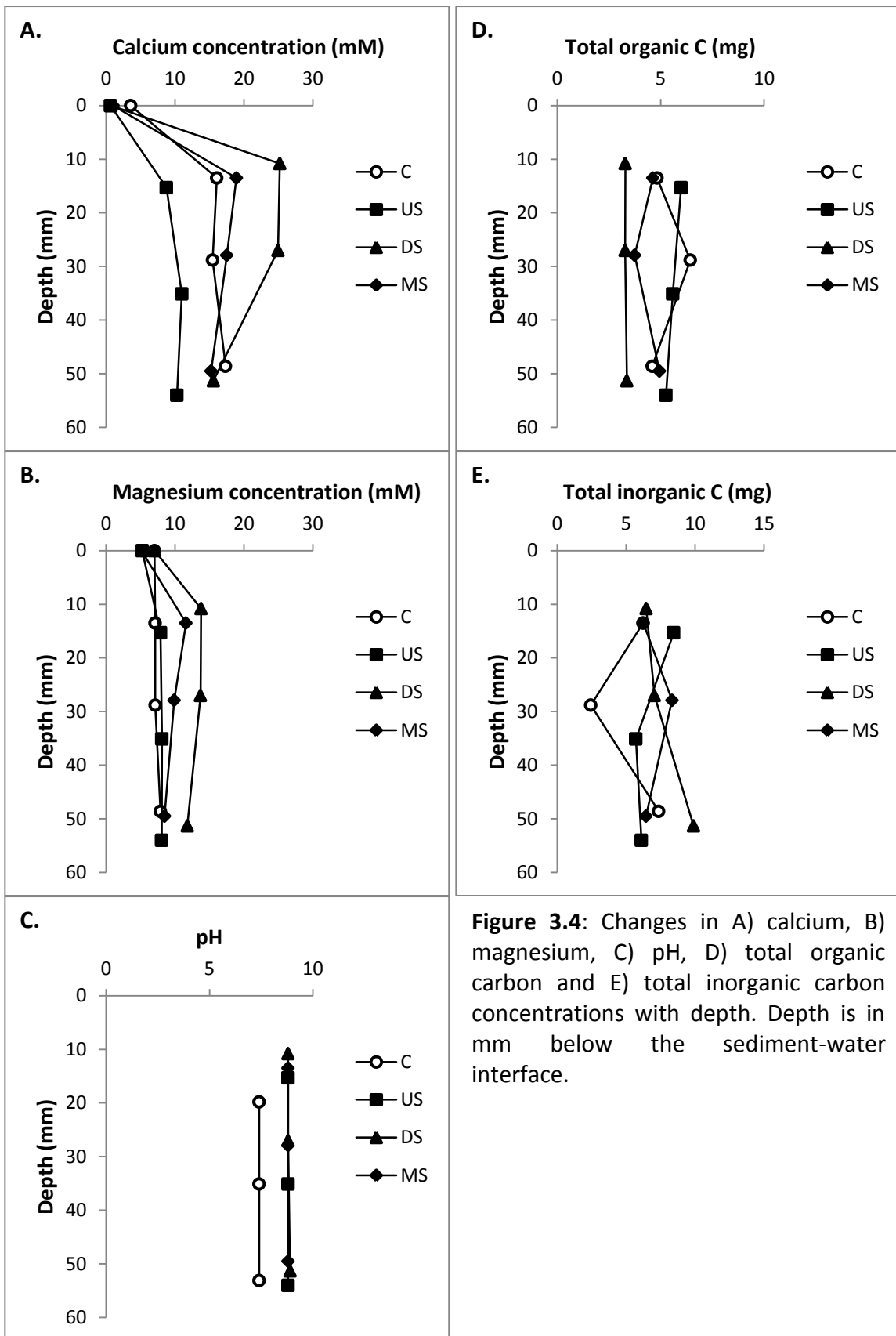


Figure 3.4: Changes in A) calcium, B) magnesium, C) pH, D) total organic carbon and E) total inorganic carbon concentrations with depth. Depth is in mm below the sediment-water interface.

upper-sulphidic columns. The SRB population was high at T = 0, but dropped to negligible levels across all phenotypes by 9 months.

Table 3.1: Changes in populations of *Shewanella oneidensis* MR-1 and the sulphate reducing bacteria (SRB) after 9 months of incubation. Microbial counts (MPN/mL slurry) are compared between upper (U) and lower (L) sediment zones.

Column Phenotype	Sampling zone (U/L)	Shewanella	SRB
0		1.7×10^5	2.2×10^7
Upper sulphidic	U	7.2×10^9	3.2
	L	5.1×10^6	3.3
Mid-sulphidic	U	6.2×10^8	5.4×10^3
	L	1.3×10^8	5.5×10^3
Diffuse sulphidic	U	1.5×10^7	1.1×10^2
	L	8.3×10^7	1.0×10^2

3.3.3 Scanning electron microscopy (SEM) and energy dispersive spectroscopy (EDS)

results

Arkona Shale and live brine shrimp were analyzed pre- and post-column set-up. The sediment was composed mainly of quartz, clays (Figs. 3.5A-D) and carbonate (Fig. 3.5E), along with some pyrite (Fig. 3.5C, F). Sparse microbial cells were observed in the shale prior to inoculation with bacterial cultures (Fig. 3.5A). The number of cells observed in the sediment using SEM did not appear to increase significantly after inoculation, *i.e.*, at time zero; however, sediments did appear more aggregated and showed colloidal iron oxide deposits throughout (Fig. 3.5B). The structure of intact *Artemia salina* organs can be seen in polished sections (Fig. 3.6) prior to undergoing diagenesis in the columns.

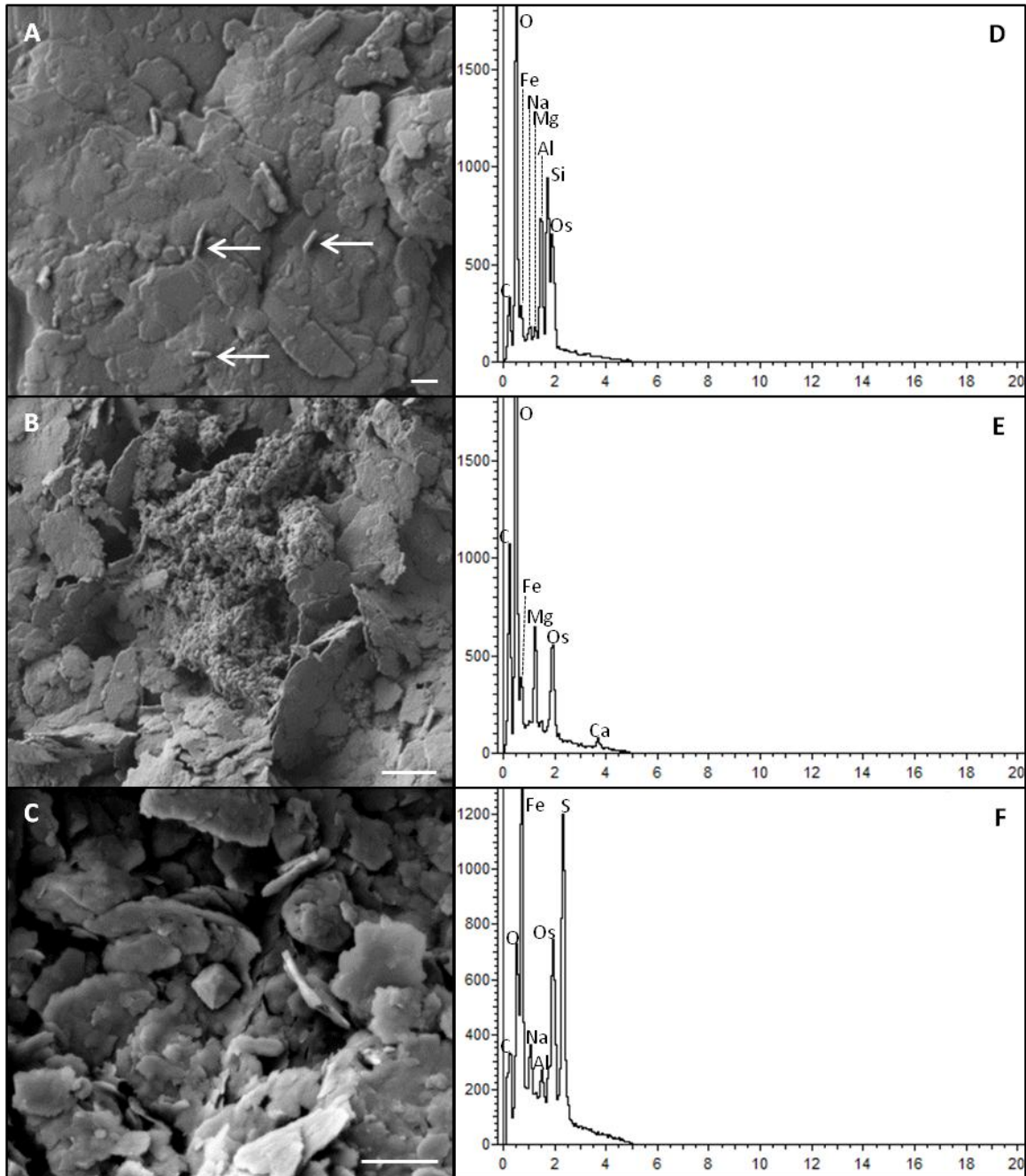


Figure 3.5: Secondary electron (SE2) SEM micrographs of: A) Microbial cells (arrows) present in uninoculated Arkona Shale, scale bar = 200 nm; B) Arkona Shale sediment with inocula and Fe³⁺-stock solution added (*i.e.* in control columns), scale bar = 1 μ m; and C) Euhedral pyrite (at centre) present in control column sediments, scale bar = 2 μ m. EDS spectra of D) clays, E) carbonate and F) pyrite, present in Arkona Shale prior to incubation. Os peaks are from the conductive coating used to prevent sample charging.

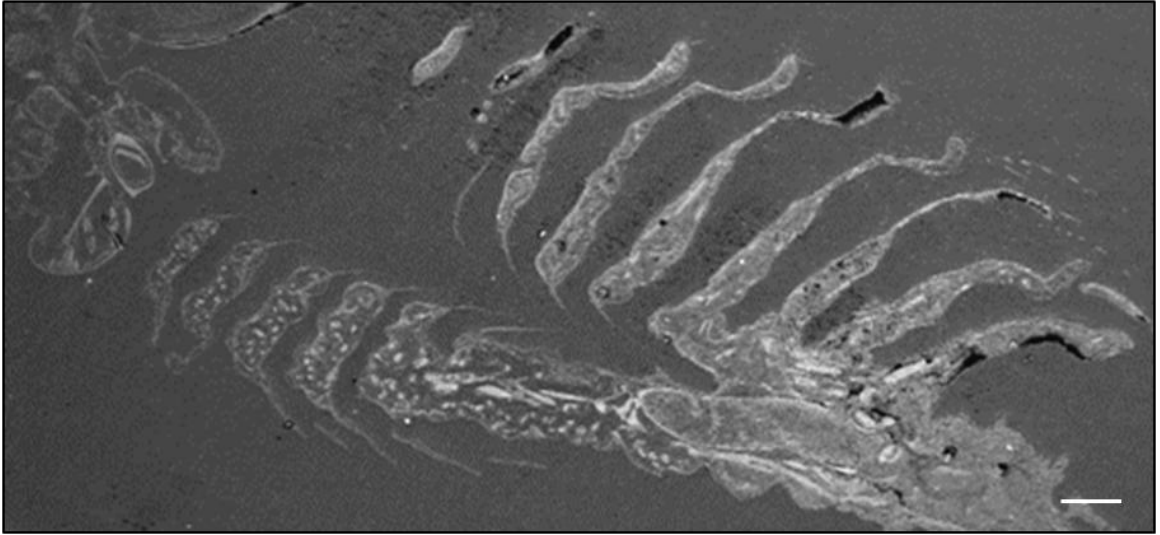


Figure 3.6: Backscattered SEM micrograph showing a lateral view of a freshly killed brine shrimp, scale bar = 200 μm .

At time zero, *A. salina* were still alive in the columns, and some escaped into the overlying water. A relatively intact thoracic segment, with attached phyllopods can be seen in one such specimen (Fig. 3.7A). Freshly killed *Artemia* have a rich indigenous microbiota, especially within the abdominal cavity (Fig. 3.7B-C).

At 2.5 months, shrimp carcasses were more degraded and encrusted with sediments (Fig. 3.7D-F). There was some disarticulation, especially of extremities and setae. Organics resembling EPS and sparse microbial cells could be seen on sediment aggregates encrusting the carcass (Fig. 3.7F). Aggregates of nanometre sized iron carbonate spheroids were found forming around native clays (Fig. 3.8).

By 5 months, the cuticle was the only intact remnant of the brine shrimp carcass (Fig. 3.9A-C). Edges of the cuticle were highly degraded, though not completely disarticulated (Fig. 3.9B). The cuticle was encrusted with sediments, mainly consisting of clays and quartz, and microbes were not readily visible (Fig. 3.9C); however, framboidal pyrite was observed, occurring within a conglomerate sediment grain (Fig. 3.10).

After approximately 9 months of incubation, cuticle remnants could be found at various states of decay and disarticulation. In the diffuse sulphidic column, a relatively intact cuticle, similar to the one at 5 months, was found (Fig. 3.9D). It was covered by a thick organic film, which was sensitive to the electron beam, and disintegrated on overexposure (Fig. 3.9E). The film consisted of sediments heavily coated by EPS (Fig. 3.9F). Within the sulphidic zone of the upper-sulphidic column, only a cuticle fragment could be found at 8.5 months (Fig. 3.9G). This fragment showed some sediment encrustation, but no obvious evidence of EPS or microbial remains (Fig. 3.9H, I). Carbon-

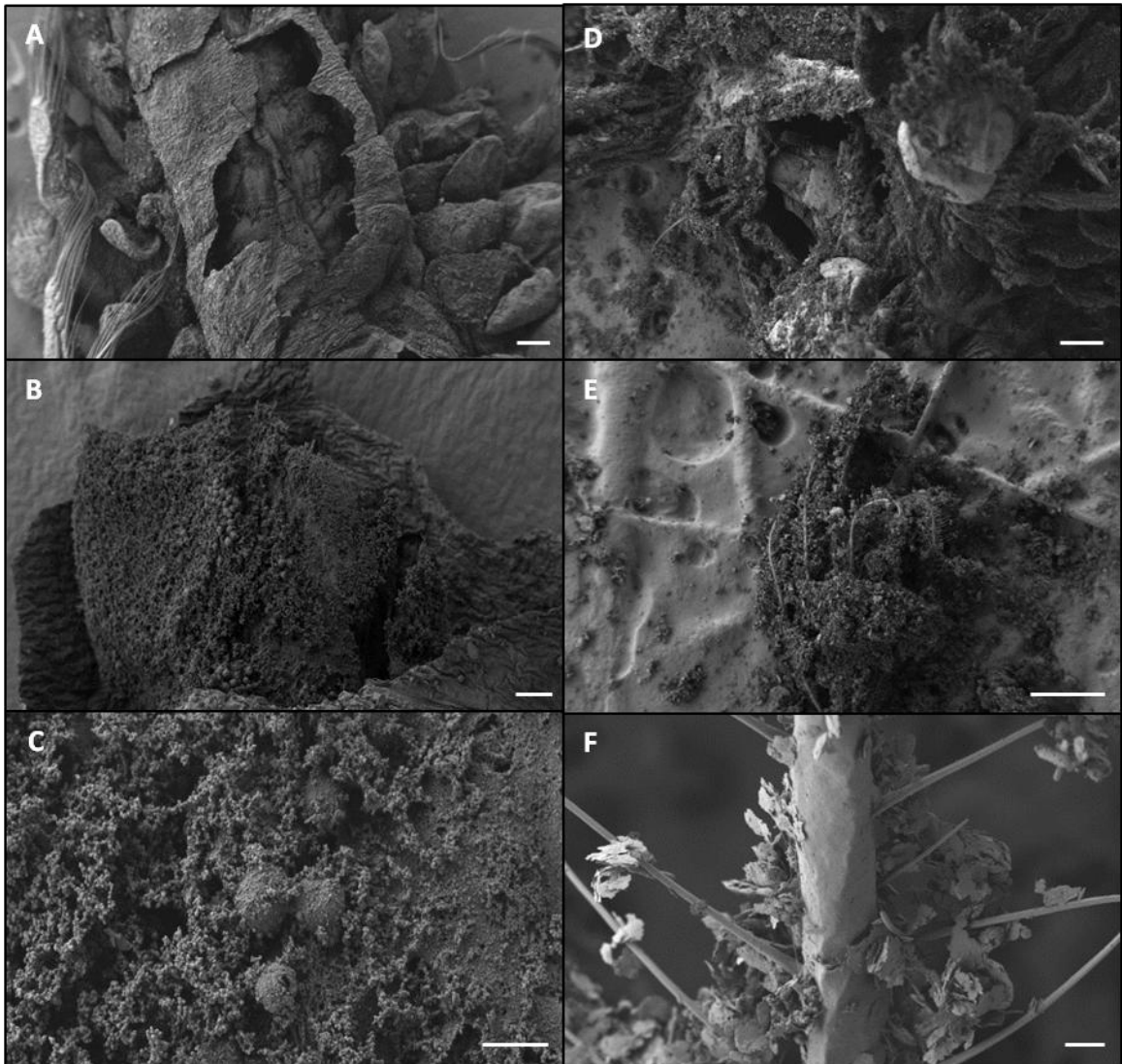


Figure 3.7: Secondary electron (SE2) SEM micrographs of a freshly killed brine shrimp showing: A) a ventral view of the open thoracic segment, scale bar = 100 μm ; B) a torn segment of the abdomen, showing a ventral view of the interior, scale bar = 40 μm ; and C) a magnified view of the gut fauna in B, scale bar = 10 μm . Secondary electron (SE2) SEM micrographs of a brine shrimp carcass at 2.5 months, showing: D) a ventral view of the open thoracic segment, scale bar = 100 μm ; E) a detached thoracopod, scale bar = 100 μm ; and F) a magnified view of the thoracopod, showing sediment encrusted setal hairs, scale bar = 2 μm .

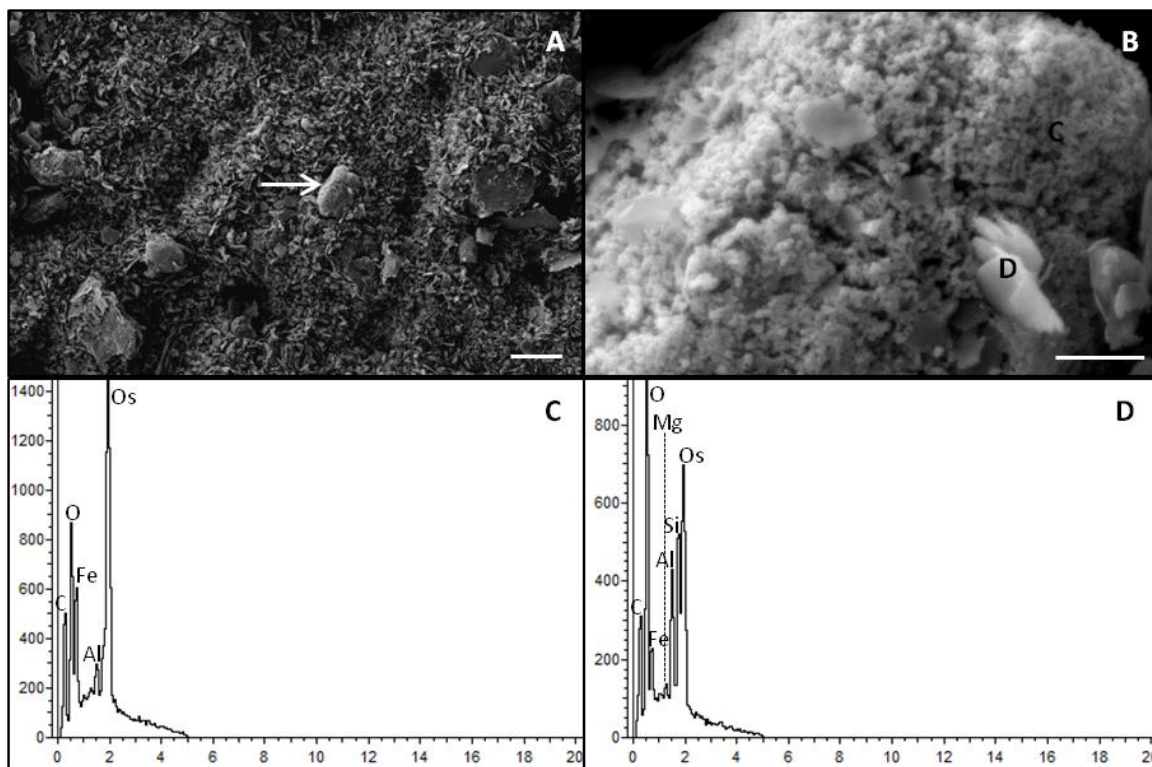


Figure 3.8: Secondary electron (SE2) SEM micrographs showing: A) an aggregate of spheroids (arrow) forming within the clay matrix at 2.5 months, scale bar = 10 μm ; and B) a magnified view of the siderite aggregate, scale bar = 1 μm . EDS spectra of the C) spheroidal aggregate and D) platy inclusions indicated in B. Os peaks are from the conductive coating used to prevent sample charging.

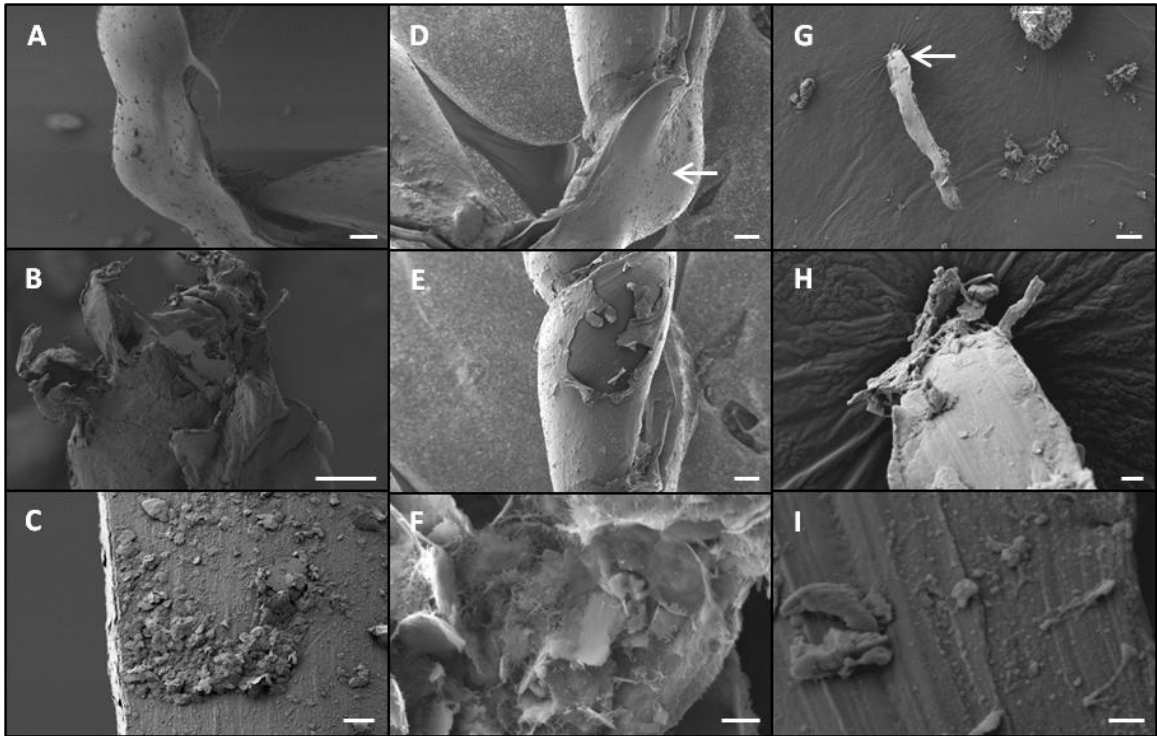


Figure 3.9: SE2 SEM micrographs showing brine shrimp remnants at 5 months: A) dorso-lateral view of the cuticle, scale bar = 200 μm ; B) antero-ventral view of a degraded cuticle, scale bar = 100 μm ; and C) a zoomed in view of the dorsal cuticle surface, scale bar = 4 μm . SE2 SEM micrographs showing brine shrimp remnants at 9 months: D) lateral view of the cuticle showing dorsal (arrow) and ventral surfaces, scale bar = 200 μm ; E) dorsal surface of a uropod, located at the abdominal posterior, scale bar = 100 μm ; and F) zoomed-in view of the organic film coating the dorsal surface, scale bar = 4 μm . SE2 SEM micrographs showing brine shrimp remnants at 8.5 months: G) a piece of cuticle, scale bar = 20 μm ; H) magnified view of the region indicated in G, scale bar = 2 μm ; and I) magnified view of the cuticle surface, scale bar = 1 μm .

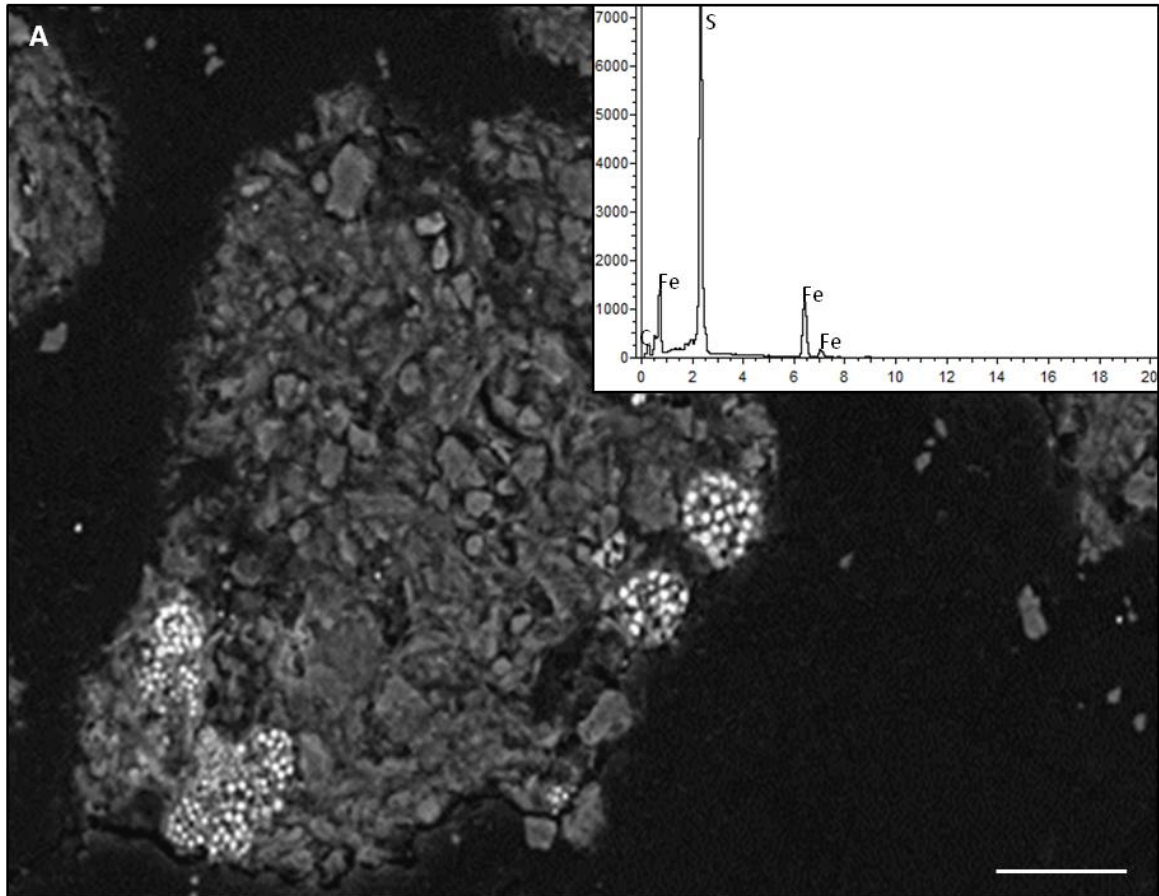


Figure 3.10: Backscattered SEM micrograph showing framboidal pyrite within an aggregate of sediment grains at 5 months, scale bar = 20 μm . The inset shows the EDS spectrum of a framboidal grain, and is indicative of pyrite.

rich regions that corresponded to the sulphidic zone, were observed within embedded sediment samples of the upper-sulphidic column (Fig 3.11A, B). The carbonaceous remains were found infiltrating consolidated sediment grains (Fig. 3.11C). Additionally, a possible articulated remain, having the same brightness as pyrite, was observed at the edge of the carbonaceous blob (Fig. 3.11D). Carbon-rich regions (Figs. 3.12A, 3.13A) corresponding to sulphidic zones, within an embedded sediment sample of the middle sulphidic column, also showed several interesting features. Framboidal and euhedral pyrite grains were found within a quartz and carbonate sediment matrix (Fig. 3.12B, D). A permineralised cellular structure (Fig. 3.12C), infilled with calcium phosphate (Fig. 3.12E) and surrounded by a carbon-enriched clay-mineralised wall (Fig. 3.12F), was also observed. Finally, a carbon-rich cell-like structure was found surrounded by sediment grains (Fig. 3.13).

3.4 DISCUSSION

3.4.1 Column phenotypes, geochemistry and microbial populations

The increased level of organic carbon in the middle of the T = 0 column is accompanied by increases in sulphate, phosphate and nitrite within the overlying sediment. The addition of the shrimp layer, along with residual aquarium water, may have caused this spike in organic carbon and sulphur, phosphorus and nitrogen containing ions within overlying sediment.

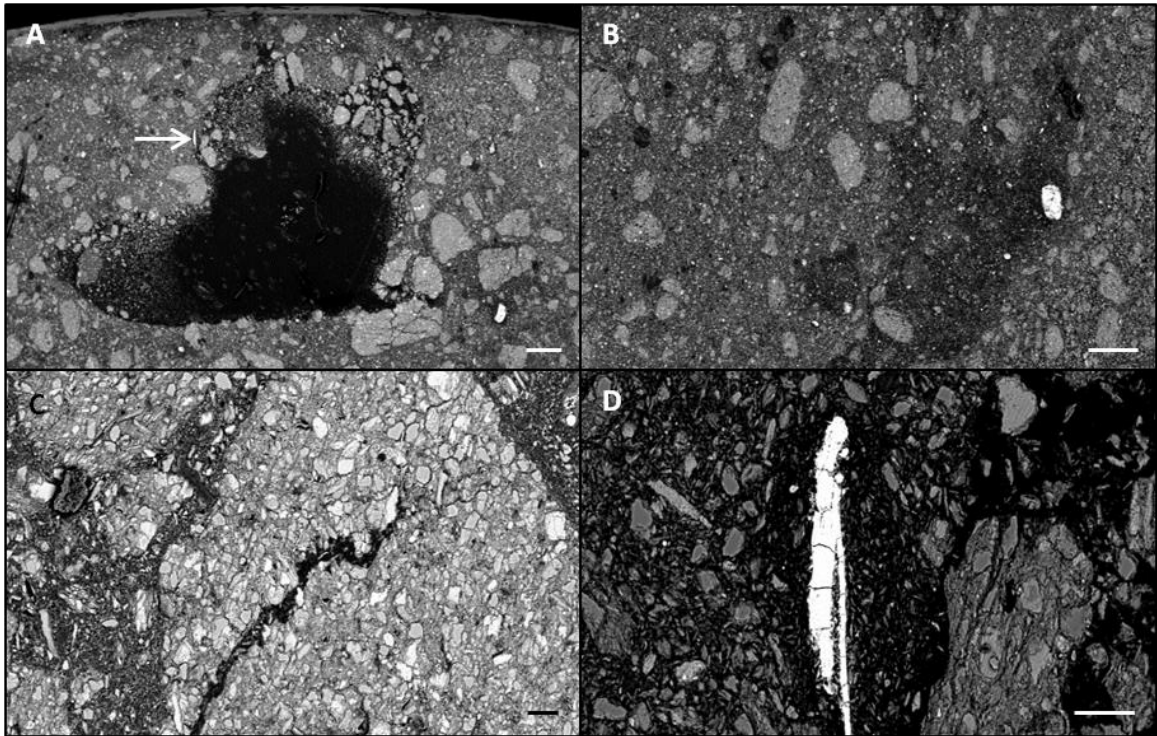


Figure 3.11: Backscattered SEM micrographs showing: A), B) carbon-rich regions within 8.5 month old embedded sediments, scale bars = 200 μm ; C) a magnified view of a carbon-rich region within an aggregate of sediment grains, scale bar = 20 μm ; and D) a magnified view of the articulated remain indicated in A, scale bar = 20 μm .

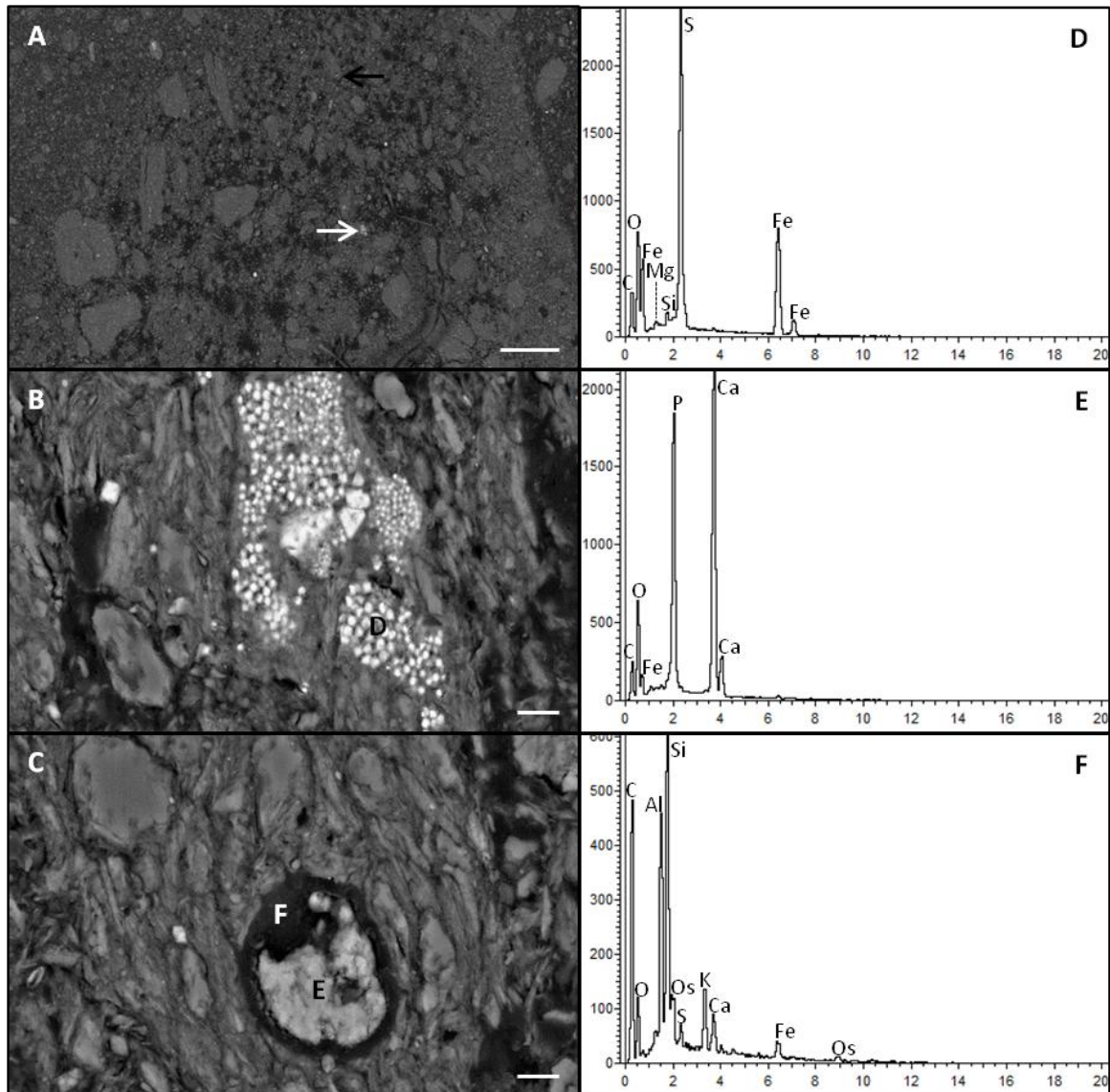


Figure 3.12: Backscattered SEM micrographs showing: A) carbon-rich regions within 9 month old embedded sediments, scale bar = 20 μm ; B) a magnified view of framboidal and euhedral pyrite occurring within an aggregate of sediment grains in A (white arrow), scale bar = 4 μm ; and C) a magnified view of the permineralised cell-like structure indicated in A (black arrow), scale bar = 4 μm . EDS spectra of: D) the pyrite framboid indicated in B; E) and F) the mineralised cellular regions indicated in C. Os is from the conductive coating used to prevent sample charging.

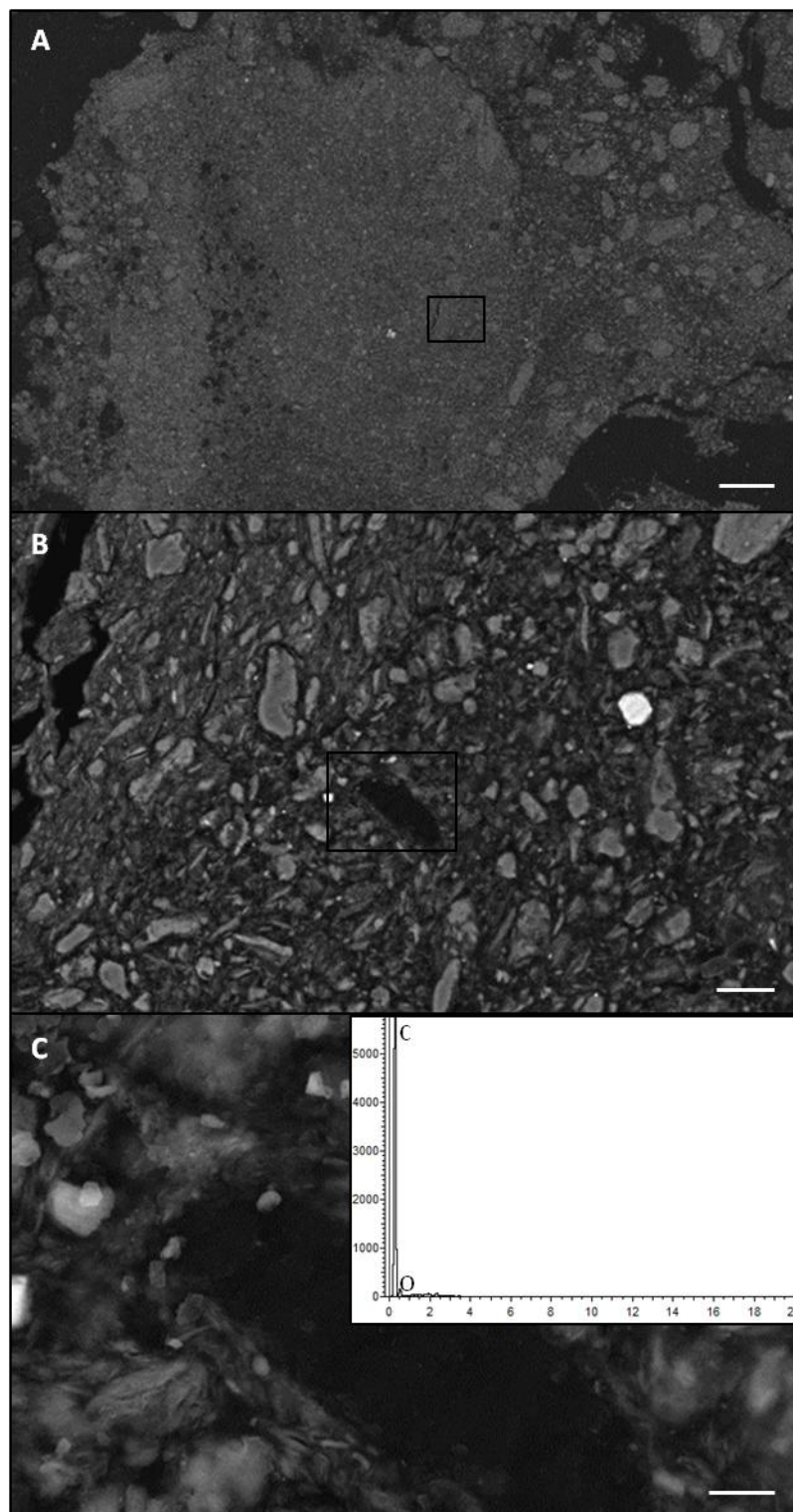


Figure 3.13: Backscattered SEM micrographs showing: A) carbon-rich regions within 9 month old embedded sediments, scale bar = 200 μm ; B) a magnified view of the boxed region in A, showing a cell-shaped structure, scale bar = 10 μm ; and C) a magnified view of the boxed region in B with an inset EDS spectrum of the cell-shaped structure showing it to be carbon-rich, scale bar = 2 μm .

Based on visual phenotypes, the taphonomic model developed heterogeneous redox zonation. The range of phenotypes, *i.e.*, upper-sulphidic, mid-sulphidic and diffuse-sulphidic, produced by this model presumably reflect the post-burial survival strategies of the live brine shrimp. The sulphidic zones observed at the sediment-plastic interface were found to be edge-effects, intuitively caused by increased diffusion around the periphery of the column. The similarity in water chemistry throughout the column suggests that there were also significant diffusion effects within the sediment, as well as between the sediment and overlying water. Several observations suggest that the system became more oxidizing with time: 1) the competitiveness of *Shewanella oneidensis* MR-1 coupled with the decline of SRB, despite continued availability of sulphate; 2) the increase in nitrate and decrease in nitrite; and 3) formation of an orange-coloured mineral in non-sulphidic zones, first observed at two weeks at the sediment-water interface and at four months within underlying sediment. *Shewanella* can outcompete SRB in environments that are low in labile organics and in conditions that are moderately reducing (Southam and Saunders, 2005). *Shewanella oneidensis* MR-1 is a metabolically diverse bacterium capable of using oxygen, nitrate, nitrite and ferric iron as an electron acceptor (Gao *et al.*, 2009; Wang *et al.*, 2010b; Qian *et al.*, 2011).

During diagenesis, the natural organic carbon in the sediment and, after their death, the organic carbon provided by decomposing shrimp carcasses is oxidised to $\text{CO}_{2(\text{aq})}$ (which dissociates to $\text{HCO}_3^-_{(\text{aq})}$ and $\text{CO}_3^{2-}_{(\text{aq})}$) and intermediate organics by heterotrophs, *i.e.*, sulphate reducing bacteria (SRB) and *Shewanella oneidensis* MR-1.

Initially, the decomposition environment created by the decaying shrimp provides a competitive advantage to the SRB. This is indicated by formation of blackened zones in the sediment within two to six weeks of diagenesis. The significant drop in SRB and increase in *Shewanella* populations after nine months supports the idea that iron sulphide formation is an early diagenetic phenomenon.

Ammonium is a by-product of protein degradation and can accumulate in anaerobic soils (Dedhar and Mavinic, 1986). It is also found fixed in clays and other geological materials (Stevenson, 1986). Nitrate can be formed from ammonium through aerobic nitrification or anaerobic ammonium oxidation (Anammox) pathways (McElroy and Glass, 1956; Wang *et al.*, 2010a; Madigan *et al.*, 2012). In aerobic nitrification, nitrite is formed chemolithoautotrophically by ammonium oxidation, and nitrate is subsequently formed by nitrite oxidation (McElroy and Glass, 1956; Madigan *et al.*, 2012). In the Anammox pathway, anaerobic ammonium oxidisers, which require oxygen limited conditions to function, utilise nitrite to oxidise ammonium to nitrate and hydroxide (Mulder *et al.*, 1995; Wang *et al.*, 2010a; Madigan *et al.*, 2012). Denitrification from nitrate may be inhibited in environments with low oxygen and organic carbon availability, and would explain why columns at 9 months show nitrate accumulation (McElroy and Glass, 1956; Madigan *et al.*, 2012). Nitrite is a reactant in both nitrification and Anammox pathways, which may account for its decreased levels within columns. These pathways can occur in the same environment, but may not necessarily occur simultaneously or go to completion.

3.4.2 Carbonate formation and pH

Oxidation of organic carbon by SRB resulted in the formation of early diagenetic iron monosulphides. Oxidation by *Shewanella oneidensis* MR-1 would have resulted in the reduction of multiple species, *e.g.*, ferric iron, nitrate and nitrite. Reduction of ferric iron oxyhydroxides to ferrous iron presumably contributed to formation of iron sulphides and, subsequently or simultaneously, iron carbonates within the sediments. This is further supported by low soluble iron concentrations in sediments, increased inorganic carbon levels at 9 months, and SEM micrograph images (Fig. 3.8A, B) suggesting formation of siderite as early as 2.5 months. Iron-reducing bacteria have been shown to precipitate calcian and magnesian siderite in room-temperature solutions containing Fe(III) oxyhydroxides, and 3-8 mM and 4-13 mM aqueous calcium and magnesium respectively (Romanek *et al.*, 2009). Carbonate precipitation is enhanced in environments with high pH. The pH in columns increases from 7.4 to 8.8 over the course of the incubation. This increase can be facilitated by: 1) microorganisms that consume CO₂ autotrophically, *i.e.*, through CO₂ reduction during methanogenesis; 2) release of OH⁻ groups into the environment during dissimilatory metal reduction; or 3) ammonification of organic compounds (Romanek *et al.*, 2009).

Despite increased pH and inorganic carbon levels, calcium levels in pore water did not change over the course of the incubation, and magnesium concentrations increased. This may be explained by the release of cations from dissolution of clays in acidic microenvironments, and preferential formation of calcian siderite and ferroan calcite over magnesian carbonates. Free divalent cations in solution are surrounded by

hydration shells (Romanek *et al.*, 2009). The ions' surface charge density determines how easily they can shed their hydration shells to be incorporated into solid minerals. Charge densities, and thus dehydration energies, increase from Ca^{2+} to Fe^{2+} to Mg^{2+} . In abiotic carbonate precipitation experiments, incorporation of magnesium into iron and calcium carbonates required high concentrations of the former. Magnesian calcites and siderites were found within sediments at nine months (data not shown). The dehydration energy barrier for magnesium, as well as iron and calcium, may have been overcome by carbonate precipitation on pre-existing mineral surfaces or the presence of organic metabolites and exudates, which can help stabilise transition states (Romanek *et al.*, 2009).

3.4.3 Organism diagenesis and preservation of organics

In all instances where shrimp carcasses were present at the sediment-water interface, the top sulphidic phenotype was observed, and no sulphidic zones developed in control columns without microbial inocula. This suggests that iron sulphides formed preferentially around shrimp carcasses, which were serving as an organic carbon source for the SRB. The inability to extract intact mineralised soft tissue from columns after nine months of diagenesis indicates that decay progressed too rapidly to fossilise delicate structures (Allison, 1988). High water content within column sediments (~50% by weight) may have allowed for too much diffusive exchange of soluble constituents, as indicated by IC and ICP results. This transfer of metabolic products and reactants across redox boundaries would have supported higher levels of biological activity throughout

the column. High levels of biological activity degrade labile tissue too rapidly for mineralisation of structural details. Intact and highly deteriorated cuticle remains were recovered at 9 months. The location of the sulphidic zone had an effect on deterioration rate, with the cuticle from the top-sulphidic zone showing much more disintegration and deterioration. Top-sulphidic zones may have been exposed to more oxygen than underlying diffuse-sulphidic zones, resulting in more rapid aerobic degradation of recalcitrant organic matter after initial decay of labile organics by the SRB (Briggs and Kear, 1993a). The relatively intact cuticle recovered from the diffuse-sulphidic column at 9 months was covered by an organic coating that resembled EPS. Microbial cells were no longer visible; however, the coating may have acted as a protective barrier against further cuticle decay. Despite distortion, disintegration at the extremities and bacterial pitting, especially on ventral surfaces, survival of the cuticle shows that more recalcitrant organic matter can withstand decay, especially in anaerobic environments (Gostling *et al.*, 2009).

Biofilms were not observed in the sediment or on carcasses after $T = 0$; however, there was evidence of microbial activity. In addition to the formation of iron sulphides and spheroidal siderite aggregates, framboidal pyrite was observed within sediment at 5 and 9 months. Visible sulphidic zones in embedded sediment samples corresponded to carbon-rich regions when observed under SEM backscatter. In the 9 month sample, the frambooids, and adjacent euhedral pyrite, were found in a sediment grain within the carbon-rich, sulphidic zone. At low temperatures, framboidal pyrite has been found to form within an organic polymer matrix, in which EPS can be a major component.

Formation of framboidal as opposed to euhedral pyrite crystals requires an environment that is supersaturated with respect to pyrite, in which the nucleation rate exceeds the crystal growth rate (MacLean *et al.*, 2008). This can be achieved in reducing, alkaline organic decay microenvironments (MacLean *et al.*, 2008).

Articulated remains and permineralised cell-like structures were also found within the carbon-rich, sulphidic zones at 5 and 9 months respectively. The articulated remnant was about 100 μm in length, and resembled an adult shrimp antenna. It appeared pyritised under SEM backscatter. The calcium phosphate in-filled cell is about 8 μm across, and is presumably of eukaryotic origin. Calcium phosphate preservation can be induced by microbial action (Briggs and Kear, 1993b). It occurs preferentially in acidic microenvironments around decaying carcasses, and usually mineralises soft tissues. It can preserve fine anatomical details if decay does not occur too rapidly; however, some decay is necessary to provide the phosphate (Briggs and Kear, 1993b). The drop in pH necessary to promote phosphatisation over carbonate mineralisation occurs early in the diagenetic process (Briggs and Kear, 1993b). The cell wall is enriched in carbon and composed of clay minerals. The second cell-like structure is a carbon-enriched region surrounded by sediment grains, and is about 16 μm long and 8 μm wide.

3.4.4 Future recommendations

Mazon Creek fossils are often surrounded by one or more pyrite halos, which may have formed by pyritisation of microbial halos and organic breakdown products surrounding decaying carcasses (Borkow and Babcock, 2003). The sulphidic zones

forming around shrimp carcasses in this taphonomic model were potentially a precursor to pyrite halos; however, their structures were severely compromised during sampling. Adding a compaction element to the diagenetic model soon after formation of sulphidic zones would limit diffusion of biologically active ions and organic decomposition products, thereby decreasing the A_w of the system and limiting biological activity. This would prevent rapid decay of labile organics, and aid in the dewatering of mineralised sedimentary structures and the formation of protoconcretions within columns that could be more easily sampled.

3. REFERENCES

- Allison, P.A., 1988, The role of anoxia in the decay and mineralization of proteinaceous macro-fossils: *Paleobiology*, v. 14, no. 2, p. 139-154.
- Allison, P.A., and Pye, K., 1994, Early diagenetic mineralization and fossil preservation in modern carbonate concretions: *Palaios*, v. 9, no. 6, p. 561-575.
- Baird, G.C., 1979, Lithology and fossil distribution, Francis Creek Shale in northeastern Illinois. *in* Nitecki, M.H., ed., *Mazon Creek fossils*: New York, NY, Academic Press, p.41-67.
- Baird, G.C., 1997, Francis Creek Diagenetic Events, *in* Shabica, C.W., and Hay, A.A., eds., *Richardson's Guide to the Fossil Fauna of Mazon Creek*: Chicago, Northeastern Illinois University, p 30-34.
- Baird, G.C., and Sroka, S.D., 1990, Geology and geohistory of Mazon Creek area fossil localities, Illinois, *in* Hammer, W.R., and Hess, D.F., eds., *Geology Field Guidebook: Current Perspectives on Illinois Basin and Mississippi Arch Geology*: Macomb, IL, Geological Society of America, 24th Annual Meeting of the North-Central Section, p. C1-C70.
- Baird, G.C., Shabica, C.W., Anderson, J.L., and Richardson, E.S., Jr., 1985a, Biota of a Pennsylvanian muddy coast: habitats within the Mazonian delta complex, northeast Illinois: *Journal of Paleontology*, v. 59, no. 2, p. 253-281.
- Baird, G.C., Sroka, S.D., Shabica, C.W., Beard, T.L., Scott, A.C., and Broadhurst, F.M., 1985b, Mazon Creek-type fossil assemblages in the U.S. midcontinent Pennsylvanian: their recurrent character and palaeoenvironmental significance [and discussion]: *Philosophical Transactions of the Royal Society of London. Series B, Biological Sciences*, v. 311, no. 1148, *Extraordinary Fossil Biotas: Their Ecological and Evolutionary Significance*, p. 87-99.
- Baird, G.C., Sroka, S.D., Shabica, C.W., and Kuecher, G.J., 1986, Taphonomy of middle Pennsylvanian Mazon Creek Area fossil localities northeast Illinois, USA: significance of exceptional fossil preservation in syngenetic concretions: *Palaios*, v. 1, no. 3, p. 271-285.
- Balch, W.E., Fox, G.E., Magrum, L.J., Woese, C.R., and Wolfe, R.S., 1979, Methanogens - re-evaluation of a unique biological group: *Microbiological reviews*, v. 43, no. 2, p. 260-296.

- Berner, R.A., 1984, Sedimentary pyrite formation - an update: *Geochimica et Cosmochimica Acta*, v. 48, no. 4, p. 605-615.
- Borkow, P.S., and Babcock, L.E., 2003, Turning pyrite concretions outside-in: role of biofilms in pyritization of fossils: *The Sedimentary Record*, v. 1, no. 3, p. 4-7.
- Bottjer, D.J., 2002, Exceptional fossil preservation: a unique view on the evolution of marine life: New York, Columbia University Press, 403 p.
- Briggs, D.E.G., and Kear, A.J., 1994, Decay and mineralization of shrimps: *Palaios*, v. 9, no. 5, p. 431-456.
- Briggs, D.E.G., and Kear, A.J., 1993a, Decay and preservation of polychaetes: taphonomic thresholds in soft-bodied organisms: *Paleobiology*, v. 19, no. 1, p. 107-135.
- Briggs, D.E.G., and Kear, A.J., 1993b, Fossilization of soft tissue in the laboratory: *Science*, v. 259, no. 5100, p. 1439-1442.
- Dedhar, S., and Mavinic, D.S., 1986, Ammonia removal from a landfill leachate by nitrification and denitrification: *Water Pollution Research Journal of Canada*, v. 2, no. 3, p. 126-137.
- Foster, I.S., 2009, Characterization of halophilic microorganisms and sulfate salts from the hypersaline lakes of British Columbia, Canada: an astrobiological perspective [M.Sc. thesis]: London, University of Western Ontario, 133 p.
- Foster, M.W., 1979a, A reappraisal of *Tullimonstrum gregarium*, in Nitecki, M.H., ed., *Mazon Creek Fossils*: New York, NY, Academic Press, p.269-302.
- Foster, M.W., 1979b, Soft-bodied coelenterates in the Pennsylvanian of Illinois, in Nitecki, M.H., ed., *Mazon Creek Fossils*: New York, NY, Academic Press, p.191-267.
- Gao, H., Yang, Z.K., Barua, S., *et al.*, 2009, Reduction of nitrate in *Shewanella oneidensis* depends on atypical NAP and NRF systems with NapB as a preferred electron transport protein from CymA to NapA: *Isme Journal*, v. 3, no. 8, p. 966-976.
- Gostling, N.J., Dong, X., and Donoghue, P.C.J., 2009, Ontogeny and taphonomy: an experimental taphonomy study of the development of the brine shrimp *artemia salina*: *Palaeontology*, v. 52, p. 169-186.
- Kuecher, G.J., Woodland, B.G., and Broadhurst, F.M., 1990, Evidence of deposition from individual tides and of tidal cycles from the Francis Creek Shale (host rock to the Mazon Creek Biota), Westphalian D (Pennsylvanian), northeastern Illinois: *Sedimentary Geology*, v. 68, no. 3, p. 211-221.

- MacLean, L.C.W., Tyliszczak, T., Gilbert, P.U.P.A., Zhou, D., Pray, T.J., Onstott, T.C., and Southam, G., 2008, A high-resolution chemical and structural study of framboidal pyrite formed within a low-temperature bacterial biofilm: *Geobiology*, v. 6, no. 5, p. 471-480.
- Madigan, M.T., Martinko, J.M., Stahl, D.A., and Clark, D.P., 2012, *Brock biology of microorganisms*, 13th edition: San Francisco, Benjamin Cummings, 1152 p.
- McElroy, W.D., and Glass, B., editors, 1956, A symposium on inorganic nitrogen metabolism: function of metallo-flavoproteins, sponsored by the McCollum-Pratt Institute of the Johns-Hopkins University: Baltimore, Johns Hopkins Press, 728 p.
- Middleton, H.A., and Nelson, C.S., 1996, Origin and timing of siderite and calcite concretions in late Palaeogene non- to marginal-marine facies of the Te Kuiti Group, New Zealand: *Sedimentary Geology*, v. 103, no. 1-2, p. 93-115.
- Mulder, A., Vandergraaf, A.A., Robertson, L.A., and Kuenen, J.G., 1995, Anaerobic ammonium oxidation discovered in a denitrifying fluidized-bed reactor: *FEMS Microbial Ecology*, v. 16, no. 3, p. 177-183.
- Nitecki, M.H., editor, 1979, *Mazon Creek fossils*: New York, NY, Academic Press, 69 p.
- Phillips, T.L., Peppers, R.A., and Dimichele, W.A., 1985, Stratigraphic and interregional changes in Pennsylvanian coal-swamp vegetation - environmental inferences: *International Journal of Coal Geology*, v. 5, no. 1-2, p. 43-109.
- Potter, P.E., and Pryor, W.A., 1961, Dispersal centers of Paleozoic and later clastics of the Upper Mississippi Valley and adjacent areas: *Geological Society of America Bulletin*, v. 72, no. 8, p. 1195-1249.
- Qian, Y., Shi, L., and Tien, M., 2011, SO2907, a putative TonB-dependent receptor, is involved in dissimilatory iron reduction by *Shewanella oneidensis* strain MR-1: *Journal of Biological Chemistry*, v. 286, no. 39, p. 33973-33980.
- Romanek, C.S., Jimenez-Lopez, C., Rodriguez-Navarro, A., Sanchez-Roman, M., Sahai, N., and Coleman, M., 2009, Inorganic synthesis of Fe-Ca-Mg carbonates at low temperature: *Geochimica et Cosmochimica Acta*, v. 73, no. 18, p. 5361-5376.
- Schellenberg, S.A., 2002, Mazon Creek: preservation in late Paleozoic deltaic and marginal marine environments, *in* Bottjer, D.J., Etter, W., Hagadorn, J.W. and Tang, C.M., eds., *Exceptional fossil preservation: a unique view on the evolution of marine life*: New York, Columbia University Press, p. 185-203.

- Schopf, J.M., 1979, Evidence of soft-sediment cementation enclosing Mazon plant fossils, *in* Nitecki, M.H., ed., Mazon Creek fossils: New York, NY, Academic Press, p. 105-128.
- Schut, F., de Vries, E.J., Gottschal, J.C., Robertson, B.R., Harder, W., Prins, R.A., and Button, D.K., 1993, Isolation of typical marine bacteria by dilution culture: growth, maintenance, and characteristics of isolates under laboratory conditions: *Applied and Environmental Microbiology*, v. 59, no. 7, p. 2150-2160.
- Seilacher, A., Reif, W.E., and Westphal, F., 1985, Sedimentological, ecological and temporal patterns of fossil lagerstätten [and discussion]: *Philosophical Transactions of the Royal Society of London, Series B: Biological Sciences*, v. 311, no. 1148, p. 5-24.
- Shabica, C.W., and Hay, A.A., editors, 1997, Richardson's guide to the fossil fauna of Mazon Creek: Chicago, Northeastern Illinois University, 308 p.
- Southam, G., and Saunders, J.A., 2005, The geomicrobiology of ore deposits: *Economic Geology*, v. 100, no. 6, p. 1067-1084.
- Stevenson, F.J., 1986, Cycles of soil: carbon, nitrogen, phosphorus, sulfur, micronutrients: Toronto, Wiley-Interscience, 380 p.
- USDA, F., 2008, Microbiology laboratory guidebook, appendix 2.03: most probable number procedure and tables, 9 p.
- Wang, C., Lee, P., Kumar, M., Huang, Y., Sung, S., and Lin, J., 2010a, Simultaneous partial nitrification, anaerobic ammonium oxidation and denitrification (SNAD) in a full-scale landfill-leachate treatment plant: *Journal of hazardous materials*, v. 175, no. 1-3, p. 622-628.
- Wang, H., Hollywood, K., Jarvis, R.M., Lloyd, J.R., and Goodacre, R., 2010b, Phenotypic characterization of *Shewanella oneidensis* MR-1 under aerobic and anaerobic growth conditions by using fourier transform infrared spectroscopy and high-performance liquid chromatography analyses: *Applied and Environmental Microbiology*, v. 76, no. 18, p. 6266-6276.
- Woodland, B.G., and Stenstrom, R.C., 1979, The occurrence and origin of siderite concretions in the Francis Creek Shale (Pennsylvanian) of northeastern Illinois, *in* Nitecki, M.H., ed., Mazon Creek fossils: New York, NY, Academic Press, p. 69-103.

CHAPTER 4

GENERAL DISCUSSION

4.1 SYNTHESIS AND CONCLUSIONS

The fossiliferous Mazon Creek concretions consist mainly of siderite cement, with clay- to silt-sized sedimentary particles (individual grains of clay and quartz, plus clay rip-up clasts) dispersed throughout (Baird, 1979; Baird *et al.*, 1986; Shabica and Hay, 1997). Fossil remains of soft tissues contained within the concretions are typically pyritised (see Figs. 2.1, 2.6) and/or occur as impressions of soft-bodied organisms (see Fig. 2.10) (Shabica and Hay, 1997; Schellenberg, 2002). The impressions can be covered by a network of reticulate cracks that have been attributed to sub-aerial exposure during early diagenesis (Foster, 1979), but more likely reflect early compaction and syneresis.

As the exceptional preservation of 'soft-bodied' organisms might suggest, the concretions also possess microbial fossils that occur as C-rich mineralised voids, at the cellular level, within the siderite 'glue' that holds the concretions together (see Figs. 2.7, 2.8, 2.12). This novel observation on the microtexture of Mazon Creek concretions is consistent with the claim of Preston *et al.* (2011) that if microbial autolytic enzymes are adequately inhibited after cell death and mineralisation occurs before significant cellular decay, organic structures can be preserved through permineralisation. Perhaps more specifically, Mazon Creek-type preservation may well manifest the importance of high iron concentrations in binding the extracellular surfaces of dead microbes and inhibiting autolysins (Preston *et al.*, 2011), ultimately favouring the preservation of microbial fossils.

The combined use of multiple analytical techniques (SEM, EDS and ToF-SIMS) permits the observation of micrometre-scale cocci, rods and filaments within the siderite-cemented matrix of the Mazon Creek concretions – a diverse assortment of microbial morphologies that suggest the participation of a variety of microbes in concretion formation. The cement-supported fabric of the concretions, as revealed by the imaging techniques employed in this study, is also significant; concretion formation must have been initiated when the sediment had a very high water content (as indicated by up to 80% cement between sediment-hosted grains at concretion centres), thus confirming their rapid formation very soon after burial (Baird *et al.*, 1986). The concretion matrix was also found to contain a wide range of organics; further study of these organic molecules may provide significant insight on fossilisation processes in the context of early diagenetic concretion development.

ToF-SIMS proved to be an especially powerful analytical method for characterizing the presence and distribution of organic biomarkers within the Mazon Creek concretions, due to its combined ability to create high mass-resolution scans and high-resolution (μm -scale) two-dimensional ion maps by separating secondary ions based on charge and mass (Thiel *et al.*, 2007; Wanger, 2008; Orphan and House, 2009). The challenge with interpreting this ToF-SIMS data is the large number of organic compounds recovered from the concretions that need to be identified. The next step in the analysis of microbial organic biomarkers in geologic material using ToF-SIMS (or perhaps Nano-SIMS (Orphan and House, 2009)) is to examine how a series of standard biological macromolecules and their constituent components, *e.g.*, peptidoglycan and N-

acetyl muramic acid, fragment on exposure to the ion beam (Thiel *et al.*, 2007). With this database of biomarker standards, these complex patterns of organic compounds preserved in geologic material can be deciphered. ToF-SIMS could also be used as a screening tool to triage samples for other analytical techniques (*e.g.*, lipid extraction and stable isotope studies (Brady *et al.*, 2010)), as a more comprehensive geobiological method for identifying biomarkers and examining biodiversity (Pearson and Nelson, 2005; Slater, 2009). As biomarker analytical techniques and databases improve, the microbes and diagenetic changes involved in the preservation of organics may be determined from fossilised remnants within these concretions (see Figs. 2.5, 2.9, 2.13).

The formation of siderite concretions around the pyritised Mazon Creek fossils (see Figs. 2.1, 2.6) indicates that that pyrite was a very early diagenetic product (Woodland and Stenstrom, 1979; Baird *et al.*, 1986; Schellenberg, 2002). The formation of pyrite halos around fossil organisms within some concretions suggests that the chemical conditions leading to concretion formation may have been cyclic, perhaps influenced by tides, which would have replenished pore water sulphate periodically. Siderite precipitation would have begun once initial interstitial sulphate was removed through sulphate reduction and pyritisation. If the tides replenished sulphate around decaying organisms after siderite precipitation had begun, viable SRB could restart sulphate reduction at some distance from the carcass. This could continue over several tidal cycles, producing halos, as long as diffusing labile organics were still present around the carcass and SRB remained viable in-between phases of sulphate availability.

The mechanism of formation of pyrite halos within the Mazon Creek concretions is still a point of debate. Recent studies have implicated the Liesegang ring formation mechanism for formation of pyrite halos in anoxic marine environments (Bektursunova and L'Heureux, 2011). This would require quiescent conditions for the formation of diffusion gradients (Allen, 2002; Bektursunova and L'Heureux, 2011), whereas the Mazon Creek area was a tidally influenced estuary with periodic influxes of terrigenous sediment from major distributary deltas (Baird *et al.*, 1986; Kuecher *et al.*, 1990). Water, and consequently porewater, geochemistry at Mazon Creek may have ranged from more freshwater during ebb tides to more marine during flood tides (Woodland and Stenstrom, 1979; Kuecher *et al.*, 1990). The model used by Bektursunova *et al.* (2009) assumes that solid components are not compacted and have spatially constant porosity, pH and density. This would not hold true for decaying carcasses buried in the Mazon Creek area. As well, for formation of a Liesegang ring pyritisation pattern, the flux of sulphide and iron diffusing towards each other must be comparable. If aqueous sulphide is much lower than aqueous iron, pyritisation will occur immediately around or within the sulphide source (Bektursunova and L'Heureux, 2011).

Siderite precipitation and concretion lithification must also have begun early in order to protect fossilizing soft tissue details from destruction by tides, sediment movement and compaction (Baird *et al.*, 1986; Schellenberg, 2002). The presence of siderite colloids (see Fig. 3.7) and framboidal pyrite (see Figs 3.10, 3.11) in the laboratory diagenesis experiments shows that these minerals can form within 2 to 5 months of organism burial, and based on macroscopic observations, i.e., blackening of the

sediment, they presumably began forming much earlier. The mechanism(s) of concretion formation are not completely understood, although microbial activity is likely to play a factor. Microbial colonies surrounding the carcass would create geochemical variations on the 1 to 10's of micrometre-scales, meaning siderite and iron monosulphides and pyrite could potentially be formed simultaneously in microenvironments within concretions. Some microbes can switch their metabolic pathways depending on nutrient availability, adding to the complexity of this process (Balch *et al.*, 1979; Southam and Saunders, 2005; Falkowski *et al.*, 2008). SRB and Fe-reducers are the likely candidates in concretion diagenesis (Duan *et al.*, 1996), but methanogens, anaerobic methane oxidisers (ANME), nitrifiers and anaerobic ammonia oxidizing Bacteria and Archaea may also play a role (Orphan *et al.*, 2001; Nannipieri and Eldor, 2009; Orphan *et al.*, 2009; Wang *et al.*, 2010). Laboratory diagenesis experiments have improved our understanding of the early stages of fossilisation, and of the permineralisation of microbes involved in decay. The characterisation of organic compounds discovered within concretions may provide important clues about the microbes involved in concretion formation. Incorporating this knowledge into future diagenesis experiments will lead to more accurate experimental designs and paleoenvironmental interpretations.

Mazon Creek concretion pyrite levels vary from no pyrite to completely pyritic (see Section 1.6.1). Concretions forming further west, *i.e.*, in more marine conditions, contained dense pyritic cores and lacked fossils. Intuitively, concretion formation varies along an inversely related iron-to-sulphate continuum based on geographic area, with

concretions located closer to the paleoshore forming in more freshwater conditions (*i.e.*, higher iron, lower sulphate) and concretions located further out to sea forming in more marine conditions (*i.e.*, lower iron, higher sulphate). This suggests increased sulphate reduction in increasingly marine conditions, either due to increased bacterial reduction rates or increased porewater sulphate concentrations. The changes in iron and sulphate concentrations over the Mazon Creek area may have been important in determining level of pyritisation. Microcosm experiments that vary these two parameters and keep all others constant would be one way to test this theory.

4.2 FUTURE EXPERIMENTS

The diagenesis model developed for this project could be modified to answer some of the lingering questions about concretion formation and soft tissue preservation. Adding a compaction element (see Section 3.4.4) would limit diffusion during later months of diagenesis, minimizing the flow of nutrients within columns and thereby preventing continued microbial activity and perhaps, dissolution of previously formed minerals. It would also promote sediment dewatering and lithification, allowing for easier extraction of *in situ* mineralised carcasses for analysis. Adding a fluid flow element would mimic the effect of tides during initial burial, changing interstitial water chemistry. Varying the sulphate and iron concentrations within columns could also shed light on the level of soft body pyritisation, development of framboids and halos, and siderite formation in brackish-estuarine environments. A more in depth understanding

of these diagenetic processes and the preservation potential of various organic tissues will lead to more accurate paleoecosystem modelling, improving phylogenetic and paleoenvironmental interpretations.

Mazon Creek siderite concretions are still opened using freeze-thaw cycles or hammer blows (Shabica and Hay, 1997); however, both methods can inflict damage on the contained fossils. The use of natural freeze-thaw cycles to promote weathering to open concretions causes oxidation (especially of pyrite), and produces secondary minerals that destroy some fossil details (see Section 2.4.2). Introducing water into concretion fractures (as part of the freeze-thaw method) means that physicochemical attributes of the concretions (including preserved organics), are no longer pristine. This complicates concretion analysis, and adds a potential for error. Some concretions take years to open with the freeze-thaw mechanism, and others never do. Breaking fossils open by hammering is the quickest method, but when concretions do not break open along the fossil plane, the specimen is destroyed.

There has been recent interest in X-ray micro-computed tomography (X-ray micro-CT) scanning of carbonaceous chondrites and stony-iron meteorites (McCausland *et al.*, 2010). Computed tomography (CT), most commonly used in medical applications, can be used to reconstruct three-dimensional images of object interiors from a series of slices taken by passing X-rays through successive 360° planes of rotation (Cierniak, 2011). CT scanning has been used for paleontological applications in the past; however, the use of micro-CT in paleontology is relatively new (Tafforeau *et al.*, 2006). Micro-CT scanners can reach high (sometimes micrometre scale) spatial resolutions, and so would

be particularly useful in the imaging of microbial textures and small organism details preserved within concretion-hosted fossils. CT image contrast is achieved by variable attenuation of X-rays in materials of different electron density and/or thickness (McCausland *et al.*, 2010; Cierniak, 2011); therefore, metallic minerals will attenuate X-rays more rapidly than less dense minerals (*e.g.*, clays, feldspars and quartz) and will appear brighter in CT scans. It is not unreasonable to extrapolate this technique to concretions containing metallic mineral fossils cemented in a sedimentary matrix. If feasible, this technique holds potential to revolutionise the way fossils are analyzed. The ability to see what is inside without exposing a fossil specimen would allow researchers to better allocate samples for analysis and preservation.

4. REFERENCES

- Allen, R.E., 2002, Role of diffusion-precipitation reactions in authigenic pyritization: *Chemical Geology*, v. 182, no. 2-4, p. 461-472.
- Baird, G.C., 1979, Lithology and fossil distribution, Francis Creek Shale in northeastern Illinois, *in* Nitecki, M.H., ed., *Mazon Creek fossils*: New York, NY, Academic Press, p.41-67.
- Baird, G.C., Sroka, S.D., Shabica, C.W., and Kuecher, G.J., 1986, Taphonomy of middle Pennsylvanian Mazon Creek Area fossil localities northeast Illinois, USA : significance of exceptional fossil preservation in syngenetic concretions: *Palaios*, v. 1, no. 3, p. 271-285.
- Balch, W.E., Fox, G.E., Magrum, L.J., Woese, C.R., and Wolfe, R.S., 1979, Methanogens - re-evaluation of a unique biological group: *Microbiological reviews*, v. 43, no. 2, p. 260-296.
- Bektursunova, R., and L'Heureux, I., 2011, A reaction-transport model of periodic precipitation of pyrite in anoxic marine sediments: *Chemical Geology*, v. 287, no. 3-4, p. 158-170.
- Brady, A.L., Slater, G.F., Omelon, C.R., *et al.*, 2010, Photosynthetic isotope biosignatures in laminated micro-stromatolitic and non-laminated nodules associated with modern, freshwater microbialites in Pavilion Lake, BC: *Chemical Geology*, v. 274, no. 1-2, p. 56-67.
- Cierniak, R., 2011, *X-Ray computed tomography in biomedical engineering*: London, Springer-Verlag London Limited.
- Duan, W.M., Hedrick, D.B., Pye, K., Coleman, M.L., and White, D.C., 1996, A preliminary study of the geochemical and microbiological characteristics of modern sedimentary concretions: *Limnology and Oceanography*, v. 41, no. 7, p. 1404-1414.
- Falkowski, P.G., Fenchel, T., and Delong, E.F., 2008, The microbial engines that drive Earth's biogeochemical cycles: *Science*, v. 320, no. 5879, p. 1034-1039.
- Foster, M.W., 1979, Soft-bodied coelenterates in the Pennsylvanian of Illinois, *in* Nitecki, M.H., ed., *Mazon Creek Fossils*: New York, NY, Academic Press, p.191-267.
- Kuecher, G.J., Woodland, B.G., and Broadhurst, F.M., 1990, Evidence of deposition from individual tides and of tidal cycles from the Francis Creek Shale (host rock to the

Mazon Creek Biota), Westphalian D (Pennsylvanian), northeastern Illinois: *Sedimentary Geology*, v. 68, no. 3, p. 211-221.

McCausland, P.J.A., Brown, P.G., and Holdsworth, D.W., 2010, Rapid, reliable acquisition of meteorite volumes and internal features by laboratory X-ray micro-CT scanning: *LPSC Abstracts*, no. 41, p. 2584.

Nannipieri, P., and Eldor, P., 2009, The chemical and functional characterization of soil N and its biotic components: *Soil Biology & Biochemistry*, v. 41, no. 12, p. 2357-2369.

Orphan, V.J., and House, C.H., 2009, Geobiological investigations using secondary ion mass spectrometry: microanalysis of extant and paleo-microbial processes: *Geobiology*, v. 7, no. 3, p. 360-372.

Orphan, V.J., House, C.H., Hinrichs, K.U., McKeegan, K.D., and DeLong, E.F., 2001, Methane-consuming archaea revealed by directly coupled isotopic and phylogenetic analysis: *Science*, v. 293, no. 5529, p. 484-487.

Pearson, M.J., and Nelson, C.S., 2005, Organic geochemistry and stable isotope composition of New Zealand carbonate concretions and calcite fracture fills: *New Zealand Journal of Geology and Geophysics*, v. 48, no. 3, p. 395-414.

Preston, L.J., Shuster, J., Fernandez-Remolar, D., Banerjee, N.R., Osinski, G.R., and Southam, G., 2011, The preservation and degradation of filamentous bacteria and biomolecules within iron oxide deposits at Rio Tinto, Spain: *Geobiology*, v. 9, no. 3, p. 233-249.

Schellenberg, S.A., 2002, Mazon Creek: preservation in late Paleozoic deltaic and marginal marine environments, *in* Bottjer, D.J., Etter, W., Hagadorn, J.W. and Tang, C.M., eds., *Exceptional fossil preservation: a unique view on the evolution of marine life*: New York, Columbia University Press, p.185-203.

Shabica, C.W., and Hay, A.A., editors, 1997, *Richardson's guide to the fossil fauna of Mazon Creek*: Chicago, Northeastern Illinois University, 308 p.

Slater, G.F., 2009, International year of planet Earth 6. biosignatures: interpreting evidence of the origins and diversity of life: *Geoscience Canada*, v. 36, no. 4, p. 170-178.

Southam, G., and Saunders, J.A., 2005, The geomicrobiology of ore deposits: *Economic Geology*, v. 100, no. 6, p. 1067-1084.

- Tafforeau, P., Boistel, R., Boller, E., *et al.*, 2006, Applications of x-ray synchrotron microtomography for non-destructive 3D studies of paleontological specimens: *Applied Physics A-Materials Science & Processing*, v. 83, no. 2, p. 195-202.
- Thiel, V., Heim, C., Arp, G., Hahmann, U., Sjøvall, P., and Lausmaa, J., 2007, Biomarkers at the microscopic range: ToF-SIMS molecular imaging of Archaea-derived lipids in a microbial mat: *Geobiology*, v. 5, no. 4, p. 413-421.
- Wang, C., Lee, P., Kumar, M., Huang, Y., Sung, S., and Lin, J., 2010, Simultaneous partial nitrification, anaerobic ammonium oxidation and denitrification (SNAD) in a full-scale landfill-leachate treatment plant: *Journal of hazardous materials*, v. 175, no. 1-3, p. 622-628.
- Wanger, G., 2008, The deep biosphere of the Witwatersrand basin, Republic of South Africa [Doctor of Philosophy]: University of Western Ontario, 17 p.
- Woodland, B.G., and Stenstrom, R.C., 1979, The occurrence and origin of siderite concretions in the Francis Creek Shale (Pennsylvanian) of northeastern Illinois, *in* Nitecki, M.H., ed., *Mazon Creek fossils*: New York, NY, Academic Press, p.69-103.

ANDREA FERNANDES

Geology
Curriculum vitae

EDUCATION

- Master of Science, Geology:** University of Western Ontario (UWO), London, Ontario 2009-2012
- Thesis: A geobiological investigation of Mazon Creek concretions
 - Concentrations: Geomicrobiology, Mineralogy, Geochemistry, Palaeontology
 - Courses: Graduate Seminar (83%), Analytical Geochemistry (95%), Advanced Mineralogy & Crystallography (94%)
- Bachelor of Medical Sciences (Honours):** UWO, London, ON 2005-2009
- Concentrations: Pharmacology, Toxicology, Genetics, Microbiology
 - Cumulative average: 81.3%

AWARDS & DISTINCTIONS

- Western Graduate Research Scholarship** (\$3000) 2009, 2010
- Western Graduate Scholarship** (\$1700) 2009
- Millennium Excellence Award** (\$4000) 2007
- National scholarship awarded for excellence in community involvement, innovation, leadership and academic achievement
- Western Scholar** 2005, 2006
- Minimum university admission average of 90% and maintenance of minimum 80% sessional average
- Dean's Honour List** 2005, 2006
- Maintenance of minimum 80% sessional average
- Western Scholarship of Excellence** (\$2000) 2005
- University entrance scholarship for 90% admission average

CONFERENCES & PUBLICATIONS

- Goldschmidt Conference:** Knoxville, Tennessee June 2010
- Presented a scientific poster about regions of high carbon and microbial textures found in Mazon Creek concretions

Refereed Publications:

Koren, G., and Fernandes, A. (2010) Reviewers' bias against the null hypothesis: the reproductive hazards of binge drinking. *Journal of Population Therapeutics and Clinical Pharmacology*. 17(2): e281-e283.

Non-Refereed Publications:

Fernandes, A., Hills, A., Tsujita, C., and Southam, G. (2010) Organic carbon and microbial remnants in Mazon Creek fossils. *Geochimica et Cosmochimica Acta*. 74(12): A288

RESEARCH EXPERIENCE

Graduate Thesis Project: UWO, London, Ontario 09/2009-01/2012

- Characterise Mazon Creek concretions using microscopic, spectroscopic and diffraction techniques
- Study initial diagenesis during preservation of soft tissue, using brine shrimp as a model organism
- Culture sulphate reducing bacteria, methanogens and *Shewanella oneidensis* MR-1 for use in decay experiments
- Analyze organisms, sediment and pore water from decay experiments for changes in morphology, mineralogy, pH, [Ca²⁺], [Fe²⁺], [Mg²⁺], [SO₄²⁻] and bacterial population density and viability

Clinical Pharmacology and Toxicology: The Hospital for Sick Children, Toronto, Ontario 05/2009-04/2010

- Corresponded with 62 research subjects, in two test groups, to administer tests and gather responses
- Researched the bias in the scientific community against studies finding no adverse fetal effects related to maternal drug or alcohol use during pregnancy

Medical Sciences Laboratory: UWO, London, Ontario 09/2008-04/2009

- Effectively handled male, Wistar rats while using them as an animal model for atherosclerosis
- Performed ultrasound, real-time PCR and histological analyses to determine the experimental diet of the animal in a blind study
- Discovered that Simvastatin treatment in rats on a high cholesterol diet caused fatty liver disease

Physiology Laboratory: UWO, London, Ontario 09/2008-04/2009

- Examined the effect of steroid abuse on the development of the reproductive system, heart, and liver of young rats

TEACHING EXPERIENCE

Graduate Teaching Assistant: UWO, London, Ontario 09/2009-04/2011

- Supervised lab sections and weekly help sessions, assisting 120

students in grasping hands-on geological concepts

- Supported the course instructor by teaching students lab material and marking assignments

Earth Science 1086G: Origin and Geology of the Solar System 01-04/2011

- Topics: Astronomy, Solar system formation, Space travel and exploration

Earth Science 1022a/b: Earth Rocks! 01-04/2010

- Topics: Rock and mineral identification, Stratigraphy and geologic mapping, Structural geology 09-12/2010

Earth Science 1081a: Environment and Sustainability in a Material Society 09-12/2009

- Topics: Rock and mineral identification, contour mapping, natural hazards, economics of mining, air pollution, global warming, climate change, ground water, waste management

LABORATORY EQUIPMENT & TECHNICAL SKILLS

Certification, Standard first-aid and CPR-C, Animal care & handling,

Training Comprehensive WHMIS, Bio- and radiation safety training, X-ray safety

Analytical Techniques SEM, EDS, XRD, FTIR, ToF-SIMS, fluorescence and phase contrast microscopy, HPLC, paper and thin-layer chromatography, ICP-AES/MS, GC/MS, Radioligand binding assays

Sample Preparation Techniques Solid-phase extraction, titration, distillation, real-time PCR, aseptic & anaerobic culturing, bacterial plating, CPD, resin embedding, Os-staining

Software Programs MS: Excel, Word, PowerPoint, SPSS: ANOVA and Tukey tests, Analytical software: GraphPad, INCA, EVA, IonSpec, IonImage

Research Databases BIOSIS, PubMed, Web of Science, GeoRef, GEOBASE, Scholars Portal

ASSOCIATIONS

- American Association of Petroleum Geologists (member): Oct 2010-2012
- Prospectors and Developers Association of Canada (member): Sept 2010-2012
- Geochemical Society (member): Feb 2010-2012
- Society of Economic Geologists (member): Jan 2008-Apr 2008, Sept 2010-Apr 2011